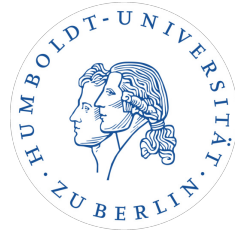


HUMBOLDT-UNIVERSITÄT ZU BERLIN



LEBENSWISSENSCHAFTLICHE FAKULTÄT
INSTITUT FÜR BIOLOGIE

BACHELORARBEIT

ZUM ERWERB DES AKADEMISCHEN GRADES BACHELOR OF
SCIENCE

A physiologically based model of pravastatin - The role of genotypes
and hepatic or renal impairment on the pharmacokinetics of
pravastatin

Ein physiologisch-basiertes Modell für Pravastatin - Die Rolle von
Genotypen und die Leber- und Nierenfunktionsstörungen auf die
Pravastatinpharmacokinetik

vorgelegt von

Helena Leal Pujol

Matrikelnummer: 578392

E-Mail: lepujolh@hu-berlin.de

Geburtsdatum und -ort: 10.11.1996, Barcelona

angefertigt in der Arbeitsgruppe Systems Medicine of the Liver

am Institut für Theoretische Biologie

Berlin, im Mai 2022

Erstprüfer: **Dr. Matthias König**

Zweitprüfer: **Prof. Dr. Hanspeter Herz**

Contents

1	Introduction	4
1.1	Pravastatin	4
1.2	Pravastatin pharmacokinetics	4
1.3	Pravastatin pharmacodynamics	7
1.4	Hepatic and renal impairment	7
1.4.1	Renal impairment	7
1.4.2	Hepatic impairment	8
1.5	Genotypes and genetic variants	8
1.5.1	OATP1B1	9
1.5.2	OATP2B1	10
1.5.3	MRP2	11
1.6	Physiologically based pharmacokinetic model (PBPK)	12
1.7	Question, scope and hypotheses	12
2	Methods	13
2.1	Data curation	13
2.2	Physiologically-based pharmacokinetics model (PBPK)	13
2.3	Parameter fitting	13
2.4	Pravastatin pharmacokinetic parameters	14
3	Results	16
3.1	Pravastatin data	16
3.2	Computational model of pravastatin	19
3.2.1	Physiologically based pharmacokinetic model (PBPK)	19
3.2.2	Intestinal model	19
3.2.3	Kidney model	21
3.2.4	Liver model	21
3.2.5	Whole-body model	22
3.2.6	Model of cirrhosis and renal impairment	22
3.3	Parameter fitting	25
3.4	Model performance	26
3.4.1	Single oral dose	27
3.4.2	Multiple oral dose	27
3.4.3	Intravenous dose	29
3.5	Model application	30
3.5.1	Hepatic impairment	30
3.5.2	Renal impairment	33
3.5.3	Hepatic import (OATP1B1)	37
3.5.4	Hepatic export (MRP2)	41
3.5.5	Intestinal absorption (OATP2B1)	45
3.6	Summary	47
4	Discussion	48
4.1	Data	48
4.2	Model	48
4.3	Disease	50
4.4	Genetic variants	50
5	Outlook	52
6	Supplement	55
References		63

Acronyms

ABC	ATP Binding Cassette
ABCC2	ATP Binding Cassette C2
ADME	Absorption, Distribution, Metabolism and Elimination
AUC	Area Under the Curve
CKD	Chronic Kidney Disease
CICr	Creatinine Clearance
Cmax	Maximum concentration
CTP	Child-Turcotte Pugh
CYP	Cytochrome P450
CYP2C9	Cytochrome P450 2C9
FDA	Food and Drug Administration
GFR	Glomerular Filtration Rate
HDL cholesterol	High-density Lipoprotein Cholesterol
HEK293	Human Embryonic Kidney cell
HMG-CoA reductase	3-Hydroxy-3-Methylglutaryl Coenzyme A Reductase
LDL cholesterol	Low-density Lipoprotein Cholesterol
MRP2	Multidrug Resistance-Associated Protein 2
NAFLD	Non-Alcoholic Fatty Liver Disease
OATP	Organic Anionic Transport Polypeptide
OATP1B1	Organic Anionic Transport Polypeptide 1B1
OATP2B1	Organic Anionic Transport Polypeptide 2B1
ODE	Ordinary Differential Equation
PBPK	Physiologically-Based Pharmacokinetics
SBML	Systems Biology Markup Language
SLCO	Solute Carrier Organic Anion Transporter
SLCO2B1	Solute Carrier Organic Anion Transporter 2B1
SNP	Single Nucleotide Polymorphism
SQ31906	3'-alpha-isopravastatin
SQ31945	3'-alpha-5'-beta-6'-beta-trihydroxypravastatin
TR-	MRP2 Transport Deficient

Abstract

English

Hypercholesterolaemia, i.e., elevated plasma levels of cholesterol, is a major risk factor for cardiovascular disease, the leading cause of death globally. Hypercholesterolaemia can be treated using statins, a class of medications which inhibit HMG-CoA reductase, a major enzyme in cholesterol synthesis.

Pravastatin is a statin used to reduce total and low-density plasma cholesterol levels and increase high-density plasma cholesterol levels in hypercholesterolaemic patients. Pravastatin is absorbed from the small intestine by the transporter OATP2B1 and subsequently transported in the liver via OATP1B1 from where it can be exported in the bile via the enzymatic exporter MRP2. Pravastatin can be excreted either in the urine via the kidneys or in the faeces due to incomplete absorption. Hepatic and renal impairment could have a large impact on the pharmacokinetics of statins as could have genetic variants of the transporters OATP2B1, OATP1B1 and MRP2. Within this thesis the pharmacokinetics of pravastatin were analysed by developing a physiologically-based pharmacokinetics model based on extensive data curation of pravastatin data. The model allows to simulate the time-concentration courses of pravastatin in various tissues and to calculate the pharmacokinetic parameters for pravastatin. Furthermore, the model was applied to investigate the effects of genotypes of the enzymatic transporters and hepatic and renal impairment on the pharmacokinetics of pravastatin. Thus, key questions such as, how pravastatin therapy would be affected in renal or hepatic disease, as well as how pravastatin therapy should be adapted based on genotypes, find an answer in this work.

German

Hypercholesterolemie, d.h. ein erhöhter Cholesterinspiegel im Plasma, ist ein wichtiger Risikofaktor für Herz-Kreislauf-Erkrankungen, die weltweit die häufigste Todesursache darstellen. Hypercholesterolemie kann mit Statinen behandelt werden, einer Medikamentenklasse, die die HMG-CoA-Reduktase hemmt, ein wichtiges Enzym bei der Cholesterinsynthese.

Pravastatin ist ein Statin, das zur Senkung des Gesamtcholesterinspiegels und des LDL-Cholesterins, und zur Erhöhung des HDL-Cholesterins bei Patienten mit Hypercholesterolemie eingesetzt wird. Pravastatin wird aus dem Dünndarm über den Transporter OATP2B1 aufgenommen und anschließend in der Leber über OATP1B1 transportiert, von wo aus es über den enzymatischen Exporter MRP2 in die Galle exportiert werden kann. Pravastatin kann entweder mit dem Urin über die Nieren oder aufgrund unvollständiger Resorption über die Fekalien ausgeschieden werden. Leber- und Nierenfunktionsstörungen können einen großen Einfluss auf die Pharmakokinetik von Statinen haben, ebenso wie genetische Varianten der Transporter OATP2B1, OATP1B1 und MRP2.

Im Rahmen dieser Arbeit wurde die Pharmakokinetik von Pravastatin durch die Entwicklung eines physiologischbasierten Pharmakokinetikmodells auf der Grundlage einer umfangreichen Datenkuratorierung von Pravastatindaten analysiert. Das Modell ermöglicht es, die Zeit-Konzentrations-Verläufe von Pravastatin in verschiedenen Geweben zu simulieren und die pharmakokinetischen Parameter für Pravastatin zu berechnen. Darüber hinaus wurde das Modell angewandt, um die Auswirkungen von Genotypen der enzymatischen Transporter sowie von Leber- und Nierenfunktionsstörungen auf die Pharmakokinetik von Pravastatin zu untersuchen. Somit werden in dieser Arbeit wichtige Fragen beantwortet, z.B. wie die Pravastatinbehandlung bei Nieren- oder Lebererkrankungen beeinflusst wird und wie die Pravastatinbehandlung auf der Grundlage eines Genotyps angepasst werden sollte.

1 Introduction

1.1 Pravastatin

Statins are a class of competitive inhibitors of 3-Hydroxy-3-Methylglutaryl Coenzyme A Reductase (HMG-CoA reductase), an important rate-limiting enzyme in cholesterol biosynthesis, which are applied to lower plasma cholesterol levels. Pravastatin (IUPAC name: (3R,5R)-7-[(1S,2S,6S,8S,-8aR)-6-hydroxy-2-methyl-8-[(2S)-2-methylbutanoyl]oxy-1,2,6,7,8,8a-hexahydronaphthalen-1-yl]-3,5-dihydroxyheptanoic acid, see figure 1) is an anionic, hepatoselective, hydrophilic statin which reduces total cholesterol, Low-density Lipoprotein Cholesterol (LDL-C) and triglyceride levels, and increases High-density Lipoprotein Cholesterol (HDL-C) in patients with hypercholesterolemia [67, 55].

Pravastatin is water-soluble and unstable under aqueous acidic conditions. In the stomach it is transformed to isomers and their lactonised compounds, amongst them 3'-alpha-isopravastatin (SQ31906) and 3'-alpha-5'-beta-6'-beta-trihydroxypravastatin (SQ31945) [29, 55].

Pravastatin has unique properties compared to other statins (e.g. simvastatin or lovastatin) [11] such as enzyme affinity, metabolic properties and chemical stability [44].

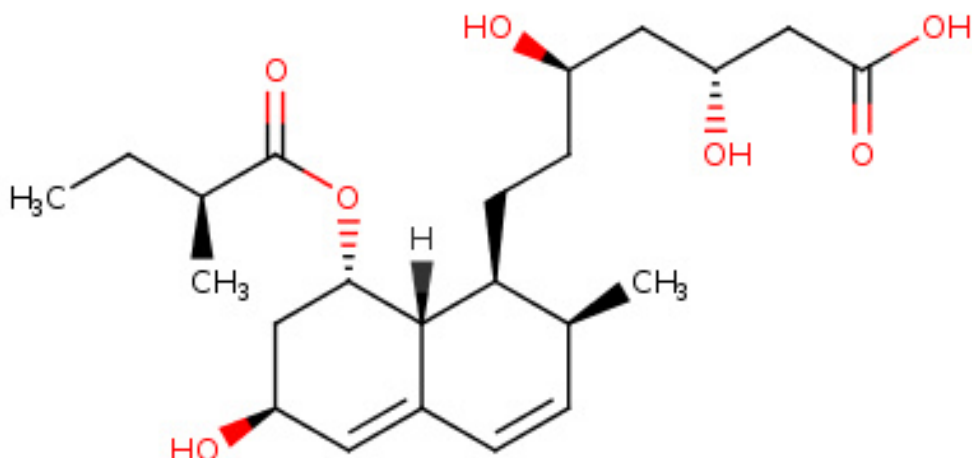


Figure 1: Structure of pravastatin; CHEBI:63618; inchikey: TUZYXOIXSAXUGO-PZAWKZKUSA-N

Due to its high hydrophilicity and its low lipophilicity, high uptake of pravastatin exists in the liver but not other tissues [11] resulting in a high hepatoselective distribution [11]. The transport into the liver is actively carried out by Organic Anionic Transport Polypeptide 1B1, OATP1B1 [11] and export from the liver in the bile via Multidrug Resistance-Associated Protein 2, MRP2. These transporters will be further discussed in section 1.5).

Pravastatin is well-tolerated in short and long-term therapy and presents only mild clinical adverse effects, such as headache, dizziness, skin rash, gastrointestinal as well as flu-like symptoms, indicating that it has relatively low toxicity [74, 44, 59].

1.2 Pravastatin pharmacokinetics

The pharmacokinetics of a drug describe the changes of the drug concentration in the body after its administration due to Absorption, Distribution, Metabolism and Elimination (ADME) [9]. An overview of the processes involved in the pharmacokinetics of pravastatin is provided in figure 2 with the involved processes presented below.

Absorption Pravastatin shows a strong first-pass effect, i.e., after oral application a smaller amount of the drug reaches the systemic circulation than after an intravenous application. After

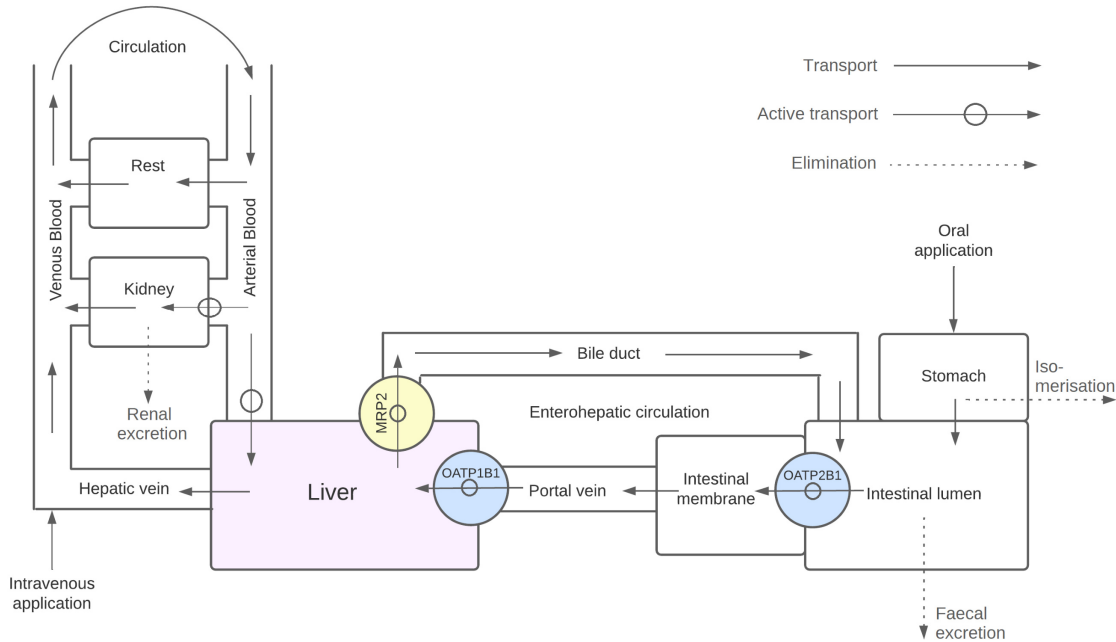


Figure 2: Overview of pravastatin pharmacokinetics, adapted from [11]. Pravastatin is transported through the body via the systemic circulation. After oral intake pravastatin passes through the stomach, where it is partly degraded into its metabolites via isomerisation. The unaltered fraction of pravastatin is subsequently transported into the intestine, where it is actively absorbed by OATP2B1 (see section 1.5.2) from the intestinal lumen via the intestinal membrane in the blood. From here it is transported via the portal vein to the liver, where it is actively imported by OATP1B1 (see section 1.5.1) into the liver. From the liver pravastatin is excreted into the bile by MRP2 (see section 1.5.3), where it undergoes enterohepatic circulation, i.e., it is transported back to the intestine. The available pravastatin is reduced via isomerisation in the stomach, excretion of unabsorbed amounts in the faeces, or renal excretion via the kidneys.

oral administration the fraction absorbed is 34%, and approximately 70% of it undergoes first-pass effect [17].

Pravastatin is unstable under aqueous acidic conditions. Therefore, after oral application part of it degrades within the gastric acid, due to its biochemical instability. This leads to the drug's oral bioavailability to be low, as radiolabelled studies have reported “oral absorption and bioavailability values of 34% and 17%, respectively” [58, 17]. Singhvi *et al.* reported that pravastatin has an absolute bioavailability of 18% and an absorption time of 2.4 hours, based on urinary excretion data [67].

A substantial fraction of pravastatin has been demonstrated to be transformed in the stomach via non-enzymatic isomerisation. Two major pravastatin metabolites are SQ31906 and SQ31945. In particular, 23.7% of the biotransformation profile of pravastatin is accounted for by SQ31906 [7, 17].

The unaltered fraction of an oral dose of pravastatin is only partly, yet rapidly absorbed by the upper part of the small intestine, whereas the remaining fraction of the unabsorbed drug is excreted into faeces [11] further contributing to the first-pass effect [58, 67].

As mentioned above, absorption of pravastatin occurs in the small intestine. Organic anion transport polypeptides (OATP) are transporters which catalyse the transfer of organic compounds across the cell membrane, and are of major importance in the uptake of pravastatin. The isoform OATP2B1 (encoded by gene SLC02B1), expressed at the apical membrane of enterocytes, facilitates the absorption of pravastatin from the intestinal lumen into the enterocytes of the intestine [29, 65]. From the intestinal cells pravastatin is exported via the basolateral membrane in the blood stream. OATP2B1 will be further discussed in section 1.5.2.

Metabolism After absorption pravastatin reaches the liver via the portal vein where it is taken up into the hepatocytes via OATP1B1 [29]. OATP1B1 will be further discussed in section 1.5.1.

In contrast to the other statins, such as simvastatin, lovastatin and atorvastatin, which are extensively metabolised in the liver by Cytochrome P450 (otherwise known as CYP enzymes), pravastatin only shows minor metabolism. The affinity for pravastatin for CYP enzymes is comparatively low [25]. Minor to no metabolism of pravastatin via the isoform CYP2C9 has been reported [19, 39, 76, 48, 79].

Pravastatin shows enterohepatic circulation. Enterohepatic circulation refers to the process in which a substance, after uptake in the liver, is secreted into the bile and subsequently released back into the intestinal lumen. In the intestine, the substance can either become reabsorbed and be transported back to the liver, or it can be excreted into faeces. Pravastatin is excreted from the hepatocyte's apical membrane into the bile via the outflow transporter multidrug resistance-associated protein 2 (MRP2) [79] from where it is transported back to the intestine via enterohepatic circulation. MRP2 will be further discussed in section 1.5.3.

Elimination Pravastatin is eliminated from the body via the urine and the faeces. One of pravastatin's major pharmacokinetic characteristics is its dual routes of elimination, i.e., renal and hepatic pathways [11].

Multiple studies corroborate that pravastatin is rapidly eliminated. For instance, an experiment by *Singhvi et al.* showed that within 12 hours of pravastatin administration over 80% of excretion could be traced in urine after oral or intravenous applications [67].

In addition, *Pan et al.* carried out a 96-hour-experiment in which oral and intravenous radiolabelled doses were given to healthy and hypercholesterolaemic patients. After an oral dose 71% and 20% of the radioactivity were recovered in faeces and urine, respectively, for intravenous doses 34% and 60% in faeces and urine, respectively [56].

Pharmacokinetic parameters Pharmacokinetic parameters are used to measure the changes that a drug undergoes in the body and are calculated mainly from plasma and urinary time courses. For instance, the terminal elimination half-life of a drug is defined as the time required for plasma concentrations of a drug to be reduced by 50% [4]. Pravastatin is rapidly eliminated from the body because its half-life is relatively short. *Pan et al.* reported half-lives of pravastatin in healthy volunteers and patients with hypercholesterolaemia between 1.3 and 2.6 hours, independently of whether the doses were administered in a single or repeated manner [56].

The protein-binding of pravastatin is low compared to other statins which are strongly bound to plasma proteins. After oral and intravenous routes of administration, the binding of total radioactivity to plasma proteins ranged between 43% and 48% [58, 67]. According to *Sigurbjörnsson et al.*, approximately 57% of pravastatin and 46% of SQ31906 bind to plasma proteins, independently of time or dose [66].

The Area Under the Curve (AUC) is the area under the concentration time curve of a drug after its administration. For instance, AUC is useful to determine if two forms of application, i.e., oral or intravenous, differ from one another in plasma exposure. For instance, *Singhvi et al.* report AUC values of 66.2 ± 32.1 ng·hr/ml for pravastatin, after providing a single, 20 mg dose in form of an oral solution [67]. In contrast, when applying a single, 10 mg intravenous dose of pravastatin, the AUC value is 171.2 ± 28.7 ng·hr/ml [67]. The oral dose is twice the intravenous dose, since oral absorption of pravastatin is reported to be less than 50% [67]. The differences between oral and intravenous application are evident in this study, showing that the AUC value after pravastatin intravenous administration is approximately 2.58-fold higher than the AUC after oral application of pravastatin.

Maximum concentration (c_{\max}) describes the peak concentration achieved by a drug in a specific body compartment, such as plasma. Multiple studies report similar c_{\max} values after a single, oral dosing of 40 mg pravastatin with values ranging from approximately 65 ng/ml to 70 ng/ml [39, 55, 38]. In contrast, *Becquemont et al.* reported a mean c_{\max} value of 91 ng/ml, with ranges from 72 ng/ml to 200 ng/ml [3].

The elimination rate constant determines the rate at which a substance becomes eliminated from the body. Multiple studies reported elimination rates for pravastatin [29, 39, 38, 10] with typical values being $k_{el} = 0.560$ 1/hr [39] and $k_{el} = 0.513$ 1/hr [38].

The clearance describes the ability of the body to excrete a drug [4]. Renal clearance refers to the process in which a drug is excreted by the kidneys. *Halstenson et al.* conducted a study in which patients with various renal function received a single 20 mg oral dose of pravastatin. The patients were categorised in four groups: Group 1 for normal renal function, group 2 for mild renal failure, group 3 for moderate renal failure and group 4 for severe renal failure. Total and renal pravastatin clearances for each group were measured. *Halstenson et al.*'s study reports a total pravastatin clearance of 265.86 ± 156.50 l/h for healthy subjects (group 1) [10]. For this same study, renal clearance Cl_{renal} values were reported for each group. For renal clearance, group 1 the reported value was 25.86 ± 9.24 l/h [10]. The corresponding values for the groups exhibiting renal dysfunction are provided in subsection 1.4.1. Hepatic clearance can be calculated as $Cl_{hepatic} = Cl_{total} - Cl_{renal}$ under the assumption that no other tissues besides liver and kidney are involved in the elimination of pravastatin. For healthy subjects this resulted in a hepatic clearance of pravastatin of 240.00 l/h. The total, renal and hepatic clearance values for the renal impairment groups are provided in section 1.4.

The volume of distribution is a virtual volume which describes the tendency of a drug to either circulate freely in the plasma or to distribute to other tissue compartments or bind to plasma proteins [43]. Pravastatin is a highly hydrophilic, hepatoselective inhibitor distributed mainly in hepatocytes [11]. Non-hepatic cells such as umbilical vascular endothelial cells, retinal pigment epithelial cells, cornea fibroblasts, granulosa cells or cerebrospinal fluid do not absorb pravastatin [11]. In addition, plasma protein binding is low compared to other statins. Consequently, pravastatin presents a relatively low volume of distribution at steady-state of 0.46 l/kg [58, 67, 11].

1.3 Pravastatin pharmacodynamics

Pharmacodynamics is defined as the body's response to a drug [5].

The main pharmacodynamic effect of pravastatin is to inhibit the activity of HMG-CoA reductase, the rate-limiting enzyme for cholesterol-biosynthesis. Pravastatin therapy results in reduced plasma concentrations of total and LDL-cholesterol, as well as lower triglyceride levels and an increase in HDL-cholesterol in patients with hypercholesterolaemia [44].

Pravastatin is a strong inhibitor of HMG-CoA reductase activity. The pravastatin metabolites SQ31906 and SQ31945 have 2.5% to 10% potency of the parent's drug for HMG-CoA reductase inhibition [1].

At a daily dose of 40 mg, pravastatin plasma LDL-cholesterol levels are reduced by 30-35% [44, 58]. In addition, plasma HDL-cholesterol levels were increased between 10% and 25%, whereas triglyceride levels were reduced between 10% and 25% [58].

Nakaya et al. conducted a study in which hypercholesterolaemic patients were divided into three groups and were provided with either 5 mg (group 1), 20 mg (group 2), or 40 mg (group 3) of pravastatin [46]. Total serum cholesterol was reduced by 11.1% in group 1, 18.8% in group 2 and 25.3% in group 3, the reduction being dose-dependent [46]. For LDL-cholesterol, group 1 showed a reduction of 16.6%, group 2 of 29.1%, and group 3 of 38.5% [46]. For HDL-cholesterol, group 1 showed an increase of 7.2%, group 2 of 4.9% and group 3 of 11.8% [46].

1.4 Hepatic and renal impairment

Both the liver and the kidneys are important in the elimination of pravastatin. Consequently, hepatic functional impairment, as well as renal functional impairment could have important effects on pravastatin pharmacokinetics.

1.4.1 Renal impairment

Chronic Kidney Disease (CKD) is an illness which results in progressive renal function failure. Kidney function can be measured using Glomerular Filtration Rate (GFR) and Creatinine Clearance (ClCr), which is an approximation of GFR [64]. For patients with normal renal function, the GFR amounts to 90 ml/min/1.73m² or higher, whereas in patients with various degrees of kidney failure the GFR is significantly decreased [10].

Halstenson et al.'s study reports a total pravastatin clearance of 265.86 ± 156.50 l/h for healthy subjects (group 1) [10]. With increased renal impairment pravastatin clearance is reduced: For

group 2 pravastatin clearance was $15.21 \pm 5.38 \text{ l/h}$, $6.23 \pm 1.49 \text{ l/h}$ for group 3 and $2.87 \pm 0.86 \text{ l/h}$ for group 4 [10]. These results are in agreement with the different degrees of renal impairment: the lower the renal function, the lower the renal clearance of pravastatin. Furthermore, their study reported fractions of pravastatin recovered in urine after 24 hours for the different groups, i.e., for group 1 the urinary fraction recovered was $12.3 \pm 7.70\%$, $8.2 \pm 9.8\%$ for group 2, $4.1 \pm 2.3\%$ for group 3 and $0.8 \pm 0.5\%$ for group 4. This data will be used for fitting and comparing the urinary data to our model's simulation in section 3.5.

Additionally, the study reported non-significant alterations in pravastatin's pharmacokinetic parameters AUC, c_{\max} , t_{half} and V_d for dysfunctional kidneys [10].

1.4.2 Hepatic impairment

Hepatic impairment describes insufficient liver function, which can be caused by liver injury or liver disease. Most advanced liver diseases result in cirrhosis, e.g. chronic hepatitis C virus infection or Non-Alcoholic Fatty Liver Disease (NAFLD). Cirrhosis comprises degeneration of healthy liver parenchyma and necrosis of hepatocytes (resulting in subsequent scarring of the liver) in combination with distortion of the hepatic vasculature [62]. This distortion subsequently shifts the portal and arterial blood supply into the outflow hepatic vein, thus interfering in the exchange between hepatic capillaries and hepatocytes, thus leading to reduction of liver perfusion and development of portal hypertension, as well as end-stage liver disease [62]. Due to the portal hypertension and changes in hepatic vasculature hepatic shunts can form which bypass part of the liver perfusion around the organ.

The Child-Turcotte Pugh (CTP) scoring system is an indicator for the severity of cirrhosis. Class A indicates good hepatic function, whereas class B demonstrates moderate hepatic function and lastly class C signals hepatic dysfunction [75].

An important clinical question is to understand the effects of cirrhosis on the pharmacokinetics of statins, as they may vary and present challenges when treating patients with accompanying liver disease [79]. Hepatic impairment can exhibit a decrease in clearance of a drug, as well as an impact on plasma protein binding, thus altering elimination and distribution mechanisms [77]. Despite the importance of liver impairment for the elimination of pravastatin, almost no pharmacokinetics data have been reported in advanced liver disease. One exception is in patients with cirrhosis, in which pravastatin showed an 1.34-fold increase in c_{\max} and a 1.52-fold-increase in AUC [79]. An interesting observation in this context is that in patients with liver dysfunction, pravastatin's elimination via the kidneys increases, thus partly compensating for its reduced hepatic clearance [58]. To our knowledge, no clinical trial exists which systematically evaluates the effect of liver disease on pravastatin therapy and pharmacokinetics.

1.5 Genotypes and genetic variants

Genotypes of transporters and metabolic enzymes can have a large effect on the pharmacokinetics of drugs. For pravastatin, the genetic variants of the transporters OATP2B1, OATP1B1 and MRP2 are of interest.

OATPs facilitate the transfer of organic compounds across the cell membrane and are important in the uptake of pravastatin. They contribute to the initial phase of elimination via the liver, as they assist in hepatic absorption of endogenous drugs from the portal vein [71, 54]. Organic Anionic Transport Polypeptides belong to the superfamily of membrane solute carriers (SLC), and are encoded by gene Solute Carrier Organic Anion Transporter (SLCO), a subfamily of influx transporters within the SLC superfamily [63]. OATP2B1 and OATP1B1 are two important isoforms which facilitate the transport for various substrates, for instance, in the intestine and the liver.

Most genetic variants of these transporters are due to Single Nucleotide Polymorphisms (also known as SNP or 'snip'). An SNP occurs when a single nucleotide at a certain position within the DNA sequence of the gene encoding the enzyme is altered. These changes can result in changes in enzyme activity, consequently altering transport via these enzymes.

Various SNPs have been reported in SLCO genes, which code for OATP [23]. Due to an SNP in the SLCO gene, the function of an OATP may become reduced, enhanced or it may

remain unchanged. For example, an SNP in SLCO1B1*5 diminishes the activity of OATP1B1 to actively transfer pravastatin from the portal circulation into the liver. This leads to increased plasma concentrations of pravastatin and thus may conclude to a higher risk of pravastatin-induced myopathy [52]. The following subsections provide an overview over reported SNPs on the respective transporters and their activities.

1.5.1 OATP1B1

Organic anionic transport polypeptide 1B1 is expressed by gene SLCO1B1 at the basolateral membrane of hepatocytes [29]. As one of its substrates, pravastatin is actively transported through the hepatocyte's membrane via OATP1B1. This mechanism is considered as the rate-limiting step in hepatic clearance of pravastatin [12, 29].

In SLCO1B1, differences exist for SNPs and allele frequencies between different ethnicities. Notably, *Kivistö et al.* reported that 2-5% of the general population exhibit "markedly elevated plasma pravastatin concentrations due to the SLCO1B1 polymorphism" [29]. For instance, in approximately 40% of Europeans, as well as in circa 80% of Sub-Saharan African and East Asians, the frequency of the 388AG (Asn130Asp) SNP proves to be very similar. However, comparatively, the frequency of the 521TC (Val174Ala) SNP appears to be not as prevailing (approx. 2%) in the Sub-Saharan population, compared to the estimate of 10-20% allelic frequency within the European and East Asian community [23]. In turn, the allelic frequency of 521TC in the European-American population comprises about 15%, whereas in African-Americans the frequency remains at roughly 1% [12]. The following haplotypes are relevant for the understanding of the impact on OATP1B1 and thus, on the pharmacokinetics of pravastatin, namely SLCO1B1*1a, which is the reference sequence, *1b, *5, *15, *16 and *17 [54, 73, 52, 51, 23]. Table 1 provides an overview of the effects that these SNPs may have on OATP1B1 and the pharmacokinetics of pravastatin. The 521TC SNP (rs4149056) is of considerable interest for the pharmacokinetics and pharmacodynamics of not only pravastatin, but various other drugs [63, 78]. This particular SNP entails an amino acid change, from valine to alanine, at position 174 in the protein. Thereby, the structure and function of the protein are altered, and the transport rate of OATP1B1 decreases, thus lowering uptake of pravastatin into the hepatocyte. Additionally, the 388AG SNP (rs2306283) is frequently observed alongside the 512TC SNP, as it has been discovered that these two SNPs comprise four different haplotypes: (388A - 521T) comprises the reference sequence *1a, (388G - 521T) *1b, (388A - 521C) *5 and (388G - 521C) *15 [78]. The carriers of these SNPs exhibit elevated pravastatin plasma concentrations (up to 100% higher than non-carriers), significantly higher mean AUC values compared to carriers of *1a or *1b, and decreased OATP1B1-regulated absorption into hepatocytes [12, 29]. To underline the impaired function of OATP1B1 due to the 521TC SNP, *Kameyama et al.* analysed Human Embryonic Kidney cells (HEK293) expressing alleles *5, *15 or *15 +1007CG. The results demonstrated that v_{max} , as well as v_{max}/K_m were significantly reduced compared to the reference sequence *1a [24, 63]. *Ho et al.* showed that the 521TC SNP was related to increased pravastatin $AUC_{(0-5)}$ and increased c_{max} values, emphasising that European-American individuals presented significantly higher values than those of African-Americans [12]. European-Americans displayed total $AUC_{(0-5)}$ values of 98.3 ± 60.7 ng·h/ml and total c_{max} values of 53.3 ± 33.3 ng/ml, whereas the total $AUC_{(0-5)}$ values for African-American patients were of 69.5 ± 56.3 ng·h/ml and 37.4 ± 29.2 ng/ml [12]. Moreover, heterozygous carriers of SLCO1B1*1a/*15 presented 45-80% higher $AUC_{(0-5)}$ values than homozygous *1a and *1b carriers, respectively [12]. Furthermore, homozygous carriers of SLCO1B1*15 exhibited an increase of 92-149% in $AUC_{(0-5)}$ compared to homozygous carriers of *1a and *1b, respectively [12].

The SLCO1B1*17 haplotype contains the following SNPs: -11187GA, 388AG and 521TC [50]. Carriers of this particular haplotype and its respective SNPs have previously been related to increased pravastatin plasma concentrations as well as increased AUC values [50]. This suggests an impaired function of OATP1B1, which reduces the uptake of pravastatin into the hepatocytes [50, 63]. Because of the decreased absorption of pravastatin, the inhibitory activity of the lipid-lowering agent on HMG-CoA reductase becomes limited, thus affecting the pharmacodynamics of pravastatin.

Table 1: Genetic variants of SLCO1B1. Shown in this table are genes, alleles, protein polymorphisms, SNPs or haplotypes, as well as the possible effects on the pharmacokinetics of pravastatin. N.R. stands for 'Not Reported'.

Gene	Allele	Protein polymorphism	SNP or haplotype	Effect
SLCO1B1	*1a	Reference sequence	Reference sequence	Normal function [60, 45]
SLCO1B1	*1b	Asn130Asp	388AG	Normal function, increased relative bioavailability for homozygotes and carriers of Asn130Asp + Val174Ala, reduced AUC compared to *1a [16, 45, 60]
SLCO1B1	*5	Val174Ala	521TC	Potential risk of myopathy, increased c_{max} and AUC compared to wildtype [52, 49]
SLCO1B1	*15	Asn130Asp Val174Ala	388AG 521TC	Small inhibitory activity of pravastatin on cholesterol biosynthesis, reduced transport activity, increased plasma AUC [61]
SLCO1B1	*16	Val174Ala	521TC	N.R.
SLCO1B1	*17	Val174Ala	-11187GA 521TC 388GA	Impaired absorption of pravastatin, reduced inhibitory activity of pravastatin on HMG-CoA reductase and cholesterol synthesis, elevated plasma pravastatin concentration levels [63, 50]

1.5.2 OATP2B1

Much less information is available about OATP2B1 than OATP1B1. This enzyme is commonly expressed at the apical membrane of enterocytes [29, 65]. OATP2B1 is responsible for the absorption of pravastatin into the enterocytes within the intestinal lumen [30, 53].

Upon studying the kinetics of pravastatin absorption, *Kobayashi et al.* observed a pH-dependent pravastatin OATP2B1 uptake, stating that the absorption rate of pravastatin proves higher at a more acidic pH-value (pH=5.0) and lower at a more basic pH-value (pH=7.4) [30]. *Nozawa et al.* propose that, at an acidic pH, pravastatin is transported "with a K_m value of the order of millimolar concentrations", reported as 2.25 mM at pH=5.0 for OATP2B1 [53]. This is further supported by K_m and v_{max} values of 2.25 ± 0.94 mM and 41.6 ± 6.4 nmol/mg·protein/10min, respectively, implying that OATP2B1 expansively selects endogenous substrates, such as pravastatin, at a more acidic pH-value [53].

Despite the suggestion regarding the engagement of a carrier-mediated transport mechanism [72], and the pH-susceptible absorption of pravastatin via OATP2B1 [53, 30], the intestinal uptake of pravastatin via OATP2B1 requires further clarification.

Whereas the SNPs of OATP1B1 have been studied thoroughly, the available information on SNPs and the effects these SNPs have on OATP2B1 activity and the pharmacokinetics of pravastatin is very limited (see table 2). SLCO2B1*2 and *3 haplotypes and their allelic frequencies

were studied in Japanese volunteers [54, 71]. The effects of these haplotypes were investigated on estrone-3-sulfate, another SLCO2B1 substrate. Although the SLCO2B1*2 haplotype was not found in the Japanese volunteers, it was nonetheless discovered that the value for the maximal velocity v_{max} of the SLCO2B1*3 haplotype was 50% lower than that of the reference sequence [63]. However, since the analysed substrate was not pravastatin, these genetic variants warrant further investigation for pravastatin pharmacokinetics.

Table 2: Genetic variants of SLCO2B1. Shown in this table are genes, alleles, protein polymorphisms, SNPs or haplotypes, as well as the possible effects on the pharmacokinetics of pravastatin. N.R. stands for ‘Not Reported’.

Gene	Allele	Protein polymorphism	SNP or haplotype	Effect
SLCO2B1	*1	Reference sequence	Reference sequence	N.R.
SLCO2B1	*2	p.Thr392Ile	1175CT	N.R.
SLCO2B1	*3	p.Ser486Phe	1457CT	50% lower v_{max} than v_{max} of wildtype [52]

1.5.3 MRP2

Multidrug resistance-associated protein 2 is an ATP Binding Cassette efflux transporter of the ABC superfamily, which in turn belongs to the human ABCC subfamily [21]. MRP2 is encoded by ATP Binding Cassette C2 (ABCC2) and it is expressed in the apical membrane of polarised cells, such as hepatocytes, as well as the kidney’s proximal tubule, and enterocytes (in the duodenum and jejunum, respectively) [29]. In the context of pravastatin, MRP2 functions as an efflux transporter exporting pravastatin from hepatocyte into the bile. MRP2 excretes hepatic pravastatin with a K_m value of $7.2 \pm 0.8 \mu\text{M}$, a maximum velocity of v_{max} of $39.1 \pm 1.0 \text{ nmol/min/mg}$ as well and an intrinsic clearance of v_{max}/K_m of 5.4 (dimensionless) as determined in human *in vitro* [6].

A deficiency in MRP2 activity may induce hyperbilirubinaemia (Dubin-Johnson Syndrome), i.e., an abnormal increase of bilirubin in the blood, which leads to important alterations in the hepatic elimination of pravastatin as shown by knockdown of MRP2 in mouse [29, 54, 51]. In Kivistö *et al.*’s study, the role of MRP2 was characterised in the pharmacokinetics of orally and intravenously administered pravastatin in rodents. MRP2 Transport Deficient (TR-) rats were compared to rats with the MRP2 wildtype. It was discovered that the MRP2 TR- rats presented a 6.1-fold increase in AUC after oral application and a 4.7-fold increase in AUC after intravenous application compared to the wildtype mice. In addition, the total clearance in the TR- rats was 4.6-fold higher than the wildtype, and the renal clearance was 16.5-fold higher in the TR- rats compared to the wildtype [28].

A SNP in ABCC2 may result in alterations in the pharmacokinetics of pravastatin, as shown in table 3, e.g., reduced oral bioavailability, as well as diminished gastrointestinal uptake of pravastatin due to increased MRP2 expression in enterocytes [21]. For instance, the c.1446CG genotype affects mRNA MRP2 expression, which is 95%-100% higher compared to the c.1445CC genotype. This is brought in association with compensated biliary and renal excretion of pravastatin [29, 49]. Furthermore, the c.1446CG SNP reduces the mean AUC and c_{max} of pravastatin to approximately 70%, compared to the non-carriers of this SNP in particular [29]. Ho *et al.* argue that “neither ABCC2, ABCB11, nor ABCG2 genotypes are associated with differences in pravastatin pharmacokinetics”, so that the effect of SNPs on the statin’s pharmacokinetics are still debated and remain to be clarified [12].

Table 3: Genetic variants of ABCC2. Shown in this table are genes, the ABCC2 regions, the protein polymorphisms, the SNPs or haplotypes, as well as the possible effects on the pharmacokinetics of pravastatin.

Gene	ABCC2 region	Protein polymorphism	SNP or haplotype	Effect
ABCC2	Exon 10	Reference sequence	Reference sequence c.1446CC	N.R.
ABCC2	Exon 10	p.Thr482Thr	c.1446CG	Decreased AUC and C_{max} in ABCC2's heterozygous carriers (but non-carriers of SLCO1B1) [29]

1.6 Physiologically based pharmacokinetic model (PBPK)

A Physiologically-Based Pharmacokinetics model (PBPK) allows to study the pharmacokinetics of a given substance based on computational modelling [31, 32, 22]. Such models allow to predict the absorption, distribution, metabolism and elimination of a substance in the human body based on a system of Ordinary Differential Equation (ODEs). A PBPK model consists of various defined compartments, representing either different organs or tissues, which are connected to one another via blood flow. They consist, among other objects, of defined compartments, species, parameters and reactions. These models can be useful to understand how one entire system is affected by minor changes in components, for example, different haplotypes in transporters. PBPK models are especially useful in studying the effect of physiological changes or alterations in disease on the pharmacokinetics of drugs, e.g., various degrees of cirrhosis [31, 32].

1.7 Question, scope and hypotheses

Within this project the effects of hepatic and renal impairment and genetic variants (genotypes) of key proteins relevant for pravastatin pharmacokinetics and pharmacodynamics were studied by the means of computational modelling. Specifically, a PBPK model of pravastatin was developed to systematically analyse the following questions:

- (i) What are the effects of renal (renal insufficiency) and/or hepatic impairment (cirrhosis) on pravastatin pharmacokinetics?
- (ii) What is the effect of genetic variants of OATP2B1, OATP1B1 and MRP2 on pravastatin pharmacokinetics?

The main objective was to describe the influence of disease and of functional variability due to genotypes on pravastatin pharmacokinetics and apply the model to clinically relevant questions such as: How is pravastatin therapy affected in renal or hepatic disease? How should pravastatin therapy be adapted based on genotype (individualised therapy)?

2 Methods

To develop the PBPK-model of pravastatin various methods were applied. Data for model calibration and validation was curated from the literature (section 2.1), the model was constructed and simulated (section 2.2), model parameters were optimised using parameter fitting (section 2.3) and pharmacokinetics parameters were calculated from time-course data and time-course simulations (section 2.4).

2.1 Data curation

Data curation consisted of multiple steps. Based on extensive literature research, relevant publications were selected and prioritised for digitisation. For this thesis, literature relevant to the pharmacokinetics of pravastatin, as well as publications about specific genetic variants and impairment of hepatic and renal function were of particular interest. From the relevant studies information about the subjects and groups, the treatment, application and dose and the pharmacokinetics and/or pharmacodynamics of pravastatin was extracted.

Microsoft Excel was used to store the digitised data in a standardised format. Measurements of study participants, such as weight, height, sex, health status, ethnicity, body surface area and reported genotypes of enzymes such as OATP1B1, OATP2B1 and MRP2 were curated. Likewise, the information on interventions applied in each study, i.e., the duration of the treatment, whether pravastatin was administered orally or intravenously, the dosage and the application were extracted from the publications. Tables containing reported pharmacokinetic parameters, namely AUC, c_{\max} , t_{half} , V_d , or Cl , were also curated. Figures containing pravastatin plasma or serum concentrations were digitised using “PlotDigitizer”, a tool which allows to extract numerical data from diagrams.

The open pharmacokinetics database PK-DB(see <https://pk-db.com> [9]), containing curated data about experimental and clinical studies, was used for data curation. The curated pharmacokinetics studies of this work were examined by a second curator and uploaded to the database (see table 4).

2.2 Physiologically-based pharmacokinetics model (PBPK)

A PBPK model was developed to study the pharmacokinetics of pravastatin. The model allows to simulate the time-courses of pravastatin in various tissues and to calculate pharmacokinetics parameters for pravastatin. The model is described mathematically via a system of coupled ordinary differential equations (ODEs) which can be numerically solved by an ODE solver. The model was developed using the Systems Biology Markup Language (SBML), a format for describing computational models of biological processes, based on XML [13, 26]. For this work, SBML Level 3 Version 2 was used [14]. The model was developed in Python using the package sbmlutils [34], which in turn enables to program SBML models. The ODE simulation of the model was performed using sbmlsim [33], which is based on the high-performance SBML-simulator libroadrunner [69]. Model visualisation was performed using cy3sbml [37, 35].

The PBPK-model was based on an existing template of a whole-body model for the absorption, distribution, metabolism and elimination of substances in the human body. Within this work the model was adapted for pravastatin and tissue models of the intestine, kidney and liver for pravastatin were developed. The tissue models were coupled to the whole-body model using the SBML hierarchical model composition [68]. Tissue and whole-body models are available in SBML. For simulation, the hierarchical model was flattened to a single SBML model. The detailed description of the developed models are available in section 3.2.

The individual models (intestine, liver and kidney), as well as the final whole-body model are available as SBML from <https://github.com/matthiaskoenig/pravastatin-model> [36].

2.3 Parameter fitting

Parameter fitting is an optimisation method which allows to adapt parameters $\vec{p}=(p_1, \dots, p_n)$ in a given model so that the distance between model predictions and experimental data is minimised.

Model parameters were adjusted by minimising the residuals r between model prediction $f(x_{i,k})$ and experimental data $y_{i,k}$ using an objective cost function F .

SciPy's least_square method was used as cost function F which depends on the parameters \vec{p} and adheres to a L2-norm which corresponds to the sum of weighted residuals, as described by the following equation 1:

$$F(\vec{p}) = \frac{1}{2} \sum_{i,k} (w_k \cdot w_{i,k} \cdot r_{i,k})^2 \quad (1)$$

where:

w_k describes the weighting factor of time course k ,

$w_{i,k}$ describes the weighting of the respective data point i over time k based on the error of the data point, and

$r_{i,k} = (y_{i,k} - f(x_{i,k}))$ represents the residue of time i over time k .

2.4 Pravastatin pharmacokinetic parameters

A brief description of the pharmacokinetic parameters of pravastatin is provided in section 1.2. These parameters are of importance for the understanding and evaluation of the plasma concentration time-courses presented in the results (section 3.4). The following formulas were used for calculation.

Maximum concentration, c_{\max} [μM] c_{\max} is the peak serum or plasma concentration by pravastatin. It is calculated by finding the maximal concentration value in the time-course.

Elimination rate, k_{el} [1/min] k_{el} is a measure for the elimination of a substance. The elimination rate is calculated assuming an exponential decrease of a substance following equation 2:

$$C_{\text{pra}}(t) = C_{\text{pra}}(0) \cdot e^{-k_{el} \cdot t} \quad (2)$$

Based on the experimental data a linear regression is performed in logarithmic space to calculate k_{el} .

Area Under the Curve, AUC [mg·hr/ml] AUC describes the area under the concentration time curve. This parameter can be calculated via the trapezoidal rule following equation 3:

$$AUC_{0 \rightarrow t_n} = \frac{1}{2} \sum_{i=1}^{n-1} (t_{i+1} - t_i) \cdot (C_i - C_{i+1}) \quad (3)$$

The AUC between the last measured time point t_{last} and infinity can be calculated via the following equation 4:

$$AUC_{t_{\text{last}} \rightarrow \infty} = \frac{C_{\text{last}}}{k_{el}} \quad (4)$$

$AUC_{0 \rightarrow \infty}$ describes the AUC extrapolated to infinity, and can be calculated via equation 5:

$$AUC_{\text{tot}} = AUC_{0 \rightarrow t_n} + AUC_{t_{\text{last}} \rightarrow \infty} \quad (5)$$

Volume of distribution, V_d [l] V_d is a virtual compartment which describes the tendency of a drug to either circulate in plasma or to disperse to other tissue compartments. This parameter can be calculated via the following equation 6:

$$V_d = AUC \cdot k_{el} \quad (6)$$

Clearance, Cl [ml/min] Clearance describes the ability of the body to excrete a drug. This parameter is calculated by multiplying the rate of elimination k_{el} with the volume of distribution V_d , as described by equation 7:

$$Cl = k_{el} \cdot V_d \quad (7)$$

Half life, t_{half} [min] t_{half} is defined by the time required for serum or plasma concentration of pravastatin to be reduced by 50%. This parameter can be calculated from the rate of elimination k_{el} via equation 8:

$$t_{half} = \frac{\ln(2)}{k_{el}} \quad (8)$$

Bioavailability, F [%] Bioavailability refers to the fraction of a drug which reaches the systemic circulation when comparing an oral dose with an intravenous dose. The bioavailability can be calculated from the AUC of an oral and a respective intravenous dose via equation 9:

$$F = \frac{AUC_{po}}{AUC_{iv}} \cdot \frac{dose_{iv}}{dose_{po}} \quad (9)$$

Where po stands for the oral application and iv stands for the intravenous application of pravastatin.

Renal clearance, Cl_{Renal} [l/min] Renal clearance describes the process in which a drug is excreted by the kidneys. This parameter can be calculated by dividing the amount of pravastatin recovered in urine over a given time by the AUC in plasma over the same period, i.e., via the following equation 10:

$$Cl_{Renal} = \frac{AR_{\Delta t}}{AUC_{\Delta t}} \quad (10)$$

Where AR is the amount of pravastatin recovered in urine from time 0 to time Δt hours [10].

Hepatic clearance, $Cl_{Hepatic}$ [l/min] Hepatic clearance describes the process in which a drug is eliminated by the liver. This parameter can be calculated by subtracting the renal clearance from the total clearance via the following equation 11:

$$Cl_{Hepatic} = Cl_{total} - Cl_{Renal} \quad (11)$$

3 Results

Within this thesis a physiologically-based model of pravastatin was developed to study the role of hepatic or renal impairment and genotypes on the pharmacokinetics of pravastatin. Within this chapter the following results are presented: the curated data on pravastatin clinical studies (Section 3.1), the development of individual tissue models which in turn constitute the whole body model of pravastatin (section 3.2) how the model was fitted (section 3.3), and how the model performed in predicting the pharmacokinetics of pravastatin using simulation experiments (section 3.4). The resulting model was applied to study how hepatic impairment, renal impairment and genotypes can influence the pharmacokinetics of pravastatin (section 3.5).

3.1 Pravastatin data

Articles were selected for data curation based on literature research for publications containing data on time-courses and pharmacokinetics of pravastatin. These articles provided the data basis for the development of the model. Table 4 provides an overview of the studies curated within this thesis, containing information on the applied dosing protocols, routes of administration, health status of the study participants, genotype variants and a brief description of the study. Every study is labelled with the corresponding PK-DB identifier, which allows direct access to the data. Overall, fifteen studies were curated [3, 10, 12, 39, 38, 42, 45, 51, 49, 52, 55, 56, 57, 66, 67]. In addition, four existing studies from PK-DB containing pravastatin data were used for model simulations [20, 27, 47, 70]. All data was made available as open data.

Table 4: Overview of data used for modelling. Most of the data sets were curated in the project with a subset of data used for parameter fitting.

Reference	PK-DB ID	PMD	Dosing protocol	Route of administration	Health Status	Genotype variants	Curated	Study description
Becquemont1999 [3]	PKDB00540	10226769	pravastatin: 40mg	oral	healthy	-	✓	Investigation of the effects of mibepradil on pravastatin pharmacokinetics.
Halstenson1992 [10]	PKDB00541	1613121	pravastatin: 20mg	oral	healthy and various degrees of renal impairment	-	✓	Evaluation of effect of renal impairment on the pharmacokinetics of pravastatin.
Ho2007 [12]	PKDB00544	17622941	pravastatin: 40mg	oral	healthy	OATP1B1, *5 (521TC)	✓	Evaluation of the effects of polymorphisms in OATP1B1, MRP2, BSEP and BCRP on pravastatin pharmacokinetics.
Jacobson2004 [20]	PKDB00364	15518608	pravastatin: 40mg	oral	healthy	-	-	Comparison between the pharmacokinetic interaction of pravastatin and simvastatin with other substances.
Keskitalo2009 [27]	PKDB00510	19842935	pravastatin: 40mg	oral	healthy	-	-	Investigations of the ABCG2 c.421CA genotype on the pharmacokinetics of pravastatin and other statins.
Kyrklund2003a [39]	PKDB00545	12811363	pravastatin: 40mg	oral	healthy	-	✓	Study of the effects of gemfibrozil on the pharmacokinetics of pravastatin.
Kyrklund2004 [38]	PKDB00547	14748817	pravastatin: 40mg	oral	healthy	-	✓	Investigation of the effect of rifampicin on the pharmacokinetics of pravastatin.
Maeda2006 [42]	PKDB00548	16678545	pravastatin: 10mg	oral	healthy	OATP1B1 *1a/*1a; *1b/*1b; *1a/*15, *1b/*15	✓	Investigation of genetic polymorphism of OATP1B1 on the pharmacokinetics of pravastatin.
Mwinyi2004 [45]	PKDB00549	15116054	pravastatin: 40mg	oral	healthy	OATP1B1 *1a, *1b (388AG), *5 (521TC)	✓	Comparison of the effects of OATP1B1 *1a, *1b and *5 haplotypes on the pharmacokinetics of pravastatin.

Table 4: Overview of the curated studies. This data was applied for the model's parameter fitting.

Reference	PK-DB ID	PMID	Dosing protocol	Routes of administration	Health Status	Genotype variants	Curated	Study description
Neuvonen1998 [47]	PKDB00372	9542477	pravastatin: 40mg	oral	healthy	-	-	Investigation of possible interactions of itraconazole with simvastatin and pravastatin.
Niemi2004 [51]	PKDB00550	15226675	pravastatin: 40mg	oral	healthy	OATP1B1, *5 (52[TC]), -1187GA, *15b, *17	✓	Characterisation of possible relationships between SNPs in OATP1B1 (SLCO1B1), OATP2B1 (SLCO2B1), MRP2 (ABCC2) and MDR1 (ABCB1) and the pharmacokinetics of pravastatin.
Niemi2006 [49]	PKDB00551	17047488	pravastatin: 40mg	oral	healthy	MRP2, 1446CG; OATP1B1 *17	✓	Investigation of possible effects of sequence variations in ABCC2 (coding for MRP2) on pravastatin pharmacokinetics.
Nishizato2003 [52]	PKDB00554	12811365	pravastatin: 40mg	oral	healthy	OATP1B1*1b/*1b; *1b/*15; *15/*15	✓	Investigation of the effects of OATP1B1 polymorphisms on the pharmacokinetics of pravastatin.
Pan1990 [55]	PKDB00542	2116260	pravastatin: 5mg, 10mg, 20mg	oral	primary hypercholesterolaemia healthy	-	✓	Evaluation of pharmacodynamics and safety of pravastatin.
Pan1990a [56]	PKDB00543	2125605	pravastatin: 20mg, 40mg	oral	-	-	✓	Investigation of the oral bioavailability of pravastatin and lovastatin.
Pan1993a [57]	PKDB00552	8219432	pravastatin: 20mg	oral	healthy	-	✓	Assessment of the effect of age on the pharmacokinetics of pravastatin in men and women.
Sigurbjörnsson1998 [66]	PKDB00546	9625267	pravastatin: 20mg, 40mg	oral	primary, moderate hypercholesterolaemia healthy	-	✓	Analysis of pravastatin pharmacokinetics in middle-aged and elderly subjects
Singhvi1990 [67]	PKDB00553	2106337	pravastatin: 9.9mg (iv), 19.2mg (po)	intravenous and oral	-	-	✓	Study to assess the pharmacokinetics of pravastatin after an intravenous and an oral dose of [¹⁴ C]-pravastatin sodium.
Sugimoto2001 [70]	PKDB00359	11753267	pravastatin: 40mg	oral	healthy	-	-	Study of possible interactions of itraconazole with simvastatin and pravastatin.

3.2 Computational model of pravastatin

3.2.1 Physiologically based pharmacokinetic model (PBPK)

Within this work a PBPK model was developed to study the pharmacokinetics of pravastatin. The model allows to simulate the time-courses of pravastatin in plasma and various tissues (e.g. liver, bile, urine) and to calculate pharmacokinetic parameters for pravastatin, based on plasma concentrations and urinary amounts. The model was constructed in a hierarchical manner consisting of a whole-body model coupled to tissue models of the intestine, kidney and liver. In the following subsections, each of the individual tissue models, i.e., intestinal model (section 3.2.2), liver model (section 3.2.4) and kidney model (section 3.2.3) are presented, followed by a more detailed explanation of how the whole-body model was constructed and how it performed (section 3.2.5). The overview of the whole-body model of pravastatin and the tissue models is given in figure 3.

3.2.2 Intestinal model

After oral administration and subsequent passage through the stomach, pravastatin becomes rapidly absorbed by the upper part of the small intestine. In the intestinal model, pravastatin is either actively transported by OATP2B1 from the intestinal lumen via the enterocytes into the blood stream or is excreted into faeces (unabsorbed fraction).

The fraction of the pravastatin residing in the intestinal lumen, which subsequently becomes absorbed, is defined by the parameter F_{pra_abs} (see equation 13). The remaining pravastatin which is not absorbed is excreted into the faeces. Thus, the percentage of the excreted pravastatin can be calculated by subtracting the entirety of the dose minus the absorbed fraction, as seen in equation 14.

The irreversible uptake of pravastatin via OATP2B1 in $\frac{mmol}{min}$ is modelled via Michaelis-Menten kinetics with the key parameters for the pravastatin absorption being $PRAABS_Vmax$ and $PRAABS_Km$, as seen in equation 12.

$$absorption = \frac{PRAABS_V_{max} \cdot Vgu \cdot [pra_lumen]}{([pra_lumen] + PRAABS_K_m)} \quad (12)$$

$PRAABS_Vmax$ is the maximal velocity with which pravastatin is absorbed into the liver, Vgu is the volume compartment in the intestine, $[pra_lumen]$ represents the pravastatin concentration in the intestinal lumen and $PRAABS_Km$ defines the enzyme-substrate affinity between pravastatin and OATP2B1.

To model the effect of genotypes of OATP2B1 on the absorption of pravastatin, the parameter $F_OATP2B1$ was introduced. The fraction absorbed by OATP2B1, expressed in $\frac{mmol}{min}$, is therefore defined as:

$$absorption_{pra} = f_OATP2B1 \cdot F_{pra_abs} \cdot absorption \quad (13)$$

Where absorption follows by equation 12, F_{pra_abs} determines the fraction of pravastatin absorbed in every round of the enterohepatic circulation, and $f_OATP2B1$ allows to modify OATP2B1 enzyme function. $f_OATP2B1$ was varied from 0.1 to 1.9 to systematically study the effects of changes in OATP2B1 activity due to genetic variants with 1.0 describing normal activity, values < 1.0 reduced activity, and values > 1.0 increased activity.

The fraction excreted into faeces in $\frac{mmol}{min}$, follows as:

$$excretion_{pra} = (1 - F_{pra_abs}) \cdot absorption \quad (14)$$

With the parameters being analogous to the parameters in equation 13.

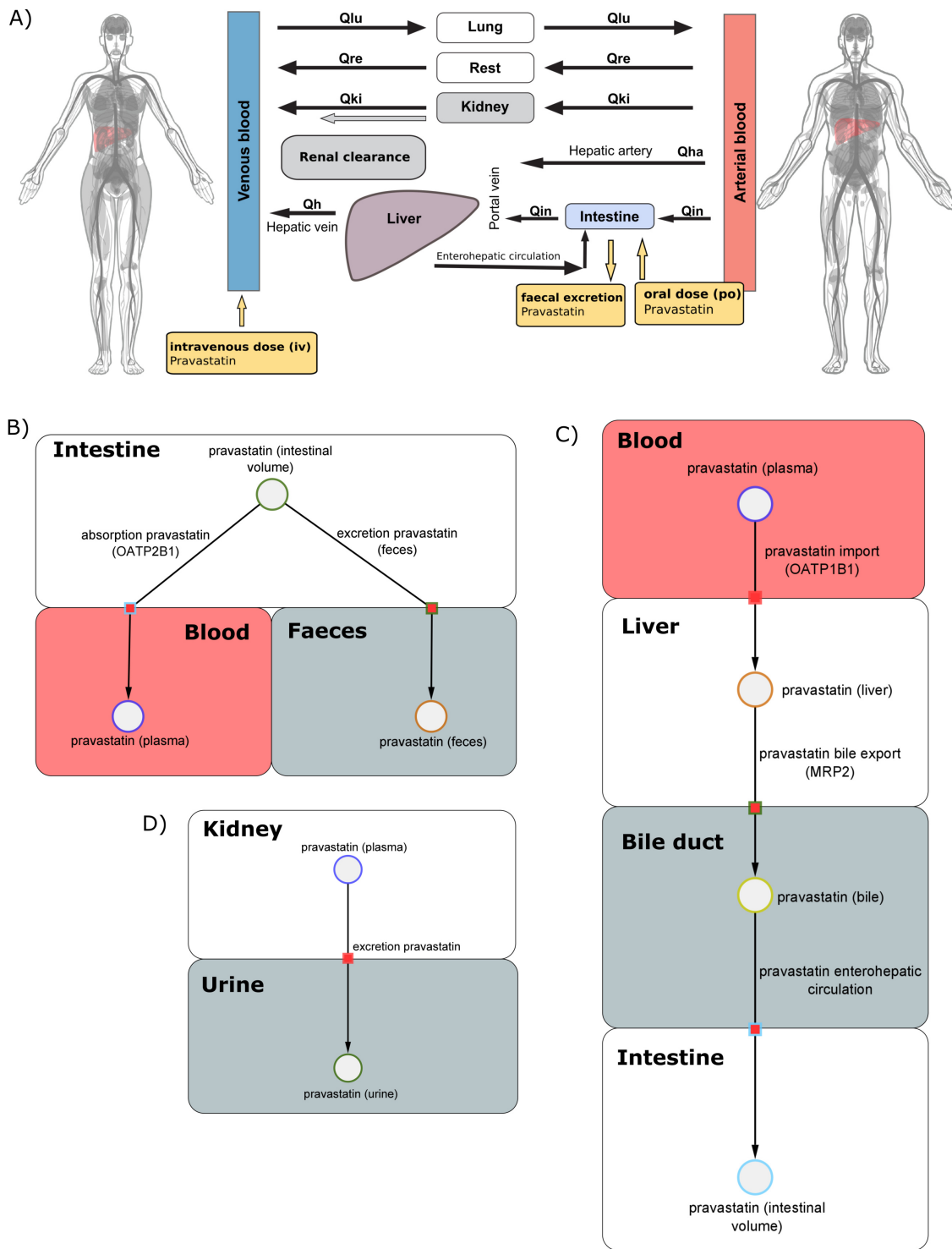


Figure 3: A) Overview body model of pravastatin. The systemic circulation connects arterial and venous blood. Pravastatin is transported via Qre, Qki, Qha and Qin flow from the arterial blood in the various body tissues. Blood leaving these tissues reaches the venous blood. Qki passes through the liver, where pravastatin is excreted by the kidneys into urine. When administered orally, pravastatin is dissolved and isomerised into its metabolites in the stomach. Once it reaches the intestine, it can either become directly excreted into the faeces, or it can undergo absorption by the intestine, and be transported into the liver via the portal vein. From there, pravastatin can either be transported into the venous blood through the hepatic vein or it can be exported into the bile, where it will pass through the enterohepatic circulation and reach the intestine anew.

Figure 3: (Continued) When applied intravenously pravastatin is injected into venous blood, where it will become distributed through the lung (Qlu) into the arterial blood. B) Intestinal model. Pravastatin is absorbed by OATP2B1 and subsequently excreted in the plasma from the enterocytes. C) Liver model. Pravastatin is taken up by hepatocyte via OATP1B1, where it inhibits the HMG-CoA reductase. Subsequently, pravastatin is excreted into the bile via MRP2. Pravastatin is transported via the enterohepatic circulation back to the intestinal lumen for either reabsorption or elimination into faeces. D) Kidney model. Pravastatin is eliminated from the kidney and is excreted into urine.

3.2.3 Kidney model

The kidney model describes the renal elimination of pravastatin in the urine by the kidneys. The excretion of pravastatin into urine in $\frac{mmol}{min}$ was modelled via mass-action kinetics by equation 15.

$$excretion = f_renal_function \cdot PRAEX_k \cdot Vki \cdot [pra_ext] \quad (15)$$

`f_renal_function` was varied from 0.1 to 1.9 to systematically study the effects of changes in renal function, with 1.0 describing normal kidney function, values < 1.0 reduced kidney function, and values > 1.0 increased kidney function. `PRAEX_k` is the rate constant describing the urinary excretion rate of pravastatin and its metabolites, `Vki` is the volume of the kidney and `[pra_ext]` the pravastatin concentration in plasma.

3.2.4 Liver model

The liver model describes the irreversible hepatic uptake of pravastatin via OATP1B1 and subsequent elimination of pravastatin in the bile via MRP2. Pravastatin enters the hepatocyte via OATP1B1 and is assumed not to be metabolised by the liver (minimal metabolism via CYP enzymes). Hepatic pravastatin can inhibit the HMG-CoA reductase in the liver (not modelled) and is subsequently exported from the apical membrane of the hepatic cell into the bile via MRP2. Once in the bile, pravastatin passes through the enterohepatic circulation and re-enters the intestine, where it can become either reabsorbed or excreted into faeces.

An important factor for the import of pravastatin into the liver is the activity of OATP1B1, since this enzyme is responsible for the active uptake of pravastatin into the hepatocytes. Analogous to OATP2B1, OATP1B1 can contain SNPs which alter the enzyme's activity. The parameter `f_OATP1B1` was varied from 0.1 to 1.9 to systematically change the OATP1B1 activity thereby allowing to simulate the effect of genetic variants.

The import of pravastatin into the liver in $\frac{mmol}{min}$ is defined by equation 16:

$$import_{pra} = f_OATP1B1 \cdot \frac{PRAIM_V_{max} \cdot Vli \cdot [pra_ext]}{([pra_ext] + PRAIM_K_m_pra)} \quad (16)$$

`f_OATP1B1` shows reduced enzyme function with values less than 1.0, and displays increased enzyme function with values greater than 1.0 (with 1.0 as reference enzyme function). `Vli` describes the volume of the liver, and `[pra_ext]` represents the pravastatin concentration in the hepatic plasma. `PRAIM_Km_pra` and `PRAIM_Vmax` are the affinity of OATP1B1 for pravastatin and the maximal velocity, respectively.

The export of pravastatin into the bile in $\frac{mmol}{min}$ is defined by equation 17:

$$export_{pra} = f_MRP2 \cdot \frac{PRAEX_V_{max} \cdot Vli \cdot [pra]}{([pra] + PRAEX_K_m_pra)} \quad (17)$$

`f_MRP2` shows reduced enzyme function with values less than 1.0 and displays increased enzyme function with values greater than 1.0 (with 1.0 as reference enzyme function). `Vli` describes the volume of the liver, and `[pra]` represents the pravastatin concentration in the liver. `PRAEX_Km_pra`, and `PRAEX_Vmax` are the affinity of OATP1B1 for pravastatin and the maximal velocity, respectively.

The enterohepatic circulation in $\frac{mmol}{min}$ was modelled via an irreversible transport of pravastatin via mass-action kinetics from the bile into the intestinal lumen, as seen in equation 18:

$$EHC_{\text{pra}} = PRAEH C_k \cdot Vli \cdot pra_bi \quad (18)$$

Where Vli describes the volume of the liver, $PRAEH C_k$ describes the rate with which pravastatin is transported within the enterohepatic circulation and pra_bi describes the pravastatin amount in the bile.

3.2.5 Whole-body model

The developed tissue models of the intestine, liver and kidney were coupled with a whole-body model for distribution of pravastatin via the systemic circulation. The whole-body model transports pravastatin via the blood to the various tissues. In addition, pravastatin can reach the intestine from the liver via the bile via the enterohepatic circulation. Figure 4 illustrates how tissues and compartments are connected via blood flow in the systemic circulation, i.e., venous blood flow and arterial blood flow, so that pravastatin is able to be distributed to various bodily tissues and ultimately to its site of action, the liver. This overview also provides information on the different routes pravastatin can take through the body, depending on whether administered orally or intravenously, and the various routes with which pravastatin can be excreted (see figure 2 for a high level description).

Table 5 provides an overview of the main parameters of the PBPK model. The individual models (intestine, liver and kidney), as well as the final whole-body model are available as SBML at <https://github.com/mattthiaskoenig/pravastatin-model> [36].

3.2.6 Model of cirrhosis and renal impairment

Hepatic impairment (cirrhosis) Liver cirrhosis entails both intrahepatic shunts of the total liver blood supply and hepatic tissue loss, as previously explained in section 1.4.2. Due to these physiological changes, a major fraction of pravastatin cannot reach the liver and the liver has a reduced effective volume for the elimination of pravastatin. As a consequence, the pharmacokinetics of pravastatin could be affected. To represent the impairment of the liver due to cirrhosis the model for cirrhosis established by *Köller et al.* was used [31, 32].

The fraction of blood being shunted around the liver is described via the parameter f_shunts ranging from 0.0 to 0.9 with 0.0 corresponding to no shunting and 0.9 to 90% shunting. The remaining blood reaching the liver is defined as $1 - f_shunts$.

In addition to the intrahepatic shunts, a cirrhotic liver is characterised by loss of functional tissue volume. The parameter f_tissue_loss was introduced ranging from 0.0 to 0.9 with 0.0 corresponding to no tissue loss due to cirrhosis and 0.9 to 90% tissue loss.

The parameter $f_cirrhosis$ is composed of both, f_shunts and f_tissue_loss changed in lockstep, and ranges from 0.0 to 0.9, where 0.0 represents a healthy liver with perfect hepatic function (no shunts, no tissue loss) and 0.9 describes a severely cirrhotic liver with greatly impaired hepatic function (90% shunts, 90% tissue loss).

Modifying this parameter allows to reproduce various degrees of hepatic function, so that substantial differences in the pharmacokinetics of pravastatin between healthy patients and patients with cirrhosis can be identified in the scans shown in section 3.5. The values used for the parameter $f_cirrhosis$ in all hepatic scans were 0.00 for the control group, 0.39 for mild cirrhosis (CTP A), 0.69 for moderate cirrhosis (CTP B) and 0.81 for severe cirrhosis (CTP C).

Renal impairment Renal impairment was simulated via the parameter $KI_f_renal_function$ ranging from 0.1 to 1.9, and modifying the capability of the kidney to excrete pravastatin in the urine. The parameter values for mild, moderate and severe renal impairment were calculated by dividing the creatinine clearance of the groups with renal impairment by the creatinine clearance in healthy subjects as reported in the study by *Halstenson et al.* [10]. Thus, the values used for $KI_f_renal_function$ were 1.00 for the control group, 0.69 for mild renal impairment, 0.32 for moderate renal impairment and 0.19 for severe renal impairment.

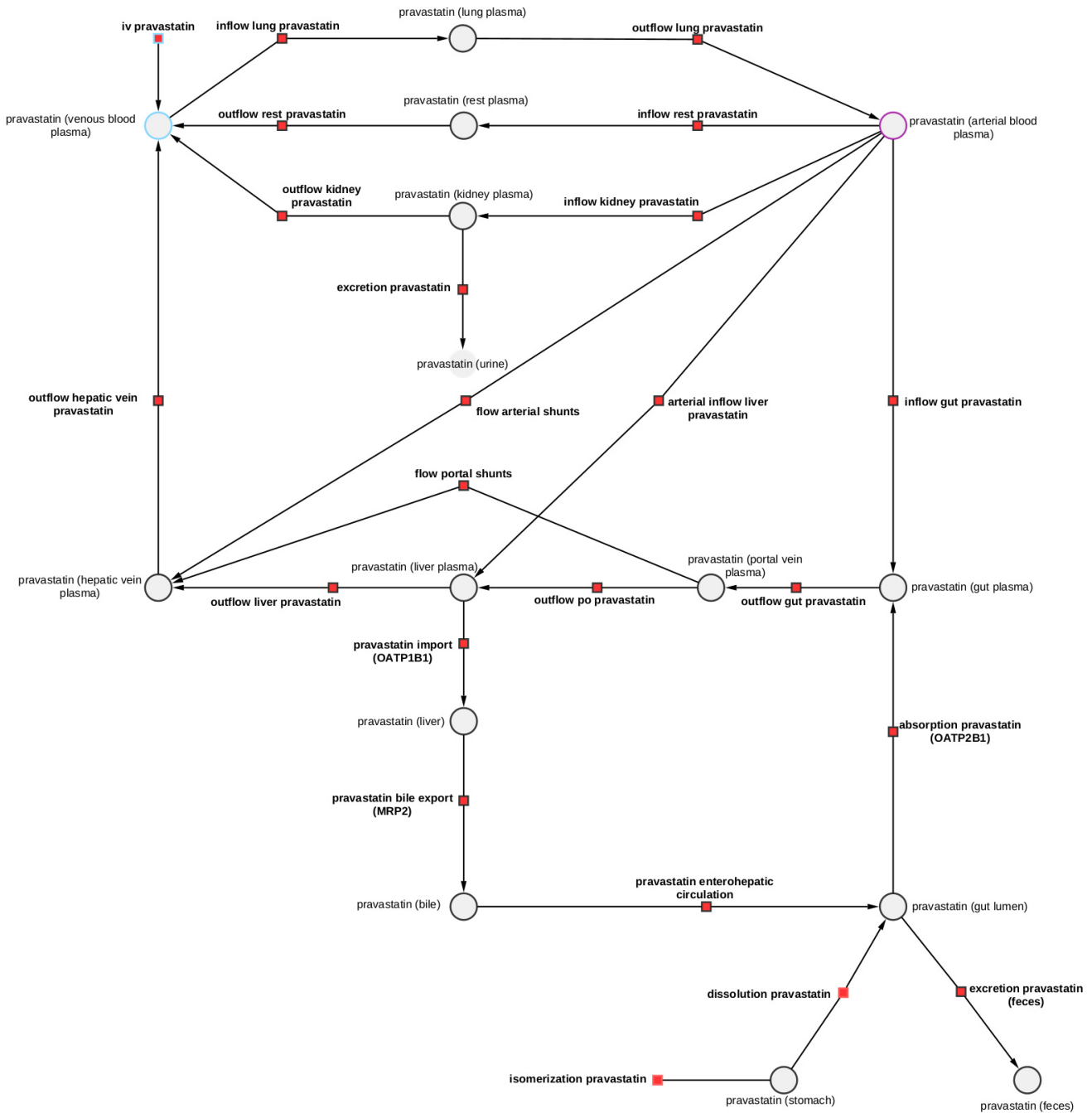


Figure 4: Overview of the whole-body model. Here, the individual tissue models are coupled to the whole-body model by hierarchical composition. For a more detailed visualisation of how pravastatin can be distributed throughout the body, see figure 3.

Table 5: Overview of the main parameters for the PBPK model. The parameter, as well as a brief description thereof, its value and unit are displayed in this table. The scan parameters were used for running the parameter scans in section 3.5. Prefixes GU, LI, and KI correspond to intestinal, liver and kidney model, respectively.

Parameter	Description	Scan	Value	Unit
KI_f_renal_function	parameter for kidney function	✓	1 [0.1, 1.9]	-
f_cirrhosis	parameter for severity of cirrhosis	✓	0 [0, 0.9]	-
LI_f_OATP1B1	parameter for OATP1B1 activity	✓	1 [0.1, 1.9]	-
LI_f_MRP2	parameter for MRP2 activity	✓	1 [0.1, 1.9]	-
GU_f_OATP2B1	parameter for OATP2B1 activity	✓	1 [0.1, 1.9]	-
f_lumen	fraction lumen of intestine	-	0.9	-
BW	body weight	-	75	kg
HEIGHT	body height	-	170	cm
HR	heart rate	-	70	$\frac{1}{min}$
HRrest	heart rate while resting	-	70	$\frac{1}{min}$
COBW	cardiac Output per body weight	-	1.548	$\frac{ml}{s \cdot kg}$
COHRI	increase of cardiac output per heartbeat	-	150	ml
HCT	hematocrite	-	0.51	-
FVgu	gut fractional tissue volume	-	0.0171	$\frac{l}{kg}$
FVki	kidney fractional tissue volume	-	0.0044	$\frac{l}{kg}$
FVli	liver fractional tissue volume	-	0.0021	$\frac{l}{kg}$
FVlu	lung fractional tissue volume	-	0.0076	$\frac{l}{kg}$
FVve	venous fractional tissue volume	-	0.0514	$\frac{l}{kg}$
FVar	arterial fractional tissue volume	-	0.0257	$\frac{l}{kg}$
FVpo	portal fractional tissue volume	-	0.001	$\frac{l}{kg}$
FVhv	hepatic venous fractional tissue volume	-	0.001	$\frac{l}{kg}$
FQgu	gut fractional tissue blood flow	-	0.18	-
FQki	kidney fractional tissue blood flow	-	0.19	-
FQh	hepatic fractional tissue blood flow	-	0.215	-
FQlu	lung fractional tissue blood flow	-	1	-
Mr_pra	Molecular weight pravastatin	-	424.53	$\frac{g}{mol}$
ti_pra	injection time pravastatin	-	10	s
Ri_pra	rate of infusion pravastatin	-	0	$\frac{mg}{min}$
Ka_dis_pra	dissolution pravastatin	-	0.6042	$\frac{l}{h}$
F_iso_pra	fraction isomerised pravastatin	-	0.5	-
KI_PRAEX_k	rate urinary excretion pravastatin metabolites	-	1.4037	$\frac{1}{min}$
LI_PRAIM_Vmax	V_{max} for pravastatin import via OATP1B1	-	0.6077	$\frac{mmol}{min \cdot l}$
LI_PRAEX_Vmax	V_{max} for pravastatin export via MRP2	-	0.0414	$\frac{mmol}{min \cdot l}$
LI_PRAEX_Km_pra	K_m for pravastatin export via MRP2	-	0.01	$\frac{mmol}{min \cdot l}$
LI_PRAEHC_k	rate of pravastatin enterohepatic circulation	-	0.2884	$\frac{l}{min}$
GU_F_pra_abs	fraction absorbed pravastatin	-	0.95	-
GU_PRAABS_Vmax	V_{max} for pravastatin absorption via OATP2B1	-	0.0253	$\frac{mmol}{min \cdot l}$
GU_PRAABS_Km	K_m for pravastatin absorption via OATP2B1	-	0.01	$\frac{mmol}{min \cdot l}$

3.3 Parameter fitting

Plasma, serum and urine pravastatin time-course data (table 7) was used from the curated studies to fit a subset of model parameters (table 6). Table 4 provides information of individual study protocols with additional information on the application and doses. With the exception of *Singhvi et al.*'s study, in which an intravenous dose of pravastatin was applied, all studies administered pravastatin orally. All curated plasma, serum and urine pravastatin were used for parameter fitting with exception of data from *Sigurbjörnsson et al.* from single subjects which showed very large residuals when included in parameter fitting [66] (the data was excluded from the fit).

Table 6: Parameters fitted in the model. Overview of the parameters, as well as a brief description thereof, optimal values rounded to their fourth digit, its upper and lower bounds and unit.

Parameter	Description	Optimal value	Lower bound	Upper bound	Unit
Ka_dis_pra	dissolution rate of pravastatin	0.6042	0.1	10	$\frac{1}{h}$
GU__PRAABS_Vmax	V_{max} for pravastatin absorption via OATP2B1	0.0253	1E-3	1E3	$\frac{mmol \cdot l}{min}$
LI__PRAIM_Vmax	V_{max} for pravastatin import via OATP1B1	0.6077	1E-3	1E3	$\frac{mmol \cdot l}{min}$
LI__PRAEX_Vmax	V_{max} for pravastatin export via MRP2	0.0414	1E-3	1E3	$\frac{mmol \cdot l}{min}$
LI__PRAEHC_k	rate of pravastatin enterohepatic circulation	0.2884	1E-3	1E3	$\frac{l}{(min)}$
KI__PRAEX_k	rate of urinary excretion pravastatin	1.4037	1E-1	1E5	$\frac{1}{min}$

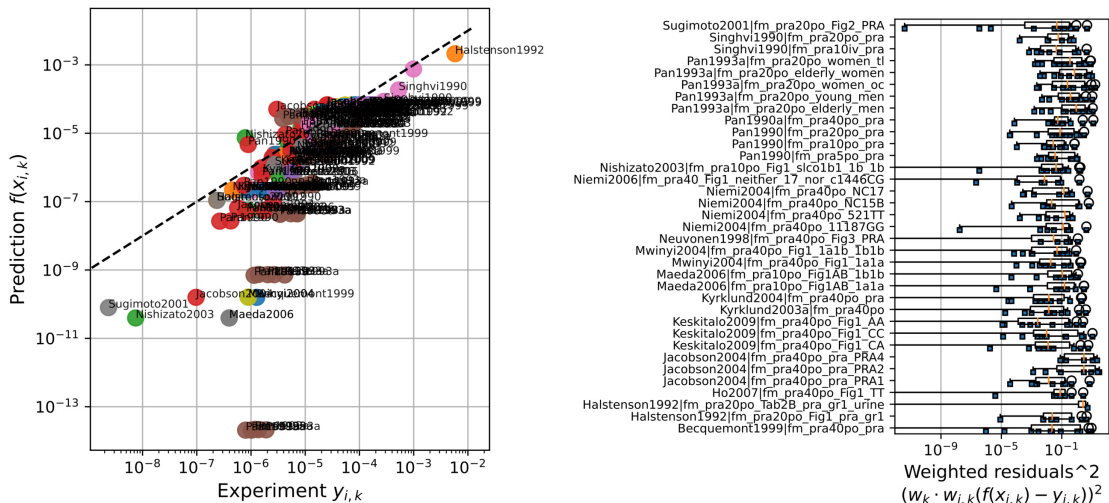


Figure 5: Results of parameter fitting. The panel on the left shows the goodness-of-fit plot between model prediction and experimental data for the resulting optimal parameters. The panel on the right shows the weighted residuals of the optimal parameter fit for the data used in parameter fitting (table 6).

Figure 5 shows an overview over the results of parameter fitting consisting of goodness-of-fit plot and residuals. Parameter fitting improved the agreement between data and model predictions with the final model showing a good agreement between experimental data and model predictions, i.e., with the exception of some outliers, e.g. Jacobson2004, Maeda2006, Mwinyi2004, Nishizato2003, Pan1993a and Sugimoto2001 for low plasma concentrations.

Table 7: Data used in parameter fitting. Overview of the application route, applied pravastatin dose, the application form in which the drug was provided, the tissue in which pravastatin was measured, and the identifier of the fit data. The fitted parameters are found in table 6

Study	Application	Dose [mg]	Form	Tissue	Fit ID
Becquemont1999 [3]	Single dose	40	-	Plasma	<code>fm_pra40po_pra</code>
Halstenson1992 [10]	Single dose	20	-	Urine	<code>fm_pra20po_Fig1_pra_gr1_urine</code>
				Serum	<code>fm_pra20po_Tab2B_pra_gr1</code>
Ho2007 [12]	Single dose	40	-	Plasma	<code>fm_pra40po_Fig1_TT</code>
Jacobson2004 [20]	Single dose	40	-	Serum	<code>fm_pra40po_pra_PRA1</code> <code>fm_pra40po_pra_PRA2</code> <code>fm_pra40po_pra_PRA4</code>
Keskitalo2009 [27]	Single dose	40	-	Plasma	<code>fm_pra40po_Fig1_CA</code> <code>fm_pra40po_Fig1_CC</code> <code>fm_pra40po_Fig1_AA</code>
				Plasma	<code>fm_pra40po_Fig1_CA</code> <code>fm_pra40po_Fig1_CC</code> <code>fm_pra40po_Fig1_AA</code>
				Plasma	<code>fm_pra40po_Fig1_CA</code> <code>fm_pra40po_Fig1_CC</code> <code>fm_pra40po_Fig1_AA</code>
Kyrklund2003a [39]	Single dose	40	Tablet	Plasma	<code>fm_pra40po</code>
Kyrklund2004 [38]	Single dose	40	Tablet	Plasma	<code>fm_pra40po_pra</code>
Maeda2006 [42]	Single dose	10	-	Plasma	<code>fm_pra10po_Fig1AB_1a1a</code> <code>fm_pra10po_Fig1AB_1b1b</code>
Mwinyi2004 [45]	Single dose	40	-	Plasma	<code>fm_pra40po_Fig1_1a1a</code> <code>fm_pra40po_Fig1_1a1b_1b1b</code>
Neuvonen1998 [47]	Single dose	40	-	Serum	<code>fm_pra40po_Fig3_PRA</code>
Niemi2004 [51]	Single dose	40	Tablet	Plasma	<code>fm_pra40po_11187GG</code> <code>fm_pra40po_521TT</code> <code>fm_pra40po_NC15B</code> <code>fm_pra40po_NC17</code>
Niemi2006 [49]	Single dose	40	-	Plasma	<code>fm_pra40_Fig1_neither_17_nor_c1446CG</code>
Nishizato2003 [52]	Single dose	10	-	Serum	<code>fm_pra10po_Fig1_slco1b1_1b_1b</code>
Pan1990 [55]	Multiple dose	5	Tablet	Serum	<code>fm_pra5po_pra</code>
Pan1990 [55]	Multiple dose	10	Tablet	Serum	<code>fm_pra10po_pra</code>
Pan1990 [55]	Multiple dose	20	Tablet	Serum	<code>fm_pra20po_pra</code>
Pan1990a [56]	Multiple dose	40	Tablet	Serum	<code>fm_pra40po_pra</code>
Pan1993a [57]	Single dose	20	Tablet	Plasma	<code>fm_pra20po_elderly_men</code> <code>fm_pra20po_young_men</code> <code>fm_pra20po_women_oc</code> <code>fm_pra20po_elderly_women</code> <code>fm_pra20po_women_tl</code>
Singhvi1990 [67]	Single dose	20	-	Plasma	<code>fm_pra20po_pra</code>
Singhvi1990 [67]	Single dose	10	Solution	Plasma	<code>fm_pra10iv_pra</code>
Sugimoto2001 [70]	Single dose	20	-	Plasma	<code>fm_pra20po_Fig2_PRA</code>

3.4 Model performance

To evaluate the performance of the developed model, the model predictions were compared to data from multiple clinical studies under various dosing protocols. The following paragraphs present the simulations for plasma and serum pravastatin concentrations for single oral dose, multiple oral doses and single intravenous dose of pravastatin.

Every plot compares the simulated and the curated data for the respective time-courses. The

solid lines represent the prediction of the PBPK model of the plasma pravastatin concentrations over time, whereas the data points (with error bars if reported) and dotted lines correspond to the curated data. The legend in the upper right corner of the plot provides information about the name of the study, the number of subjects analysed for each study, denominated n , and the standard deviation (SD), as far as the curated data reported it.

3.4.1 Single oral dose

In the majority of the studies, pravastatin was administered as a single oral dose. In figure 6 we show a representative study to demonstrate the effect of single oral pravastatin application. The complete set of all time-course simulations is available in the supplement section 6 (see figures 24, 25, 26, 27, 28, 29, 30, 34, 33, 32, 35, 36, 37, 38, 39).

In *Kyrklund et al.*'s study in 2004 (figure 6), a single oral 40 mg dose of pravastatin was administered to ten healthy volunteers [38]. Over the course of 12 hours, pravastatin plasma concentrations were measured every 1 to 2 hours.

The simulation shows that pravastatin is rapidly absorbed by the intestine, demonstrated by the plasma concentration peak c_{\max} , which is reached after 1.5 hours. The elimination half-life t_{half} is approximately 2 hours. After eight hours almost the complete amount of pravastatin was eliminated from the plasma. Overall, the curated data and the predicted time-course simulation are in good agreement with one another. The large error bars can be attributed to the relatively low sample size in the study and the large intraindividual variability. Reported plasma concentration peaks are higher than the model predictions, but the overall dynamics after an oral pravastatin dose is captured very well by the model.

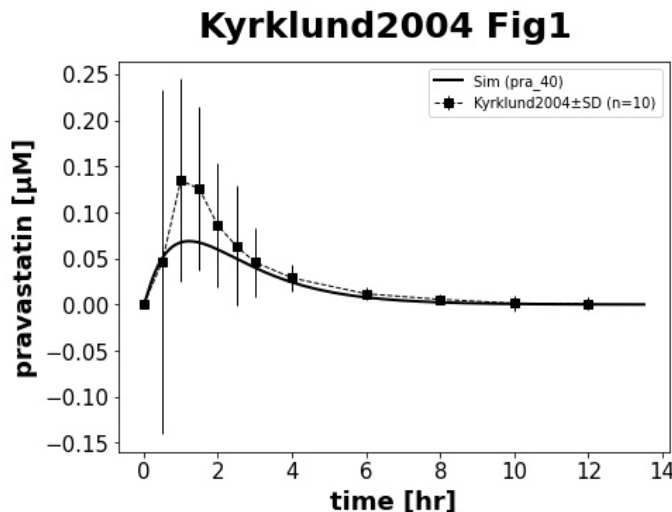


Figure 6: Simulation experiment Kyrklund2004 [38]. In this study, ten subjects were provided with a single 40mg oral dose of pravastatin. The dotted line represents the curated data, and the solid line is the time-course simulation predicted by the PBPK model.

3.4.2 Multiple oral dose

Next, model performance was evaluated for multiple oral pravastatin applications in two studies conducted by *Pan et al.*

The first study comprises twenty healthy subjects provided with multiple oral 40 mg doses of pravastatin. Pravastatin was administered once daily over the course of one week [56]. Figure 7 shows the comparison between the simulation and the curated study data on the last day. The simulation shows the multiple dosing in form of multiple concentration peaks every 24 hours, consistent with pravastatin being administered once daily. The curated data is only plotted once for the last application in line with the reported study protocol (i.e. pharmacokinetics was only

measured after the last application). The second study shows the simulation and data for thirty-three subjects with primary hypercholesterolaemia provided with multiple oral 5 mg, 10 mg and 20 mg doses of pravastatin [55]. Pravastatin was provided twice daily over the course of four weeks, as depicted in figure 8.

In both studies, and for all doses, pravastatin is rapidly absorbed and reaches its maximum concentration peak around 2 hours, and is completely eliminated in less than 12 hours. Simulation and data are in good agreement with each other for multiple dose applications under various doses ranging from 5 mg up to 40 mg daily. As with the single dose, the overall dynamics is captured very well by the model with peak concentrations being lower in the model predictions compared to the clinical data.

Pan1990a Fig2

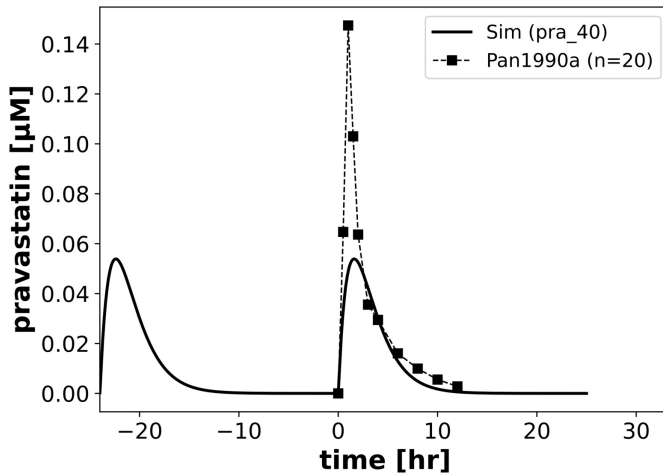


Figure 7: Simulation experiment Pan1990a [56]. Twenty healthy subjects were provided with a multiple oral dose of 40 mg pravastatin over the course of a week. The dotted line represents the curated study data and the solid line is the time-course simulation predicted by the PBPK-model.

Pan1990 Fig1

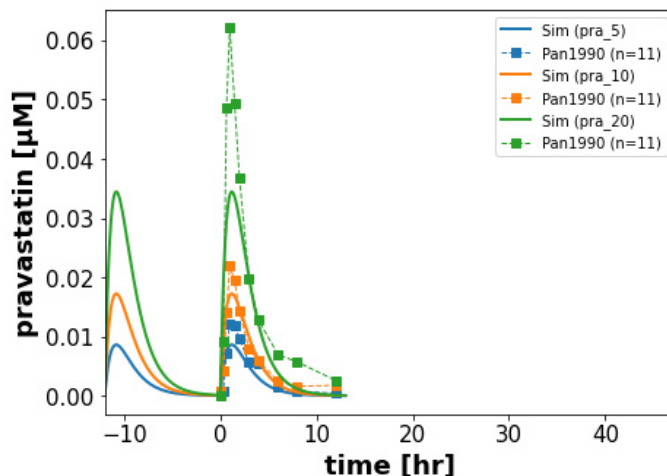


Figure 8: Simulation experiment Pan1990 [55]. Thirty-three subjects with primary hypercholesterolaemia were provided with multiple oral doses of 5 mg (blue), 10 mg (orange) and 20 mg (green) pravastatin over the course of four weeks. The dotted lines are the curated data and the solid lines are the model's prediction.

3.4.3 Intravenous dose

Next, oral and intravenous pravastatin application were compared.

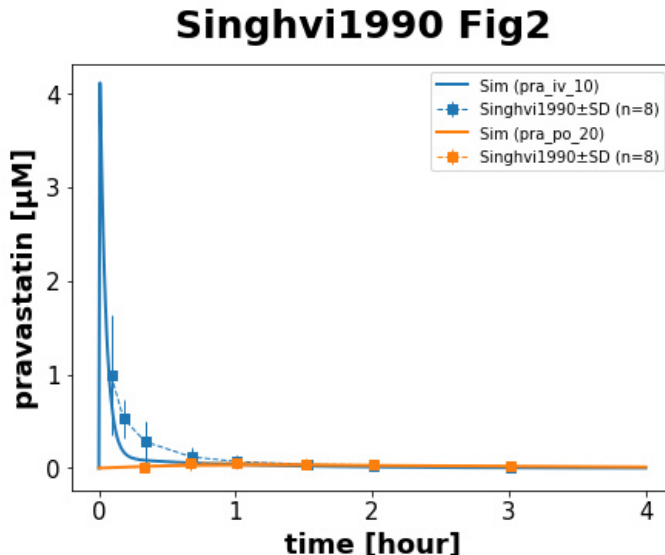


Figure 9: Simulation experiment Singhvi1990 [67]. In this study, eight subjects were provided with a single, 10 mg intravenous dose of pravastatin and with a single, 20 mg oral dose of pravastatin. The blue dotted lines represent the curated data for the intravenous administration of pravastatin and the orange dotted lines describe the oral administration of pravastatin. The blue and orange solid simulation lines are the intravenous and oral simulations predicted by the PBPK model, respectively.

Of all curated studies, *Singhvi et al.*'s study was the only study comparing oral and intravenous administration of pravastatin [67]. *Singhvi et al.* provided eight healthy subjects with a single, 10 mg intravenous dose of pravastatin and with a single, 20 mg oral dose of pravastatin. Over the course of four hours, pravastatin plasma concentrations were measured.

After intravenous pravastatin application, the simulation shows that the plasma c_{\max} peak is reached very rapidly, at approximately $c_{\max} = 4 \mu\text{M}$. No experimental data exists for this early time point. The model predicts a very short t_{half} of less than an hour and pravastatin is eliminated from the systemic circulation within one hour. In contrast, the curated study data reported a c_{\max} of $c_{\max} = 1 \mu\text{M}$ in good agreement with the model prediction at the respective time point. Within the clinical protocol the very early time points corresponding to the actual maximal concentration were not sampled. The curated data does not show an absorption time, since, with an intravenous application, pravastatin is directly injected into the blood circulation and thus bypasses the first-pass effect in the intestine. Despite of a slightly slower t_{half} , the curated data shows a very rapid elimination of pravastatin from the blood. The model simulation and the curated data are in good agreement.

The simulation for oral application is in very good agreement with the curated data. Both time-courses show a slow absorption time and a relatively flat peak for the maximum plasma pravastatin concentration in comparison to the intravenous application. Here, the consequence of the first-pass effect and the slow absorption become apparent: Only a fraction of pravastatin is absorbed slowly in the intestine compared to the intravenous distribution, thus the peak for the plasma concentration flattens and appears much later. The predictions of the PBPK model and the curated study data for oral and intravenous pravastatin application are in very good agreement for this study. In conclusion, the curated data and the predicted time-course simulation by the PBPK model are in good agreement with one another for single oral, multiple oral and intravenous application of pravastatin. The large error bars observed in many studies (figure 6) can be attributed to the relatively low sample size in combination with large interindividual variability. The overall dynamics are predicted very well by the model with correct peak times and half-lives, but peak concentrations being rather low. Intravenous pravastatin data was very limited.

3.5 Model application

The developed PBPK model of pravastatin was applied to study the differences in pharmacokinetics between healthy subjects and patients with either hepatic or renal impairment, as well as the differences between patients with either the wildtype or a specific genetic variant of the enzymatic transporters (OATP2B1, OATP1B1 and MRP2). Parameters corresponding to the different questions were scanned systematically and the corresponding changes in pravastatin pharmacokinetics were evaluated.

Thus, the scans provide answers to the main questions of this thesis, namely, (i) how the genetic variants of the transporters affect the pharmacokinetics of pravastatin, and (ii) how renal and/or hepatic impairment impact the pharmacokinetics of pravastatin.

Hepatic impairment is often associated with renal impairment and vice versa. To account for this hepato-renal interaction the cirrhosis scans were performed under various degrees of renal impairment (control, mild renal impairment, moderate renal impairment, severe renal impairment). All other scans, i.e., renal impairment and the scan of transporter activities, were performed under various degrees of hepatic impairment (control, mild cirrhosis, moderate cirrhosis, severe cirrhosis).

All scans were performed for a single oral dose of 20 mg, if not stated otherwise.

3.5.1 Hepatic impairment

Figure 10 shows time-course scans of the hepatic function in patients with liver cirrhosis for various degrees of renal impairment. The scan gradually increases the degree of severity in cirrhosis $f_{cirrhosis}$ in [0, 0.9], shown by the darkening of the blue lines. The severity of the renal dysfunction is divided into four columns and is depicted by the green-coloured axis frames, ranging from mild to severe insufficiency described by an increasingly darker green.

With increasing cirrhosis degree the pravastatin plasma AUC increases, urinary excretion of pravastatin increases, plasma pravastatin increases, pravastatin in bile increases and pravastatin in faeces decreases. The degree of liver impairment has a very strong effect on the pharmacokinetics of pravastatin.

The main effect of accompanying renal impairment is an increase in plasma pravastatin concentrations. I.e., the more severe the renal impairment, and the worse the cirrhosis, the higher the plasma pravastatin concentrations. Comparing subjects without renal impairment with severe renal impaired shows an increase by 2.5-fold (or $\Delta c_{max} \approx 0.6 \mu\text{M}$).

Interestingly, pravastatin in the urine, liver, bile and faeces, while depending strongly on the severity of cirrhosis, are not affected much by the severity of renal impairment.

Scan Cirrhosis [-]

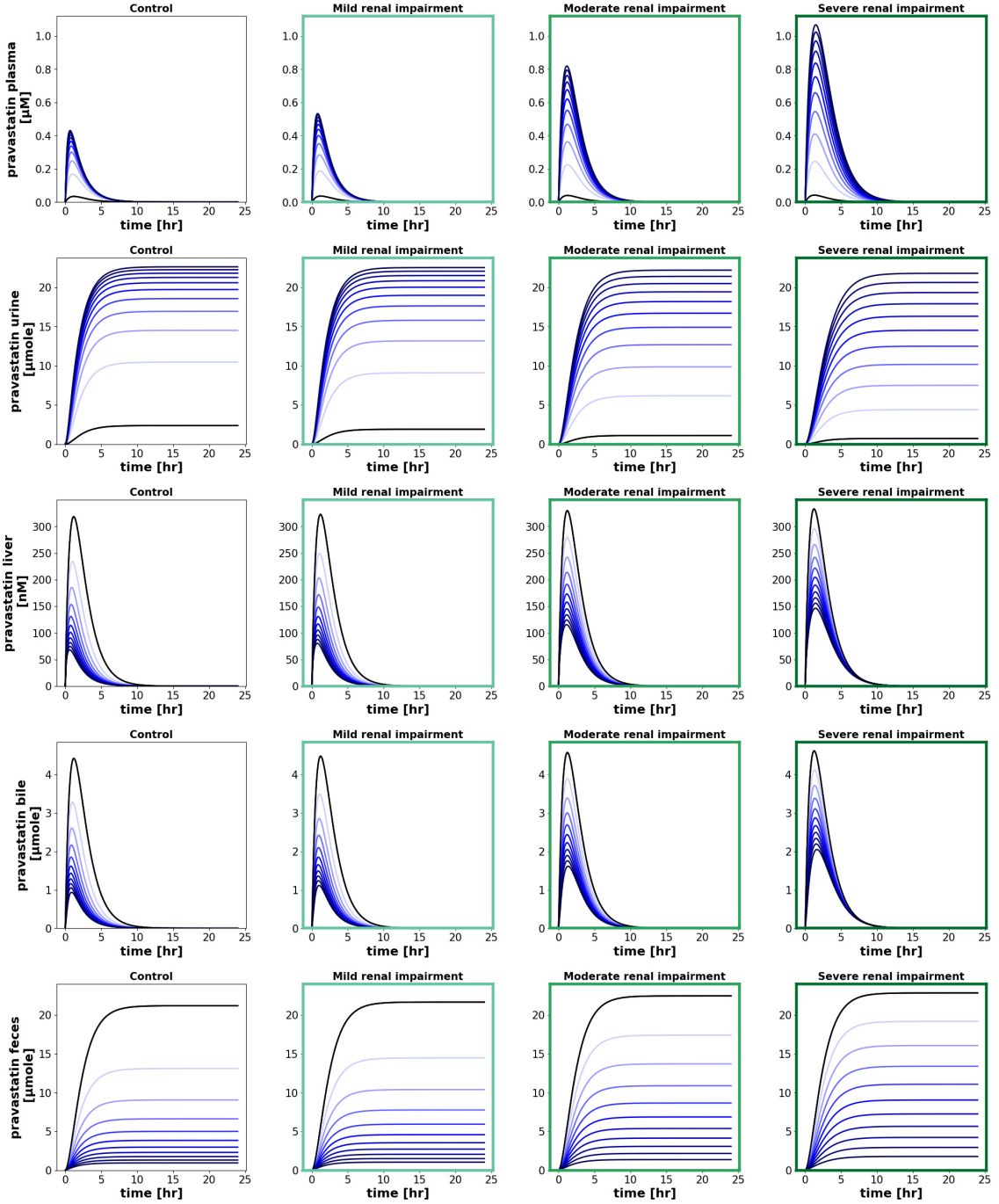


Figure 10: Time-course scan of the hepatic function via the cirrhosis degree $f_{\text{cirrhosis}}$ in $[0, 0.9]$ with increasing cirrhosis corresponding to darker blue tones. From left to right, the columns represent advancing renal impairment, ranging from control to severe, as characterised by the darkening gradient in the green-coloured axis. The rows show pravastatin concentrations and amounts in different tissues over a time period of twenty-four hours.

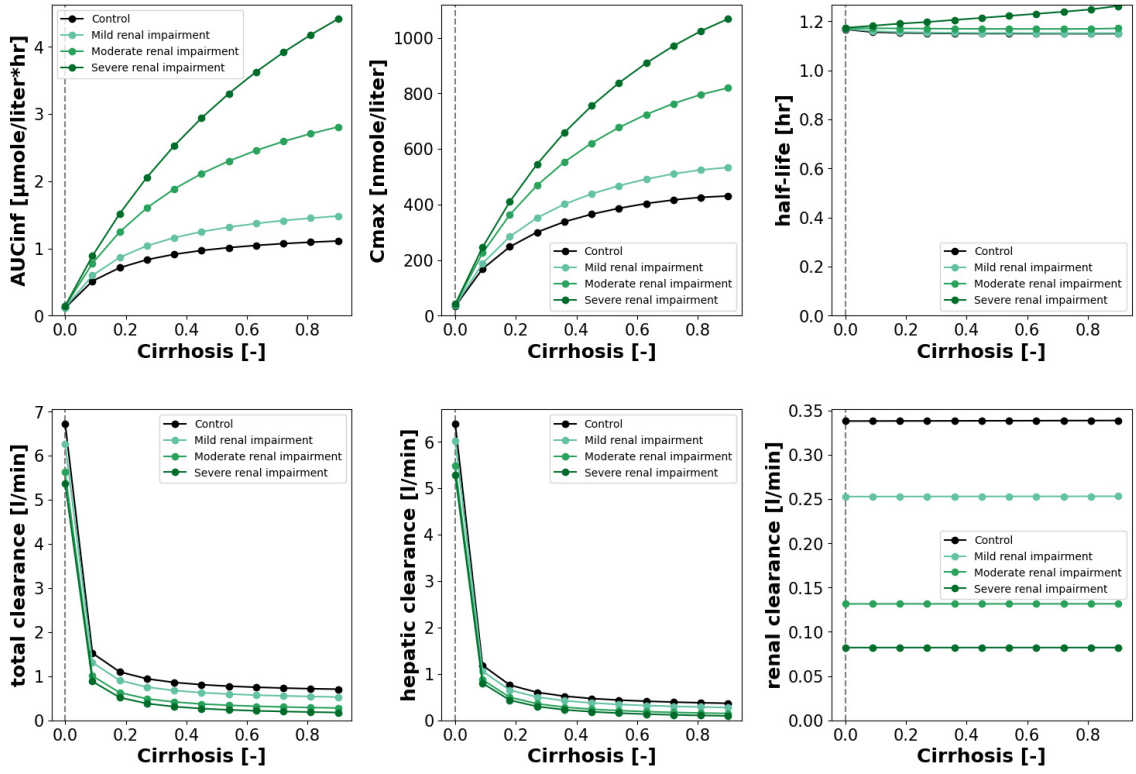


Figure 11: Pharmacokinetics parameter scan of the hepatic function via the cirrhosis degree $f_{\text{cirrhosis}}$ in $[0, 0.9]$. Varying degrees of renal impairment are depicted by the green solid lines. The dotted line represents the reference value 0.0 (healthy, no cirrhosis). This figure shows pravastatin AUC, maximum concentration, half-life, total clearance, hepatic clearance and renal clearance as functions of cirrhosis.

Figure 11 depicts the dependency on cirrhosis for the individual pharmacokinetic parameters of pravastatin, calculated from the pravastatin time-courses in figure 10 given various degrees of renal impairment.

The effect of cirrhosis and renal impairment varies for the different pharmacokinetic parameters. AUC_{inf} and c_{max} show a large dependency on both, the severity of cirrhosis and the severity of the renal impairment. The worse the renal impairment and the worse the hepatic impairment, the greater the area under the plasma pravastatin curve. A combination of hepatic and renal impairment has additive effects. Interestingly, no effect of renal impairment can be observed in subjects with healthy livers, only with cirrhosis the effect of renal impairment becomes apparent.

Almost no data exists in the literature for the effect of liver impairment on the pharmacokinetics of pravastatin. One exception is the review of *Wright et al.*, which states a 1.34-fold increase in c_{max} and a 1.52-fold-increase in AUC for pravastatin in cirrhosis (CTP class not specified), but without referencing an actual study for this observation [79]. These observed changes are in good agreement with the model predictions.

Total clearance and hepatic clearance are mainly affected by cirrhosis, but not renal impairment. Hepatic clearance and consequently total clearance decrease steeply with increasing cirrhosis. In contrast, renal clearance is greatly affected by renal impairment, but not by cirrhosis. Clearly, if the renal function is impaired, so is the renal clearance. However, since renal clearance only contributes about 10% to the total clearance of pravastatin, only a minor effect on total clearance can be observed, as the liver is able to compensate for the renal impairment.

t_{half} is neither affected much by renal impairment nor by hepatic impairment.

3.5.2 Renal impairment

The renal function scans, as opposed to the cirrhosis scans, describe the dependency of the renal function given various degrees of cirrhosis, as illustrated by figure 12. The scan changes renal function $KI_f_renal_function$ in [0.1, 1.9], with reduced renal function in red shades, increased renal function in blue shades, and normal renal function in black.

With increasing renal impairment plasma pravastatin increases, urinary excretion of pravastatin decreases, pravastatin in bile increases and pravastatin in faeces increases. Improved renal function does not change the time-courses much compared to normal function. The degree of cirrhosis has a strong effect on the pharmacokinetics of pravastatin.

The results show that the renal function can partially compensate for reduced pravastatin clearance in hepatic impairment. There exists a linear increase in plasma pravastatin concentration with worsening cirrhosis. The concentration in the liver and consequently, in the bile, show a linear decrease with increasingly severe cirrhosis. The amount of pravastatin excreted into the faeces decreases, as well. Since only a minor fraction of pravastatin reaches the cirrhotic liver, only a minor fraction will be excreted into the bile and reach the enterohepatic circulation, so that a very small amount of pravastatin can reach the intestine and become either reabsorbed or excreted. Due to the increased plasma concentrations, the kidneys can greatly compensate for the hepatic impairment by excreting pravastatin into the urine, even if impaired (due to mass action kinetics of excretion depending on plasma pravastatin concentration). For instance, when comparing the control group to the group with mild cirrhosis, it is noticeable that the amount of pravastatin excreted into urine increases by approximately 4.5-fold with good renal function. More pravastatin is excreted in the urine in the cirrhosis groups under maximal kidney damage ($KI_f_renal_function = 0.1$) than under maximal kidney function ($KI_f_renal_function = 1.9$) in the control group with healthy liver.

Scan Renal function [-]

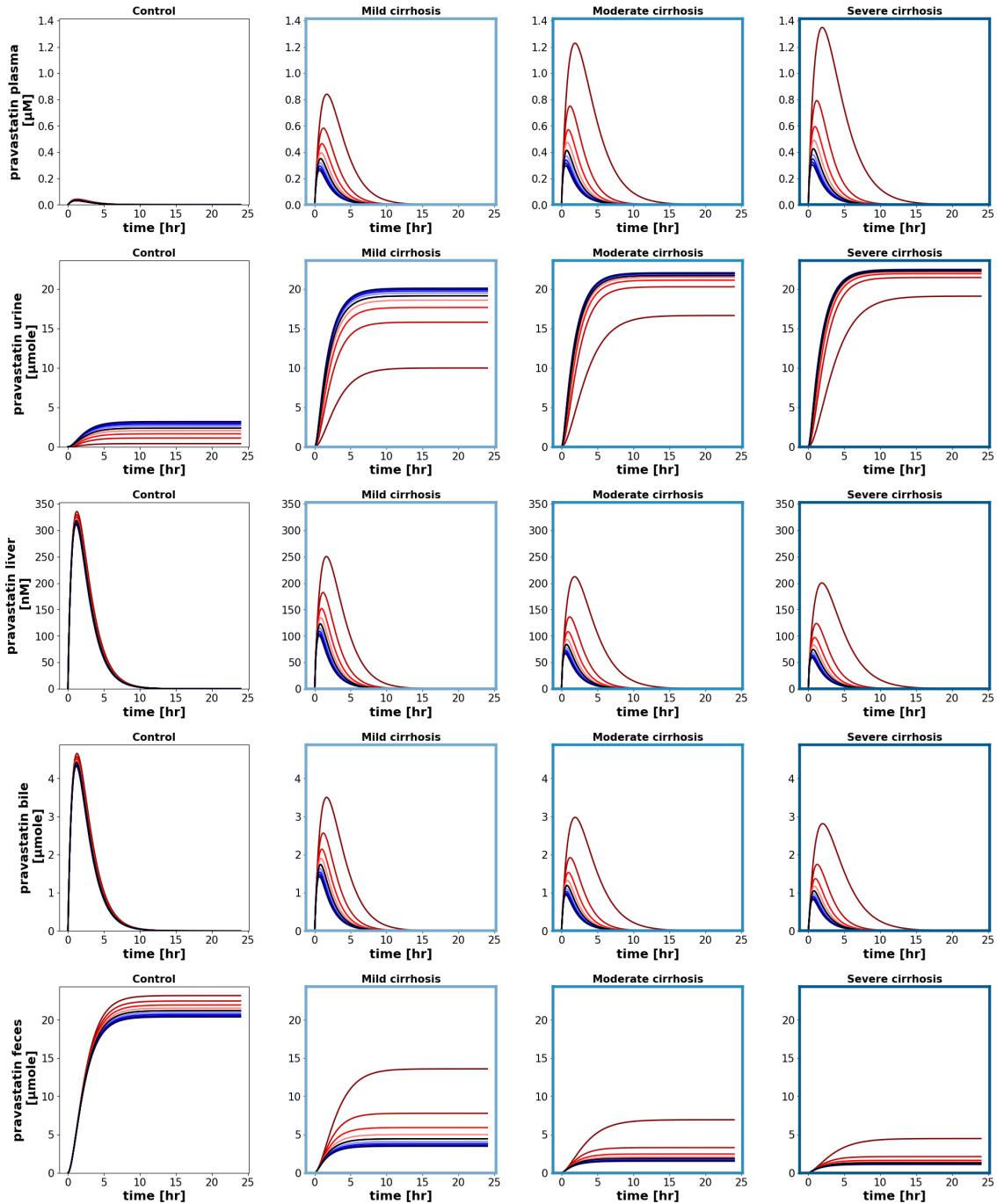


Figure 12: Time-course scan of the renal function via `KI_f_renal_function` in $[0.1, 1.9]$. The red lines represent reduced renal function and the blue lines represent increased renal function with control value depicted in black. From left to right, the columns represent advancing cirrhosis, ranging from control to severe, as characterised by the darkening gradient in the blue-coloured axis. The rows show different pravastatin concentrations and amounts in different tissue compartments over a time period of twenty-four hours.

Figure 13 illustrates the dependency of the pharmacokinetic parameters on the renal function given various degrees of cirrhosis.

AUC_{inf} and c_{max} show a strong dependency on the renal function given any degree of cirrhosis, as opposed to a healthy liver, where the dependency is almost not visible. Due to the large contribution of the liver to the total clearance of pravastatin, a strong increase in AUC_{inf} and c_{max} can be observed with cirrhosis. Both AUC_{inf} and c_{max} increase with decreasing renal function due to the decreased renal clearance. This trend could be observed in the reported pharmacokinetics parameters of *Halstenson et al.*, but this trend was not statistically significant.

t_{half} shows almost no dependency on renal function and cirrhosis with t_{half} being around 1.2 hours for most conditions. These results are in very good agreement with the data of *Halstenson et al.*, which reports no dependency of t_{half} with renal impairment with 1.86 ± 0.72 hr for control, 1.92 ± 0.68 hr for mild renal impairment, 1.26 ± 0.45 hr for moderate renal impairment, and 2.07 ± 0.77 hr for severe renal impairment.

Evidently, since cirrhosis has an impact on the liver and not the kidneys, the hepatic and consequently the total clearance will greatly be affected by cirrhosis. With any degree of cirrhosis, both scans for total and hepatic clearance show a very strong decrease by a factor of 6. The renal function has only minor influence on the total and hepatic clearances, since renal clearance only contributes about 10% to the total clearance. Absolute values of renal clearance range from 0.05 l/min under maximal renal impairment to 0.5 l/min under maximal renal function. The renal clearance is unaffected by cirrhosis, and is only influenced by changes in kidney function via `KI_f_renal_function`.

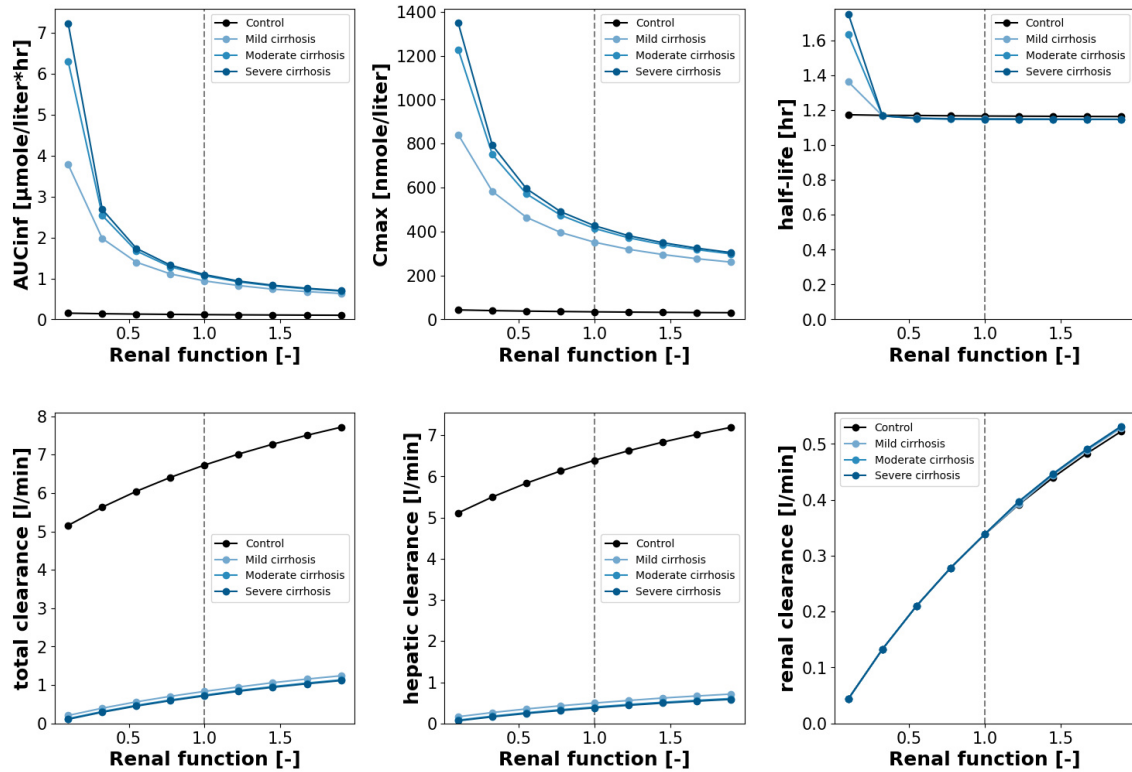


Figure 13: Pharmacokinetics parameter scan of the renal function via `KI_f_renal_function` in $[0.1, 1.9]$. Varying degrees of cirrhosis are depicted by the blue solid lines. The dotted line represents the reference value 1.0 (normal renal function). This figure shows pravastatin AUC, maximum concentration, half-life, total clearance, hepatic clearance and renal clearance as functions of renal function.

Halstenson et al. conducted a study in which sixteen subjects with various degrees of renal impairment received a single oral dose of pravastatin. Figure 14 shows the comparison for the plasma pravastatin time-course and the amount of pravastatin excreted in the urine after 24 hours between simulation and experimental data for various degrees of renal function.

The model predicts only a minor influence of renal impairment on plasma pravastatin concentrations under healthy liver condition (see above), because renal clearance contributes only around 10% to total pravastatin clearance. No clear effect of renal impairment on plasma pravastatin concentrations can be observed in the data of *Halstenson et al.*. The difference between the groups are likely due to the large intraindividual variability due to the very small sample size ($n=4$) per group. In line with simulations in the model performance (section 3.4), the predicted plasma peaks are lower then the data. In line with our simulations, no significant changes in c_{\max} and AUC_{inf} for the plasma pravastatin concentrations were observed between the groups with different renal function.

The panel on the right depicts the amount of pravastatin excreted into urine over twenty-four hours. The dots represent the reported study data by *Halstenson et al.*, and the solid lines are the predictions performed by the model. The large error bars can be attributed to a large intraindividual variability in the subjects, taking into consideration that each group consists of only four individuals (no error bars were reported for the plasma data). The predicted qualitative changes in urinary excretion of pravastatin with renal impairment are in good agreement with the data. The study reported significant changes in recovery of pravastatin in the urine for the group with severe renal impairment. With increasing renal impairment, the amount of pravastatin in the urine decreases. The reported urinary excretion amounts are twice as large as the predictions of the model.

Halstenson1992 Fig1 & Tab2

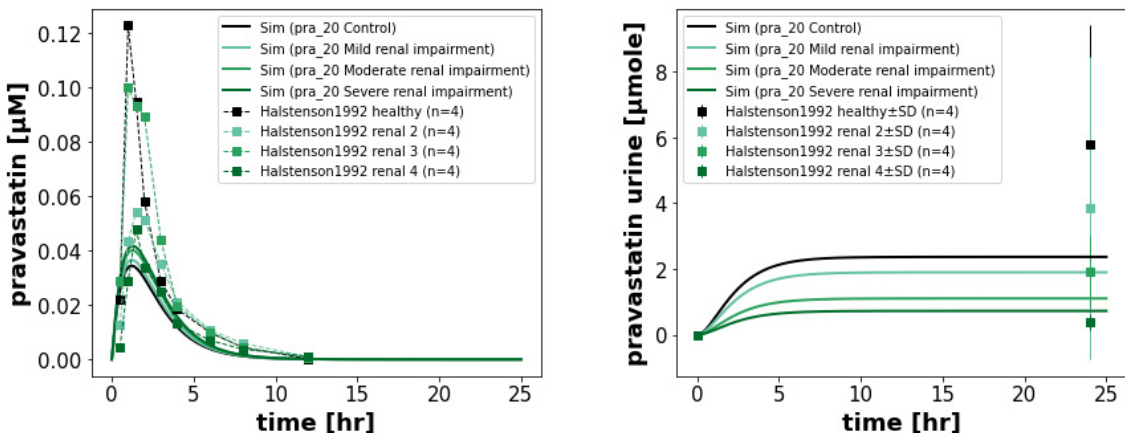


Figure 14: Time-course simulations of *Halstenson et al.*'s study. On the left, plasma pravastatin concentrations are given with dotted lines corresponding to the experimental data and solid lines representing the corresponding simulations for various degrees of renal dysfunction. On the right, the simulation for the amount of pravastatin excreted in urine for various degrees of renal impairment is depicted.

In a next step, the PBPK model prediction and *Halstenson et al.*'s study data in regards to the dependency of renal clearance on renal function were compared in figure 15.

The panel on the left represents the predicted dependency of renal clearance on renal function described by the solid line. Renal clearance improves with better renal function, i.e., with higher `KI_f_renal_function` values. The panel on the right depicts the renal function of each individual in the study. Four dots correspond to one group of renal function, e.g., the four first dots represent the group with severe renal impairment, and so forth. Here, the dots range from poor renal function to healthy renal function. When comparing the two panels, it can be concluded that the prediction of the model stands in very good agreement with the curated data. The model predicts an almost linear increase of renal clearance with increasing renal function. A similar linear increase can be observed in the data. In line with our predictions of large changes in renal clearance of pravastatin with changes in renal function, *Halstenson et al.* reported significant changes in renal clearance between the groups with different renal function.

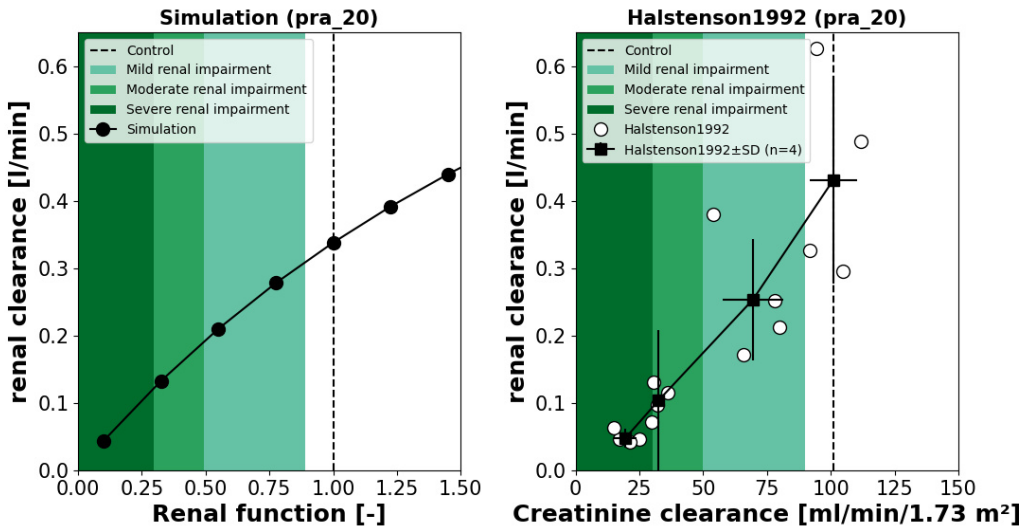


Figure 15: Comparison between the simulated dependency of renal clearance on renal function and the scatter plot in *Halstenson et al.* showing the dependency of renal clearance on creatinine clearance [10]. The green tones describe the various degrees of renal impairment.

3.5.3 Hepatic import (OATP1B1)

The scans for OATP1B1 function describe the dependency of the OATP1B1 function on various degrees of cirrhosis. The time-course simulations are shown in figure 16. The scan changes OATP1B1 function `LI_f_OATP1B1` in [0.1, 1.9], with reduced OATP1B1 function in red shades, increased OATP1B1 function in blue shades, and normal OATP1B1 function in black.

With decreasing OATP1B1 function plasma pravastatin increases, urinary excretion of pravastatin increases, pravastatin in bile decreases and pravastatin in faeces decreases. The degree of cirrhosis has a strong effect on the pharmacokinetics of pravastatin.

Examining the OATP1B1 function in regards to pravastatin plasma concentration, it is clear that differences exist between the various degrees of function for OATP1B1 in the control group. With increasing OATP1B1 function plasma pravastatin decreases due to rapid uptake in the liver, with reduced OATP1B1 function plasma pravastatin increases up to 0.2 μ M due to impaired uptake in the liver. However, given any degree of cirrhosis, plasma pravastatin concentration will strongly increase, independent of the OATP1B1 function. I.e., the effect of OATP1B1 on pravastatin pharmacokinetics is strongly reduced in cirrhosis.

With reduced function of OATP1B1 less pravastatin is taken up in the liver and pravastatin concentrations in the liver decrease. In turn, since the concentration in the liver is low, the export into the bile is also reduced, resulting in a decrease in pravastatin in the bile. Consequently, only a small fraction of pravastatin reaches the enterohepatic circulation, so that the excretion into the faeces decreases greatly.

Similarly to the time-course simulations of the renal scan (see figure 12), the reduced elimination of pravastatin by the liver can be compensated by the kidneys and the excretion into the urine increases with reduced OATP1B1 function due to the increasing plasma pravastatin concentrations.

Scan OATP1B1 function [-]

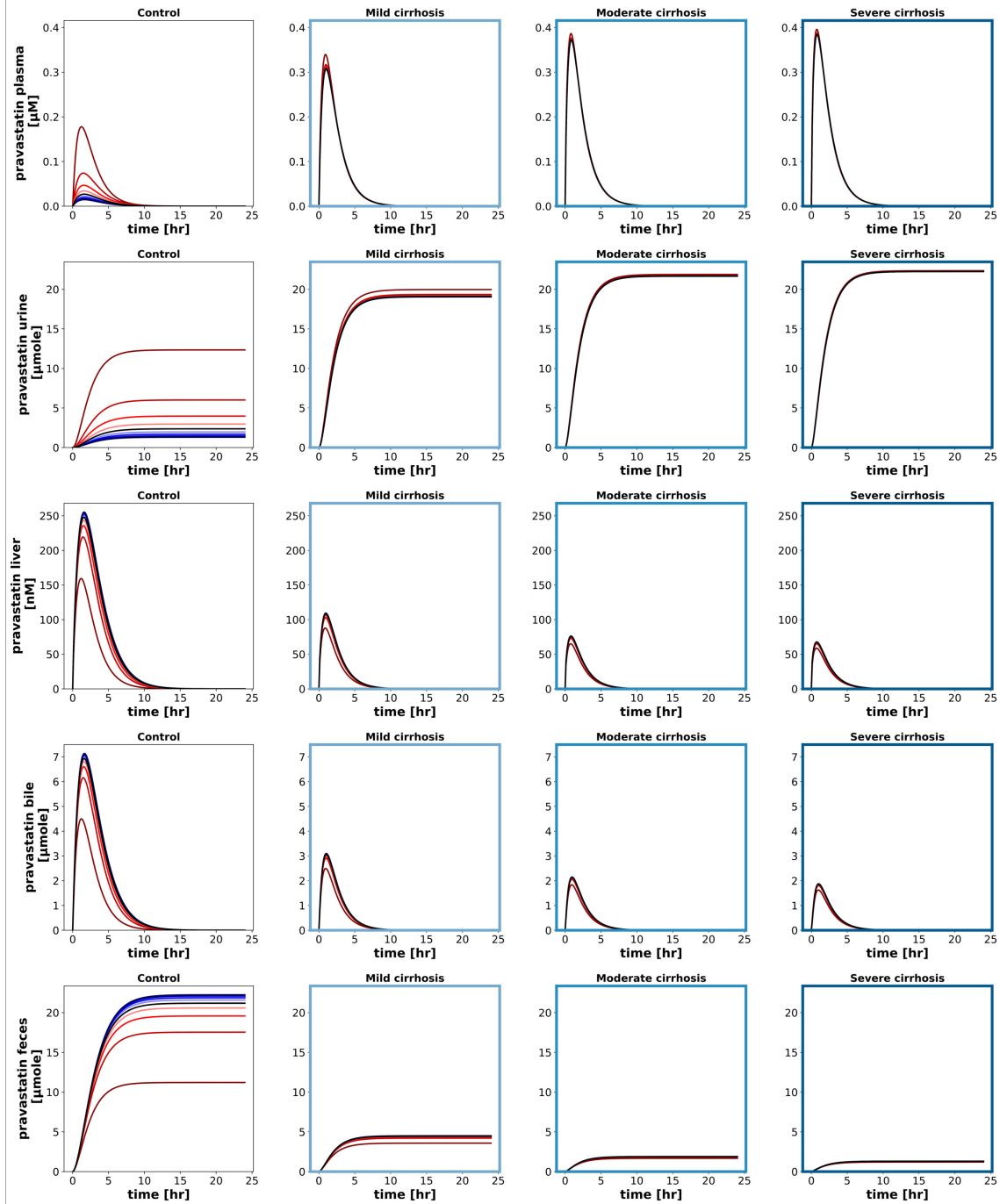


Figure 16: Time-course scan of the OATP1B1 function via LI_f_OATP1B1 in $[0.1, 1.9]$. The red lines represent reduced OATP1B1 function and the blue lines represent increased OATP1B1 function. From left to right, the columns represent advancing cirrhosis, ranging from control to severe, as characterised by the darkening gradient in the blue-coloured axis. The rows show different pravastatin concentrations and amounts in different tissue compartments over a time period of twenty-four hours.

Figure 17 illustrates the dependency of the pharmacokinetic parameters on the function of OATP1B1, given various degrees of cirrhosis.

AUC_{inf} and c_{max} are greatly affected by any degree of cirrhosis. OATP1B1 function has a strong effect on AUC_{inf} in the control group, ranging from 0.6 $\mu\text{mol/l}\cdot\text{hr}$ at minimal OATP1B1 function to less than 0.2 $\mu\text{mol/l}\cdot\text{hr}$ with increased OATP1B1 function. The difference in AUC_{max} between the control group and any group with cirrhosis is about 5-fold, given a normal OATP1B1 function of $LI_f_OATP1B1 = 1.0$.

OATP1B1 function has a strong effect on c_{max} in the control group, ranging from 200 nM with improving OATP1B1 function to approximately 25 nM with improving OATP1B1 function. The difference in c_{max} between the control group and any group with cirrhosis is approximately 7-fold, given a normal OATP1B1 function of $LI_f_OATP1B1 = 1.0$. In contrast, t_{half} remains almost unchanged at around 1.2 hours, for any group and with any value of the OATP1B1 function.

The pharmacokinetic scans for total and hepatic clearance show the impact of cirrhosis. The control groups for both, hepatic and total clearance, show a linear increase with improving OATP1B1 function, ranging from $\approx 1.5 \text{ l/min}$ for $LI_f_OATP1B1 = 0.1$ to 12 l/min for $LI_f_OATP1B1 = 1.9$. With cirrhosis present, hepatic clearance and, due to the large contribution of hepatic clearance to total clearance, also total clearance become significantly reduced, regardless of the function of OATP1B1. Consequently, the removal of pravastatin from the systemic circulation is strongly impaired in cirrhosis. In contrast, the renal clearance remains unchanged at approximately 0.35 l/min in all groups and independent of the function of OATP1B1.

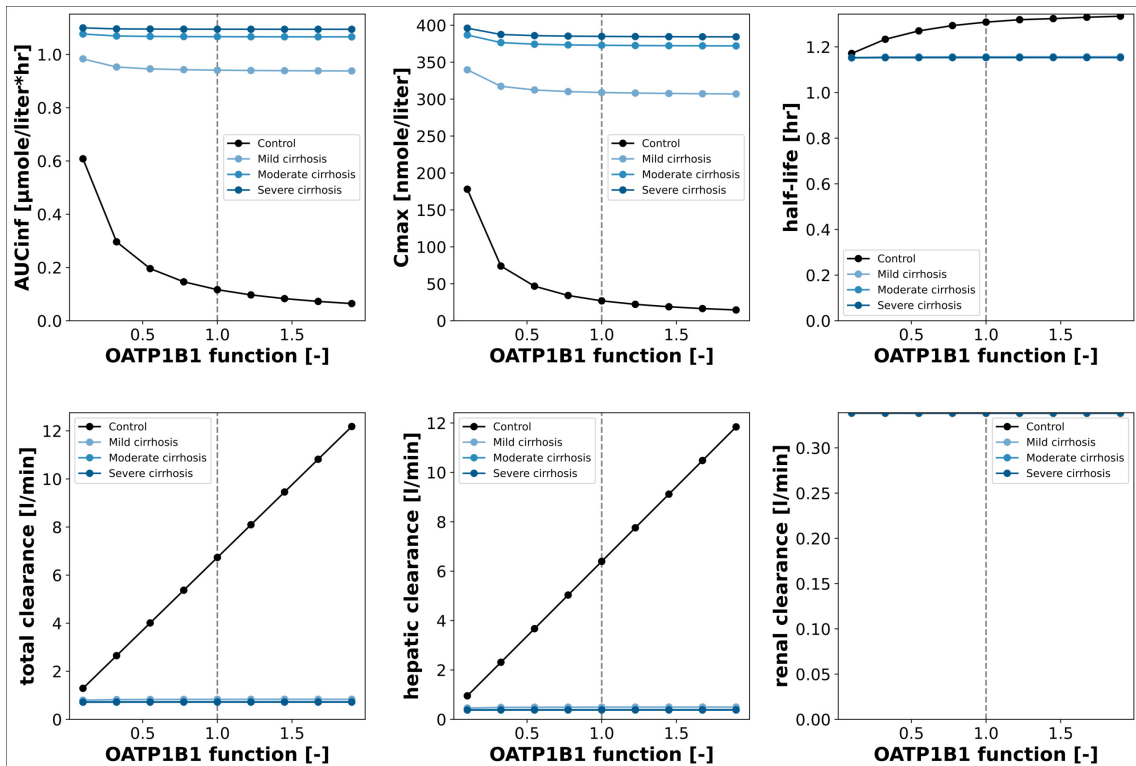


Figure 17: Pharmacokinetics parameter scan of the OATP1B1 function via $LI_f_OATP1B1$ in $[0.1, 1.9]$. Varying degrees of cirrhosis are depicted by the blue solid lines. The dotted line represents the reference value 1.0 (normal OATP1B1 function). This figure shows pravastatin AUC, maximum concentration, half-life, total clearance, hepatic clearance and renal clearance as functions of OATP1B1 function.

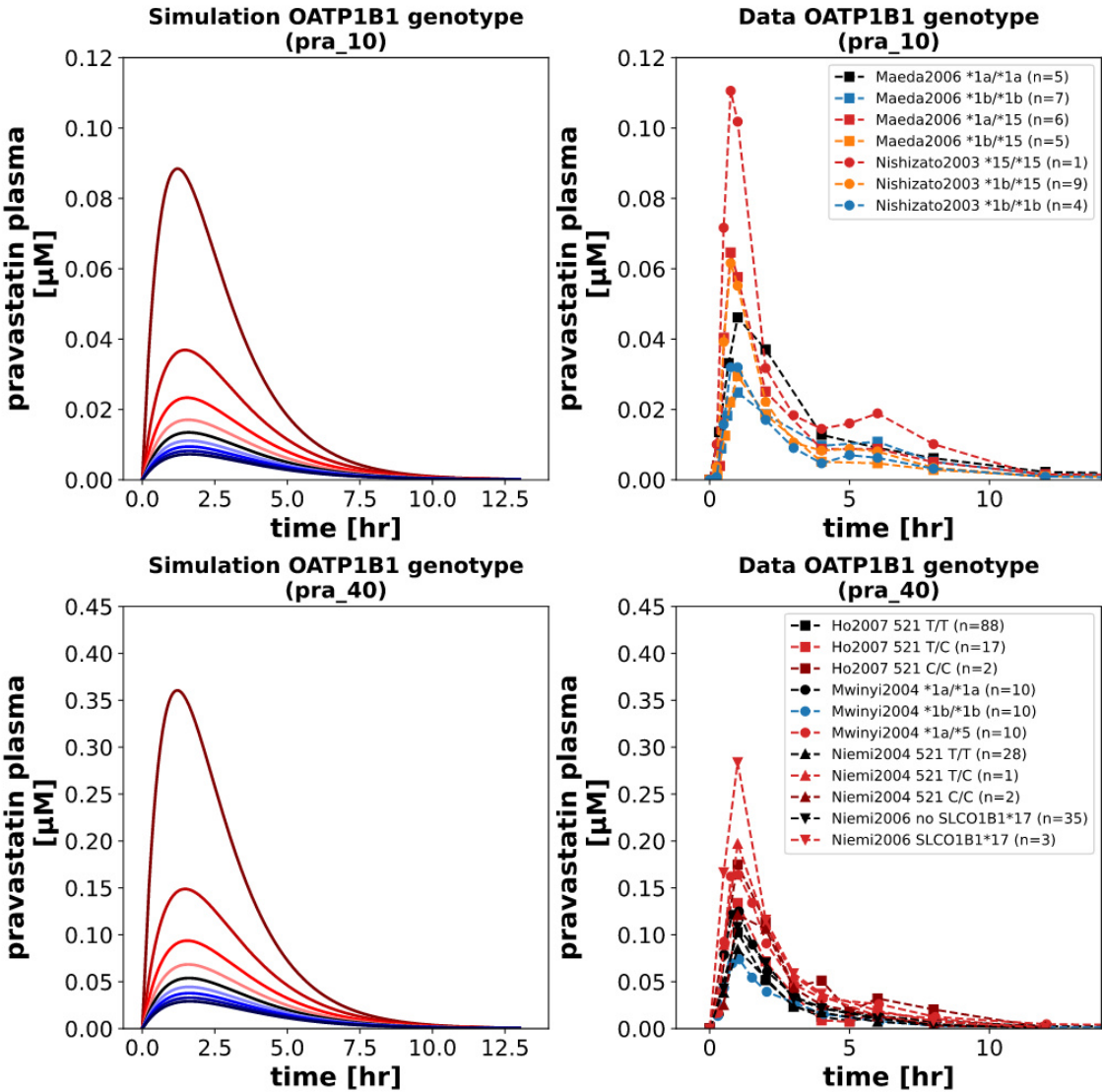


Figure 18: Scan of the effect of OATP1B1 genotypes on the pharmacokinetics of pravastatin. Upper panels: Comparison of the PBPK model’s simulation (left panel) and the study data reported in [42, 52] (right panel) for a 10mg single oral dose of pravastatin. Lower panels: Comparison of the PBPK model’s simulation (left panel) and the study data reported in [12, 45, 51, 49] for a 40mg single oral dose of pravastatin. The red lines represent reduced OATP1B1 function and the blue lines represent increased OATP1B1 function.

Figure 18 analyses the effect of the OATP1B1 wildtype *1a and its genetic variants on the pharmacokinetics of pravastatin. The upper panels illustrate the effect of the OATP1B1 genotypes on the pharmacokinetics of pravastatin for a single oral 10 mg dose of pravastatin. For *Maeda et al.*’s study, OATP1B1*1a/*1a is taken as reference sequence, illustrated as a black line in the upper right panel. The *1b genotype shows increased OATP1B1 activity and the *15 genotype reduced OATP1B1 activity. Consequently, compared to the wildtype OATP1B1*1a/*1a, the OATP1B1*1b/*1b variant (blue line) has higher activity resulting in lower pravastatin plasma concentration and lower AUC. Relative to the OATP1B1*1b/*1b (blue), the OATP1B1*1b/*15 variant (orange) shows decreased activity, as does OATP1B1*1a/*15 (red) relative to OATP1B1*1a/*1a (black). As a consequence, OATP1B1*1a/*15 shows higher pravastatin plasma concentration and higher AUC compared to the wildtype. For *Nishizato et al.*’s study the plasma pravastatin concentrations for the OATP1B1*1b/*1b (blue), OATP1B1*1b/*15 (orange) and OATP1B1*15/*15 (red) genotype were reported with plasma concentrations being twice as high for OATP1B1*15/*15

compared to OATP1B1*1b/*1b. In line with the corresponding model predictions, an increase in enzyme activity (due to the OATP1B1 genotype) results in a decrease in plasma pravastatin. From the pooled data we conclude that the OATP1B1 genetic variant activity is: *1b > *1a > *15, and consequently *1b/*1b (blue) > *1a/*1a (black) > *15/*15 (red), *1b/*1b (blue) > *1b/*15 (orange) > *15/*15 (red), *1b/*15 (orange) > *1a/*15 (red).

The lower panels show the effect of the OATP1B1 genotypes on the pharmacokinetics of pravastatin for a 40 mg single oral dose of pravastatin. For *Ho et al.*'s study, OATP1B1 SNP 521TT is taken as reference sequence, illustrated as a black line in the lower right panel. The 521TC SNP (red line) shows light increases of plasma pravastatin concentrations and AUC values compared to 521TT, whereas the concentration and AUC values for the 521CC SNP (dark red line) are twice as high as those of 521TT. For *Niemi et al.*'s data from 2004, similar effects are seen, corroborating that the genetic variants generally report higher c_{max} and AUC values than the wildtype. For *Mwinyi et al.*'s study, OATP1B1*1a/*1a is taken as reference sequence (black line with circle). OATP1B1*1b/*1b (blue line with circle) shows lower plasma concentration and AUC values than the wildtype, in contrast to OATP1B1*1a/*15 (red line with circle), which report higher concentration and AUC values. For *Niemi et al.*'s study, non-carriers of the OATP1B1*17 haplotype are taken as reference (black line with downside triangle). Compared to the carriers of the *17 haplotype (red line with downside triangle), it is evident that the haplotype has an important impact on the pharmacokinetics of pravastatin, as the c_{max} value is approximately three times as high as those who do not carry the *17 haplotype. However, the sample size is very small and consequently, the variability is quite high.

Overall, the provided data are in very good agreement with the model's simulation of the effect of OATP1B1 genotypes. In agreement with the data, the model predicts that a genotype resulting in a decreased OATP1B1 activity (red) will result in an increase in AUC and plasma pravastatin concentration, whereas an increase in activity (blue) will result in an decrease in AUC and plasma pravastatin concentration. The mixing of genetic variants on the both alleles had the expected effects in the data.

3.5.4 Hepatic export (MRP2)

The scans for MRP2 function describe the dependency of the MRP2 function on various degrees of cirrhosis. The time-course simulations are shown in figure 19. The scan changes MRP2 function **LI_f_MRP2** in [0.1, 1.9], with reduced MRP2 function in red shades, increased MRP2 function in blue shades, and normal MRP2 function in black.

Changes in MRP2 function have only minor effects on plasma pravastatin concentration and pravastatin in the urine. With increasing MRP2 function the plasma pravastatin increases, urinary excretion of pravastatin increases, pravastatin in the liver decreases, pravastatin in bile increases and pravastatin in faeces increases. The degree of cirrhosis has a strong effect on the pharmacokinetics of pravastatin.

MRP2 is responsible for the export of pravastatin from the liver in the bile. The observed effects of increases of liver pravastatin and decreases of pravastatin in the bile with functional impairment of MRP2 are in line with its function as pravastatin exporter. Cirrhosis greatly influences the function of MRP2, resulting in a strong increase in plasma pravastatin concentrations. Again, the liver can partially compensate for the reduced clearance and due to the increased plasma pravastatin concentrations the amount of pravastatin in the urine is increased.

With any degree of cirrhosis, the import of pravastatin into the liver is reduced, i.e., the more aggravating the hepatic impairment, the less uptake of pravastatin into the liver and consequently, less pravastatin can be excreted into the bile via MRP2, hence the concentration of pravastatin in the liver and bile are reduced. An inhibition in MRP2 results in pravastatin not being able to be exported into the bile and it cannot reach the enterohepatic circulation, so that reabsorption into the liver and faecal excretion become hindered.

Figure 20 provides an overview of the impact of cirrhosis on the pharmacokinetic parameters as well as the influence of the MRP2 function on each of the pharmacokinetic parameters.

Cirrhosis has a strong impact on AUC_{inf} , demonstrated by the difference between the control group and the mild cirrhotic group, which is of approximately $\Delta AUC_{inf} \approx 0.8 \mu\text{mol/l}\cdot\text{hr}$. The MRP2 function seems to have no influence on AUC_{inf} , as opposed to the hepatic, renal and

OATP1B1 scans. I.e., reduced biliary excretion of pravastatin only affects the liver concentrations and biliary concentrations, but not plasma pravastatin. Nonetheless, these changes are important because the pharmacodynamics of pravastatin at its site of action can be changed, i.e., the inhibition of HMG-CoA reductase due to changes in hepatic pravastatin concentration.

Cirrhosis has a strong effect on c_{\max} , considering that the difference between the control group and the mildly cirrhotic group is $\Delta c_{\max} \approx 275$ nM for an MRP2 function of $LI_f_MRP2 = 1.0$. c_{\max} shows a small dependency on MRP2 function compared to AUC_{inf} , with reduced MRP2 activity resulting in a reduction of c_{\max} .

With impaired MRP2 function t_{half} increases in subjects with healthy livers from ≈ 1.3 hours to ≈ 2.5 hours. Any degree of cirrhosis results in a decrease in t_{half} to around 1.1 hours and abolishes the dependency on MRP2 function.

If the liver is cirrhotic, both hepatic and total clearance are greatly reduced. Here, the plots for the total and hepatic clearances illustrate that a healthy liver shows a 7-fold increase in clearance compared to an impaired liver. Renal clearance remains at a constant value of approximately $Cl_R \approx 0.35$ l/min independent of hepatic impairment or MRP2 function. The function of MRP2 does not have any influence on the total, hepatic and renal clearance.

Figure 21 analyses the effect of the MRP2 wildtype and its genetic variant c.1446CG on the pharmacokinetics of pravastatin for a 40 mg single oral dose of pravastatin.

Only very little data exists on MRP2 and its genotypes, and the effect of MRP2 variants on pravastatin pharmacokinetics. To our knowledge *Niemi et al.*'s study from 2006 is the only study reporting such data. Here, the non-carriers of the c.1446CG genotype (black line) serve as reference (wildtype). The carriers of c.1446CG (red line) show a significant decrease in pravastatin plasma concentration compared to the non-carriers, suggesting reduced MRP2 function. The model simulations are in good agreement with the experimental data predicting a decrease in pravastatin plasma concentrations and AUC for reduced MRP2 function.

Scan MRP2 function [-]

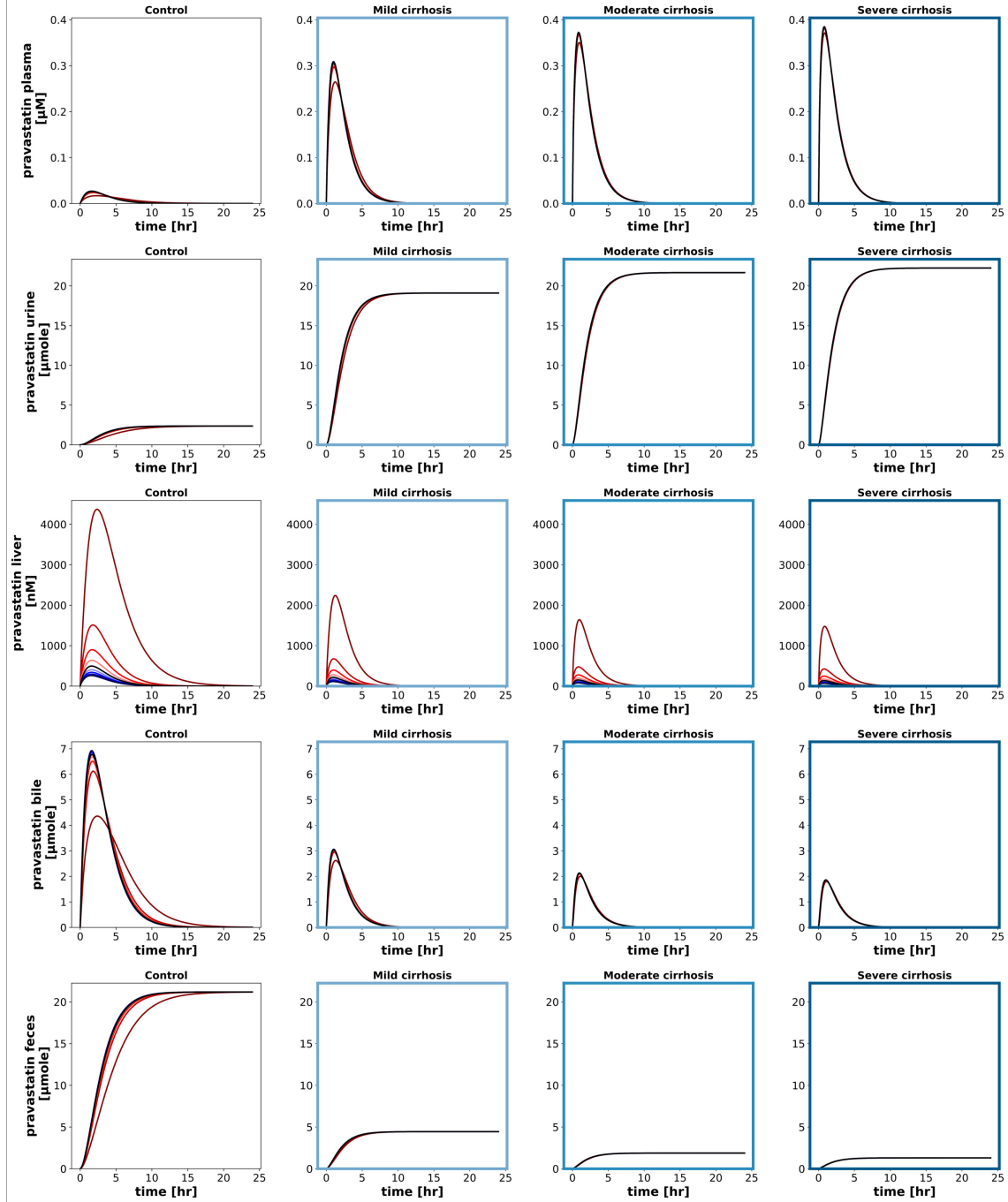


Figure 19: Time-course scan of the MRP2 function via `LI_f_MRP2` in [0.1, 1.9]. The red lines represent reduced MRP2 function and the blue lines represent increased MRP2 function. From left to right, the columns represent advancing cirrhosis, ranging from mild to severe, as characterised by the darkening gradient in the blue-coloured axis. The rows show different pravastatin concentrations and amounts in different tissue compartments over a time period of twenty-four hours.

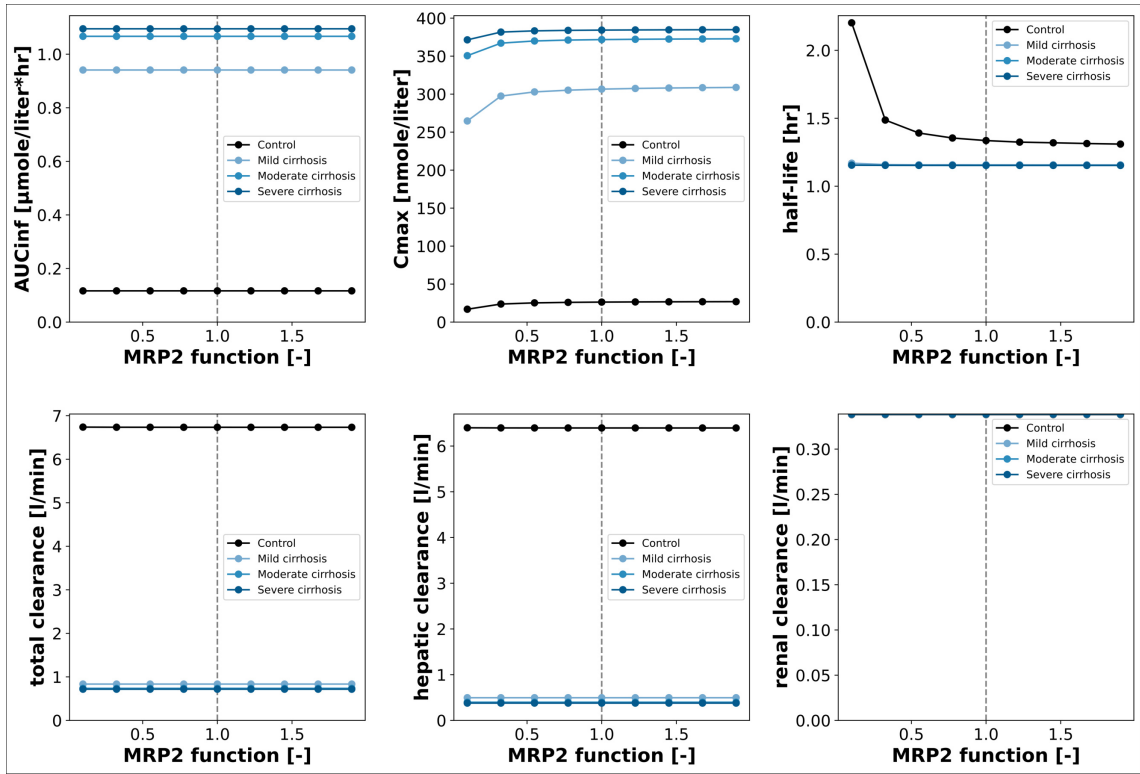


Figure 20: Pharmacokinetics parameter scan of the MRP2 function via LI_f_MRP2 in $[0.1, 1.9]$. Varying degrees of cirrhosis are depicted by the blue solid lines. The dotted line represents the reference value 1.0 (normal MRP2 function). This figure shows pravastatin AUC, maximum concentration, half-life, total clearance, hepatic clearance and renal clearance as functions of MRP2 function.

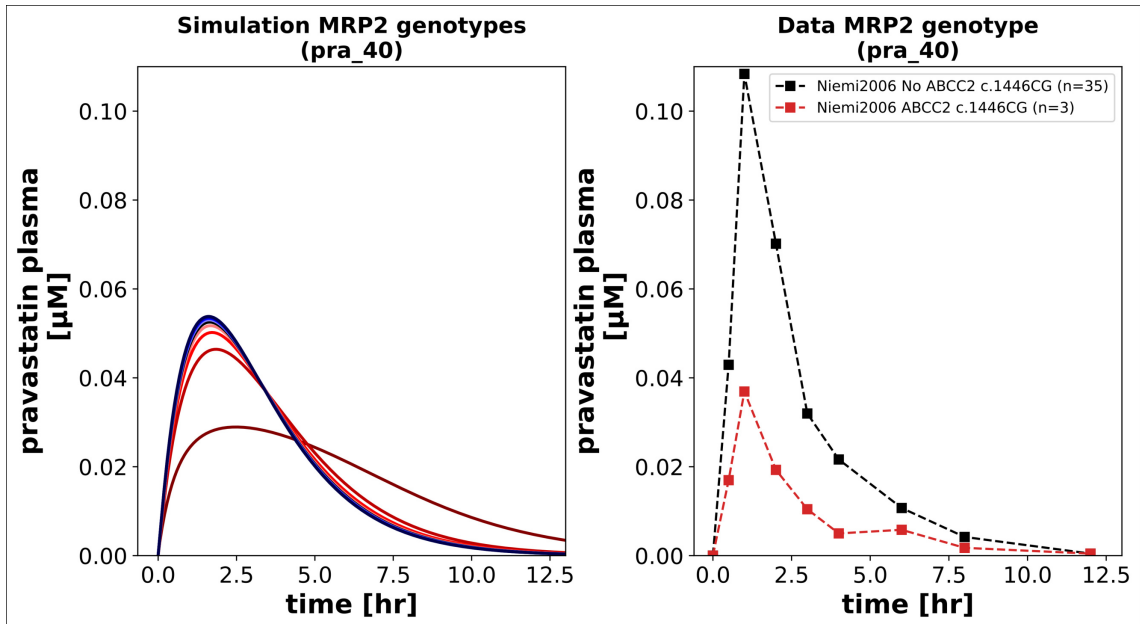


Figure 21: Scan of the effect of MRP2 genotypes on the pharmacokinetics of pravastatin. Here, the effect of the MRP2 genotypes on the pharmacokinetics of pravastatin for a 40 mg single oral dose of pravastatin are illustrated. The red lines represent reduced MRP2 function and the blue lines represent increased MRP2 function. The left panel depicts the PBPK model's simulation and the right panel shows the data reported in [49].

3.5.5 Intestinal absorption (OATP2B1)

The scans for OATP2B1 function describe the dependency of the OATP2B1 function on various degrees of cirrhosis. The time-course simulations are shown in figure 22. The scan changes OATP2B1 function $GU_f_OATP2B1$ in [0.1, 1.9], with reduced OATP2B1 function in red shades, increased OATP2B1 function in blue shades, and normal OATP2B1 function in black.

With increasing OATP2B1 function the pravastatin plasma AUC increases, urinary excretion of pravastatin increases, plasma pravastatin increases, pravastatin in bile increases and pravastatin in faeces decreases. The degree of cirrhosis has a very strong effect on the pharmacokinetics of pravastatin.

OATP2B1 is responsible for the absorption of pravastatin into the enterocytes within the intestinal lumen. Thus, in order to be transported into the systemic circulation and subsequently in the liver, good OATP2B1 function is required. Otherwise, unabsorbed pravastatin becomes excreted into the faeces. The effect is as follows: if the OATP2B1 function increases (blue solid line), the amount of pravastatin excreted into faeces will decrease and more pravastatin will become absorbed, whereas if the OATP2B1 function decreases (red solid line), the amount of pravastatin excreted into the faeces will increase and less pravastatin will become absorbed. With cirrhosis, the excretion-absorption ratio is further compromised by the small amount of pravastatin coming from the enterohepatic circulation. Since only a small fraction comes back from the liver, only a small fraction can be either excreted or reabsorbed.

The fraction of pravastatin that is absorbed by OATP2B1 is subsequently transported to the liver. Due to cirrhosis, a major fraction of pravastatin is unable to reach the liver due to shunts, and thus the concentration of pravastatin in the liver and in the bile decrease, and pravastatin concentration in the plasma increases. Since renal clearance can compensate part of the loss of hepatic clearance in cirrhosis, the amount of pravastatin excreted into urine increases.

Figure 23 provides an overview of the dependency of the pharmacokinetic parameters on the function of OATP2B1, given various degrees of cirrhosis.

AUC_{inf} and c_{max} are affected by cirrhosis and show a dependency on $GU_f_OATP2B1$, i.e., the better the OATP2B1 function, the higher the AUC_{inf} and the c_{max} due to increased absorption of pravastatin which reaches the systemic circulation. The difference in AUC_{inf} between the control group and the mild cirrhotic group for $GU_f_OATP2B1 = 1.0$ is approximately $\Delta AUC_{inf} \approx 0.75 \mu\text{mol/l}\cdot\text{hr}$. Analogously for c_{max} , the difference between the control group and the mild cirrhotic group is $\Delta c_{max} \approx 275 \text{ nM}$. Interestingly, the change in AUC_{inf} and c_{max} is almost linear in case of no liver disease, becoming non-linear in case of liver disease.

Similarly to OATP1B1, neither cirrhosis nor $GU_f_OATP2B1$ seem to affect t_{half} , which remains almost constant at $t_{half} = 1.2$ hours, for any group and with any value of the OATP2B1 function.

Hepatic clearance and total clearance are strongly reduced in cirrhosis. With $GU_f_OATP2B1 = 0.1$, the difference in total and hepatic clearances between the control group and the mildly cirrhotic group are approximately $\Delta Cl_{total} \approx \Delta Cl_{hepatic} \approx 120 \text{ l/min}$. For any degree of cirrhosis, the total and hepatic clearances remain at a value near 0.0, regardless of the function of OATP2B1. Renal clearance, which is not influenced by the function of OATP2B1 nor cirrhosis remains at a constant value of $Cl_R \approx 0.35 \text{ l/min}$.

Scan OATP2B1 function [-]

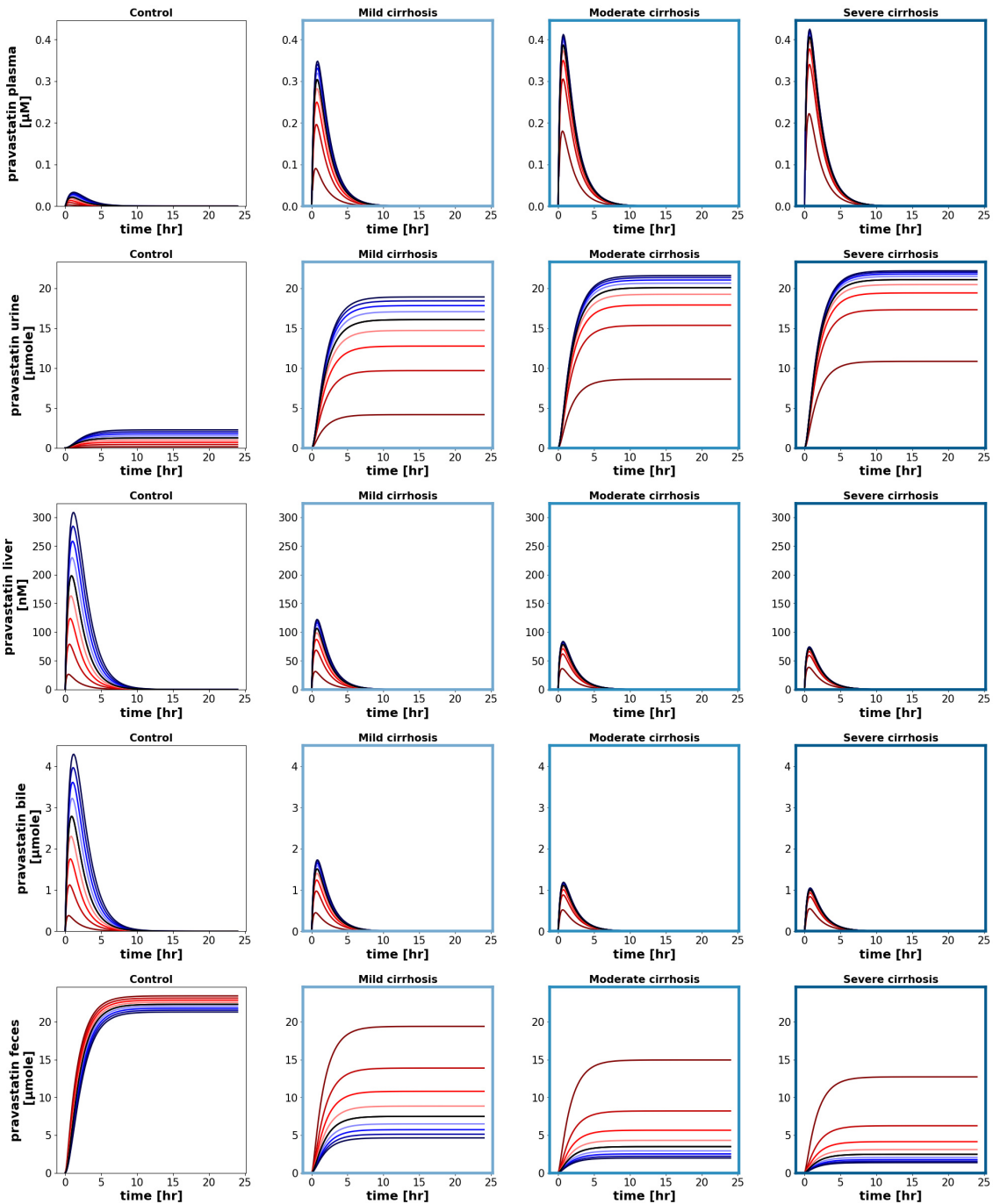


Figure 22: Time-course scan of the OATP2B1 function via GU_f_OATP2B1 in [0.1, 1.9]. The red lines represent reduced OATP2B1 function and the blue lines represent increased OATP2B1 function. From left to right, the columns represent advancing cirrhosis, ranging from control to severe, as characterised by the darkening gradient in the blue-coloured axis. The rows show different pravastatin concentrations and amounts in different tissue compartments over a time period of twenty-four hours.

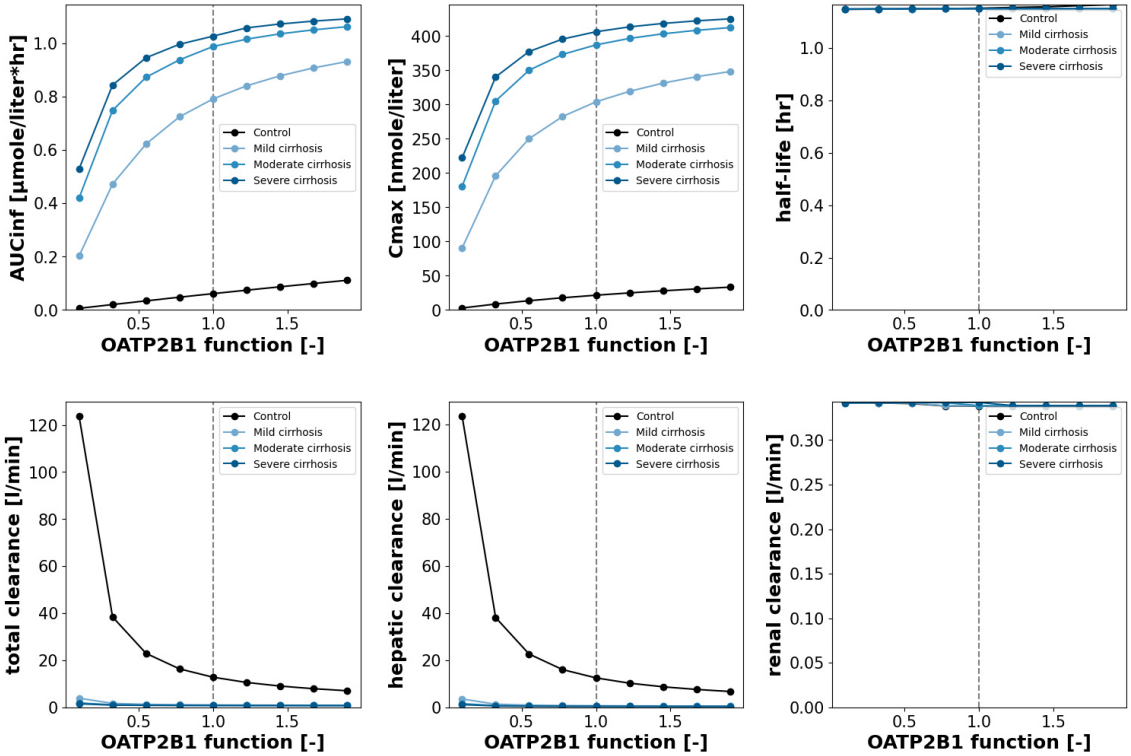


Figure 23: Pharmacokinetics parameter scan of the OATP2B1 function via GU_f_OATP2B1 in [0.1, 1.9]. Varying degrees of cirrhosis are depicted by the blue solid lines. The dotted line represents the reference value 1.0 (normal OATP2B1 function). This figure shows pravastatin AUC, maximum concentration, half-life, total clearance, hepatic clearance and renal clearance as functions of OATP2B1 function.

3.6 Summary

The ambition of this thesis was to develop a PBPK model for studying the role of genotypes and hepatic or renal impairment on the pharmacokinetics of pravastatin. For that purpose, pravastatin-related literature was researched and a total of fifteen relevant articles were selected for data curation and four additional studies for modelling. Subsequently, the computational model was constructed in a hierarchical manner consisting of a whole-body model coupled to individual tissue models of intestine, liver and kidneys. A subset of parameters of the model were fitted by using time-course data of plasma, serum and urine pravastatin. Study data and model predictions were overall in good agreement as evaluated by parameter fitting results and the model performance after single oral, multiple oral and intravenous application of pravastatin. The present model was in good agreement with data for oral and intravenous pravastatin application for multiple studies, albeit with few outliers. The model was applied to predict the effects of hepatic and renal impairments and of genetic variants affecting activity of OATP2B1, OATP1B1 and MRP2. Model predictions were in good agreement with available data for renal impairment and genetic variants of OATP1B1 and MRP2.

4 Discussion

4.1 Data

Curation of various pravastatin datasets was required for the development and evaluation of the PBPK model. Thus, fifteen studies were selected and the study data therein was curated. In addition, data from four existing studies from PK-DB were used for modelling. The clinical studies provided information on the pharmacokinetics and pharmacokinetics parameters of pravastatin, e.g., c_{\max} , t_{half} and AUC. The collection of high-quality data sets were uploaded to the pharmacokinetics database <https://pk-db.com>, where it is freely and openly accessible for future scientific research and reuse.

The clinical studies mostly included healthy volunteers, with the exception of *Pan et al.*'s study in 1990 and *Sigurbjörnsson et al.*'s study in 1998, where subjects had primary hypercholesterolaemia [55, 66], and *Halstenson et al.*'s study in 1992, where subjects exhibited various degrees of renal impairment [10]. Especially the latter data was of importance for this thesis in order to evaluate the model predictions in renal impairment (see section 3.5).

In order to assess the impact of the genetic variants of OATP1B1, OATP2B1 and MRP2 on the pharmacokinetics of pravastatin, multiple studies were included. In particular *Niemi et al.*'s studies both in 2004 and 2006 as well as *Ho et al.*'s study in 2007 were of main interest to understand the impact which various SNPs and haplotypes can have on the pharmacokinetics of pravastatin [12, 51, 49].

The administration route (oral or intravenous), form and dose of pravastatin were important information in the curation, which can have a major influence on the pharmacokinetics of pravastatin. Only *Singhvi et al.* reported intravenous pravastatin application, with all other studies applying pravastatin orally. Despite the large bias in the dataset towards oral data, intravenous as well as oral data could be very well described by the model, as can be seen in figure 9.

Overall, the data bases from the curated studies was highly consistent and reported similar values for the pharmacokinetic parameters, with the exception of the studies by *Becquemont et al.* and *Sigurbjörnsson et al.*, which report higher c_{\max} peaks than all other curated studies [3, 66]. This could be due to several reasons, including large intraindividual variability, or reporting errors in the study. For instance, the data by *Sigurbjörnsson et al.* was reported for a single subject, which could be far from the mean observed pravastatin time-courses observed in other studies. The data was therefore excluded from parameter fitting.

In the presented work, drug-drug interaction between pravastatin and other drugs was not studied. Nevertheless, the respective data was curated. The evaluation of the effect of drug-drug interactions on the pharmacokinetics of pravastatin will be of interest for future research. This will be further discussed in section 5.

4.2 Model

A physiologically-based pharmacokinetics model was developed to study the pharmacokinetics of pravastatin. The model allows to simulate the time-courses of pravastatin in various tissues and to calculate pharmacokinetics parameters for pravastatin. The overall objective was to develop a PBPK model which allows to accurately predict experimental data from a wide range of studies under oral and intravenous application routes. Thus, clinical study data were curated and the parameters were fitted using time-course data for plasma and urine (see section 2.1 and section 2.3 for more detailed information on data curation and parameter fitting).

In the development of the PBPK model, the following assumptions were made and implemented:

- (i) The isomerisation of pravastatin in the stomach reduces the fraction absorbed, i.e., only a fraction of pravastatin in the stomach reaches the intestinal lumen.
- (ii) The import of pravastatin via OATP2B1 is irreversible at the apical membrane of enterocytes.
- (iii) The hepatic import of pravastatin via OATP1B1 via Michaelis-Menten Kinetics is irreversible.

- (iv) The hepatic export of pravastatin via MRP2 via Michaelis-Menten Kinetics is irreversible.
- (v) The transport of pravastatin through the enterohepatic circulation, i.e., from the bile to the intestinal lumen, via Mass-action kinetics is irreversible.
- (vi) No metabolism of pravastatin takes place in the liver.
- (vii) Pravastatin metabolites, such as pravastatin lactone, were not included in the model.
- (viii) No tissue distribution exists for pravastatin besides the active transport in the liver.

Despite these simplifying assumptions, the model allowed to correctly describe the curated pharmacokinetic data with good agreement between model prediction and data. The model simulations for oral pravastatin application appeared to be in overall good agreement with the study data, albeit with some exceptions.

Sigurbjörnsson et al.'s time-course figures 37 and 38 could not be correctly simulated. Particularly, the simulation experiment in figure 37 presents the largest differences between model simulation and experimental data. Overall, the protocol of the study was not very well reported and values were only reported for a single subject. Due to the large intraindividual variability in the pharmacokinetics of pravastatin, this subject could be far from the mean model behaviour. All model simulations were performed with the mean model (corresponding to the fitted parameters) and no individualisation of model simulations were performed. Due to the large differences to all other data the study was removed from analysis and parameter fitting.

Becquemont et al.'s study was conspicuous in comparison to almost all other curated studies in this thesis due to excessively high concentration peaks compared to other studies under the same application route and dose, as seen in figure 24 (see supplement section 6). In their article, it was argued that the high c_{\max} peaks may be due to high interindividual variability [3]. Taking the small sample size and the large error bars into consideration, it would be likely for this argumentation to be accurate.

Within this work, only a single study applied pravastatin intravenously (see section 3.5, figure 9). In addition, only a single study by *Halstenson et al.* reported urinary data of pravastatin. The under-representation of urinary and intravenous data in parameter fitting clearly favours the oral data during parameter optimisation (data was only weighted based on subject number). Despite this unbalance in training data, the resulting optimal parameter set showed very good model performance not only for the oral clinical data, but also for the prediction of intravenous data and urinary data.

One limitation of the presented study is that the time-course model performance was only evaluated on data used within the parameter fitting. I.e., no independent time-course data was used for model validation. Based on an extension of the pravastatin data bases such a validation could be performed, but was not part of this thesis.

The following data not used for parameter fitting and was used to evaluate model predictions:

- (i) renal clearance depending on renal function (very good agreement),
- (ii) prediction of changes in plasma pravastatin time-courses with OATP1B1 function, and comparison with genotype data (good agreement for increased and reduced activity genotypes),
- (iii) prediction of changes in plasma pravastatin time-courses with MRP2 function, and comparison with genotype data (good agreement with reduced activity genotype).

Despite these predictions generally being in good agreement with the data, the availability of renal clearance and genotype data was indeed very limited. In addition, the research on genotypes focused mainly on the reference sequences and wildtypes or did not report the genotypes of the subjects at all. If genetic variant data was reported, the sample size was very small (often not very frequent variants) resulting in large variability of the results due to the low number of subjects. Out of the three enzymatic transporters analysed in this thesis, OATP1B1 was by far the most studied, whereas MRP2 and especially OATP2B1 warrant further research. Based on additional data, a more accurate description of the effect that the genetic variants have on the activity of the respective enzymes and pharmacokinetics of pravastatin could be achieved.

4.3 Disease

Understanding the effects of cirrhosis on the pharmacokinetics of statins poses an important clinical question (see section 1.4), as the pharmacokinetics may vary and present challenges when treating patients with liver disease. The simulations of hepatic impairment have shown that with increasing cirrhosis degree the pravastatin plasma AUC increases, alongside urinary excretion, plasma pravastatin and pravastatin in the bile, whereas the amount of pravastatin in faeces decreases (see figure 10). Furthermore, the pharmacokinetics parameter scan of the hepatic function shows that accompanying renal impairment does not heavily influence the pharmacokinetics of pravastatin, with the exception of renal clearance, as illustrated by figure 11. Surprisingly, data on pravastatin pharmacokinetics in subjects with liver disease such as cirrhosis is very limited. Besides a 1.34-fold increase in c_{max} and a 1.52-fold-increase in AUC for pravastatin in cirrhosis (CTP class not specified) [79] which is in good agreement with our model predictions, no data on the effect of liver disease on pravastatin pharmacokinetics could be found in our literature research. Due to the very large effect of liver impairment on pravastatin, such research would be important.

Similarly, the time-course simulations for the effects of renal impairment on the pharmacokinetics of pravastatin have demonstrated that any degree of cirrhosis does heavily influence the renal function (see figure 12). The kidneys, i.e., the renal clearance, can partly compensate for the impaired liver, since the total and hepatic clearances are heavily compromised by cirrhosis (see figure 13). As previously mentioned in section 1.4, *Halstenson et al.*'s study reported about two important things: On the one hand, non-significant alterations in pravastatin's pharmacokinetic parameters AUC, c_{max} and t_{half} were reported. This is corroborated by the model, as it can be seen in figure 13. In addition, it was stated that with increased renal dysfunction pravastatin clearance would be reduced and vice versa. Figure 15 clearly illustrates this effect, thus reinforcing this last statement. A major challenge for modelling renal impairment was the lack of study data reported about renal clearance. For instance, only *Halstenson et al.*'s study provided a more extensive research on renal clearance, with which we were able to model figures 14 and 15. The study data agreed very well with the model's simulation, which further validates the model.

In conclusion, a PBPK model that was able to predict the effects of pravastatin pharmacokinetics given hepatic or renal dysfunction was successfully established.

4.4 Genetic variants

Within this thesis, the genetic variants of the enzymatic transporters OATP1B1, OATP2B1 and MRP2 were of main interest, since they can have a large effect on the pharmacokinetics of pravastatin. The objective was to systematically predict the effect of changes in activity of these transporters due to genetic variants. For that purpose, we modelled these changes and compared the predictions with pravastatin pharmacokinetics data available for different genotypes. This comparison was possible for OATP1B1 and MRP2.

Multiple studies reported the effect of genetic variants of OATP1B1 on pravastatin pharmacokinetics [42, 52, 12, 45, 51, 49], albeit more data about the wildtype was available than about the genetic variants. Nevertheless, the curated data were in very good agreement with the model's simulation of different OATP1B1 genotypes (see figure 18), despite the sample size being relatively small for the genetic variants. In addition, the effects on enzyme activity of the genetic variants reported in table 1 were in line with the model simulations.

Only a single study reported on the effect of genetic variants of MRP2 on the pharmacokinetics of pravastatin in humans [49]. In addition, *Kivistö et al.* reported reductions of AUC and c_{max} of approximately 70% for the c.1446CG SNP in rodents, and although the reduction predicted by the PBPK model is not as pronounced, the effect of the genotype compared to the wildtype can be clearly seen in the model's prediction, showing an AUC and c_{max} reduction of $\approx 40\%$. However, it must be taken into consideration that data surrounding MRP2 in general was very limited and consequently, large interindividual variability existed. Nevertheless, the curated data were in very good agreement with the model's simulation of the MRP2 wildtype compared to its genetic variant. However, to gain a better understanding of the effect of genetic variants of MRP2 further research is warranted.

Data about the effects of OATP2B1 genotypes on the pravastatin pharmacokinetics was not available. Only the time-course simulations and the pharmacokinetics scans of OATP2B1 could

be simulated (see figures 22, 23), but a comparison between the model's prediction and genotype data could not be performed.

In conclusion, a PBPK model of pravastatin was developed to systematically analyse the effects of renal (renal insufficiency) and/or hepatic impairment (cirrhosis) on pravastatin pharmacokinetics and the effects of genetic variants of OATP2B1, OATP1B1 and MRP2 on pravastatin pharmacokinetics.

5 Outlook

The following section aims to discuss possible use cases of the present PBPK model, which could assist in future research on the pharmacokinetics of pravastatin.

Drug-drug interactions The evaluation of drug-drug interactions between pravastatin and other medications would be of particular interest for future research, taking into consideration the impact that it may have on the pharmacokinetics (see also section 4.1). Especially in a population growing older and with elderly often prescribed multiple drugs in addition to cholesterol lowering medication via statins, the possible effects of these interactions would be important to know.

Drugs which can be combined with pravastatin are, for example, cyclosporine, boceprevir or telaprevir [79]. These drugs inhibit OATP1B1 mediated transport, thus increasing c_{max} levels and AUC values of pravastatin by 1.32-fold and 1.52-fold, respectively [79]. The increased exposure at the site of action will result in increased inhibition of the HMG-CoA reductase and increase the risk of possible adverse effects. When administering these substances in conjunction with pravastatin, researchers warn that therapy should be either monitored or modified, since such drug-drug interactions have been discovered to alter the pharmacokinetics of some statins and significantly increase the risk of statin-related muscle injury [79, 40].

Furthermore, grapefruit juice has been reported to inhibit the uptake of pravastatin by the high-affinity side of OATP2B1 (alongside non-significant inhibition of the low-affinity side of OATP2B1) [65]. As a consequence, the pharmacokinetics of pravastatin are affected when consuming grapefruit juice during therapy.

By including the effects of drug-drug interactions in the PBPK model (e.g., by inhibiting OATP1B1 or OATP2B1) the effect of drug-drug interaction on pravastatin could be studied. As an important note, the current thesis already provides the predictions of these drug-drug interactions in form of activity scans of OATP1B1, OATP2B1 and MRP2. I.e., drug-drug interaction resulting in an activation of these transporters correspond to the respective scan results with increased activity, drugs inhibiting these transporters (e.g. via competitive inhibition) correspond to the respective scans with decreased activity. For instance, our model predicts lower plasma pravastatin concentrations and AUC with inhibition of OATP2B1, resulting in a decreased bioavailability of pravastatin due to grapefruit juice (see figure 16 and 17). In line with this prediction, *Lilja et al* showed a non-significant decrease in pravastatin AUC from $111.7 \pm 68.1 \mu\text{mol/l}\cdot\text{hr}$ to $102.8 \pm 49.6 \mu\text{mol/l}\cdot\text{hr}$ and a similar decrease in active HMG-CoA reductase inhibitors when comparing placebo with grapefruit juice during 40 mg oral pravastatin [41].

Thus, predictions by the presented model would seem plausible, as a better understanding of drug-drug interaction could be provided and, consequently, polypharmacy-therapy could be better adapted.

Circadian rhythm Another future direction could be the application of the model to study the possible effects of the circadian rhythm on pravastatin therapy.

Cholesterol biosynthesis follows a circadian rhythm. Consequently, pravastatin could be an interesting drug for chronotherapy, i.e., adapting the time of application of pravastatin to optimise the treatment effects. It is an open question whether the timing of statin administration might be of importance for clinical outcomes [18]. Statins are usually administered once per day without time specifications (except simvastatin, which is recommended to be taken in the evening).

In a nine-week time period of statin administration, only low-quality evidence was reported by *Izquierdo-Palomares et al.*, showing no major differences between morning and evening statin administration in total cholesterol, LDL-cholesterol, HDL-cholesterol or triglyceride levels [18]. Ultimately, they concluded that the limited and low-quality evidence indicated that no significant differences existed between chronomodulated treatment and conventional treatment with statins [18].

For pravastatin, *Hunninghake et al.* conducted an eight-week study in which the differences in efficacy of pravastatin were compared in subjects with hypercholesterolaemia. I.e., pravastatin was administered either once daily as (i) a single, 40 mg oral dose in the morning, (ii) in the evening, or (iii) twice daily as a 20 mg oral dose [15].

It was reported that in the 40 mg evening group, all patients achieved > 15% LDL-C level reduction. Additionally, 75.5% of those patients presented a >25% LDL-C level reduction and a 8.2% increase in HDL-C levels. In comparison, in the 40 mg morning group, 96% patients achieved a >15% LDL-C level reduction [15]. In summary, the reported effects of the treatment showed that the pharmacodynamic effects of pravastatin were slightly greater when pravastatin was administered in the evening rather than in the morning, due to cholesterol synthesis reaching a peak around midnight [15].

Application of the developed model to this question could provide important information relevant for the chronotherapy with pravastatin.

Pharmacodynamics The presented thesis focused on the pharmacokinetics of pravastatin. The pharmacodynamics of pravastatin, i.e., especially the lipid-lowering effect on LDL-C due to HMG-CoA reductase inhibition in the liver, have not been studied. However, the study of the pharmacodynamics of pravastatin, as well as its implementation in the PBPK model, would be of interest for future research. Future work will address this by coupling the developed model to existing computational models of the effect of HMG-CoA reductase inhibition on plasma lipids [2]. Modelling the pharmacodynamic effects of pravastatin would be a prerequisite to study the dependency of pravastatin therapy on the time of dose due to daily variation in cholesterol synthesis.

According to a large number of studies, pravastatin has been indicated to have rather low toxicity and thus can be administered in a relatively safe manner, only causing mild adverse clinical effects. Typical adverse effects of pravastatin include headache, dizziness, skin rash, gastrointestinal and flu-like symptoms [74, 44, 59]. These secondary effects are not frequent. For instance, the Food and Drug Administration (FDA) reports adverse clinical effects of less than 2% for pravastatin-treated patients [8]. By better understanding the pharmacokinetics and pharmacodynamics of pravastatin and factors resulting in the large interindividual variability, a model-based approach could help in reducing these adverse effects.

Acknowledgements

I would like to sincerely thank Dr. Matthias König for giving me a chance to take on this project, and making it such an enjoyable learning experience. His knowledge, support and kindness throughout all of my time in his group were beyond remarkable and I am very grateful that I was able learn so many new things under his guidance. Thank you.

Further, I would like to thank Jan Grzegorzewski. He has helped me with every little doubt I have had, regarding both, data curation and modelling, and has always been beyond supportive, patient and kind. Thank you.

Lastly, I would like to express my sincerest gratitude for all my family and friends for believing in me, especially my mother, my sister and Sven Ladusch. Thank you so much for your immense emotional and moral support, not only throughout this thesis, but throughout all of my bachelor's degree in general. Thank you so much.

6 Supplement

Becquemont1999 Fig1

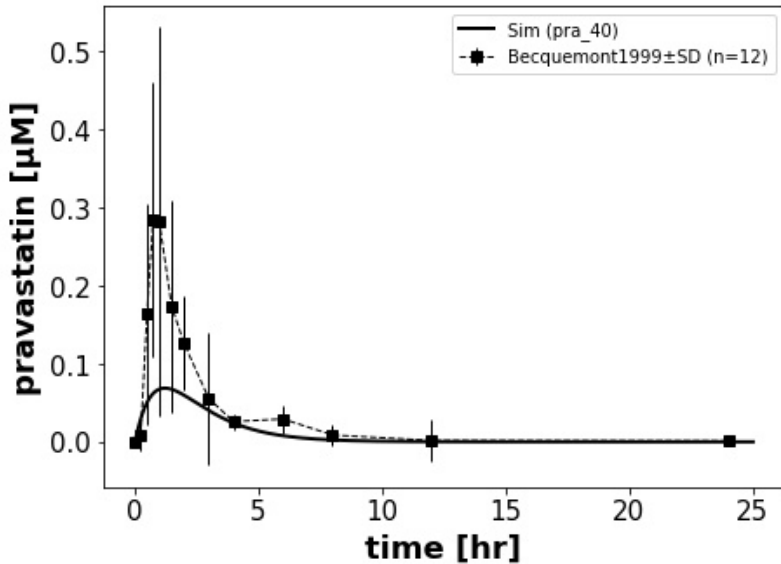


Figure 24: Simulation experiment Becquemont1999 [3]

Ho2007 Fig1

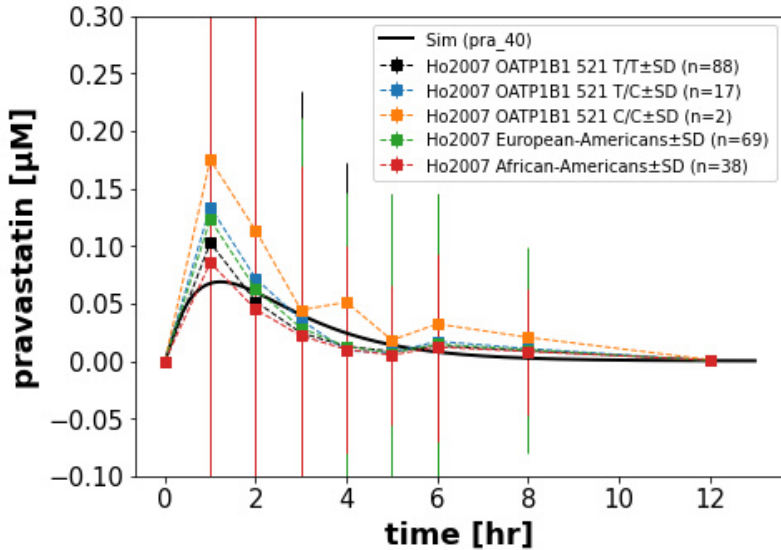


Figure 25: Simulation experiment Ho2007 [12].

Jacobson2004 Fig1,2,4

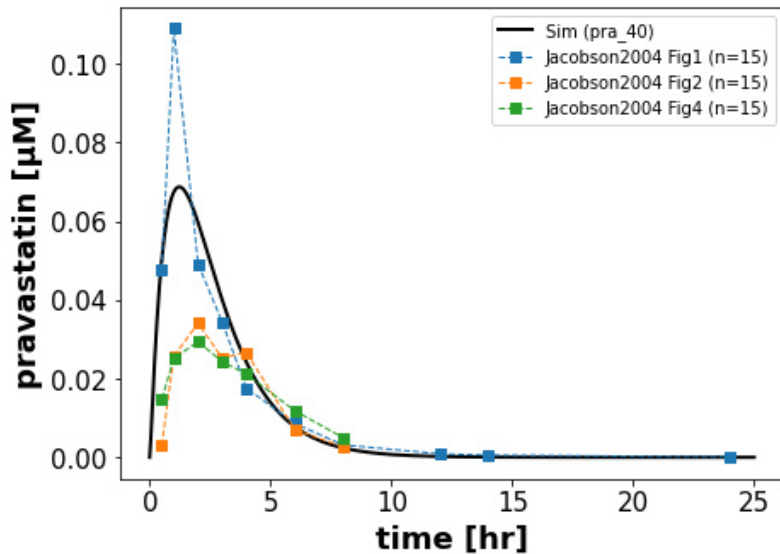


Figure 26: Simulation experiment Jacobson2004 [20].

Keskitalo2009 Fig1

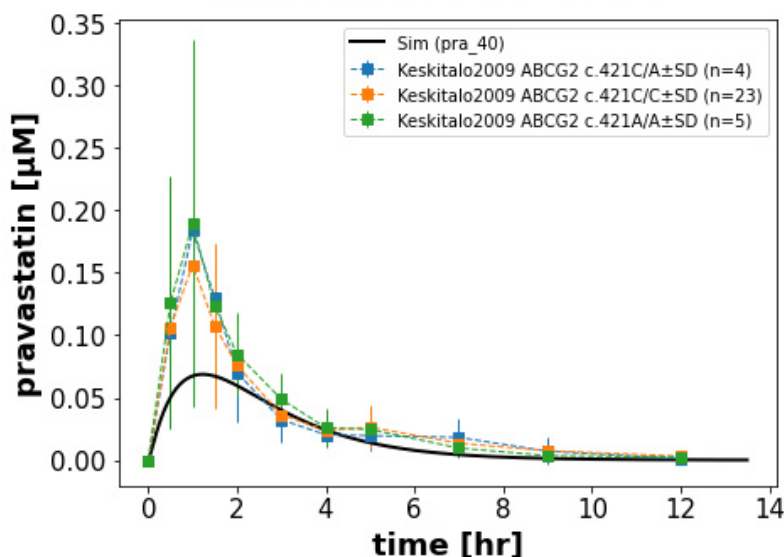


Figure 27: Simulation experiment Keskitalo2009 [27].

Kyrklund2003a Fig1

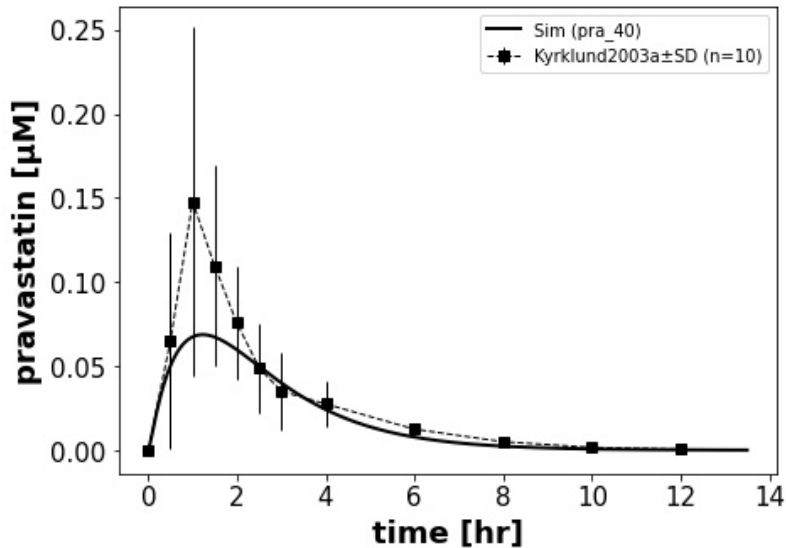


Figure 28: Simulation experiment Kyrklund2003a [39].

Maeda2006 Fig1

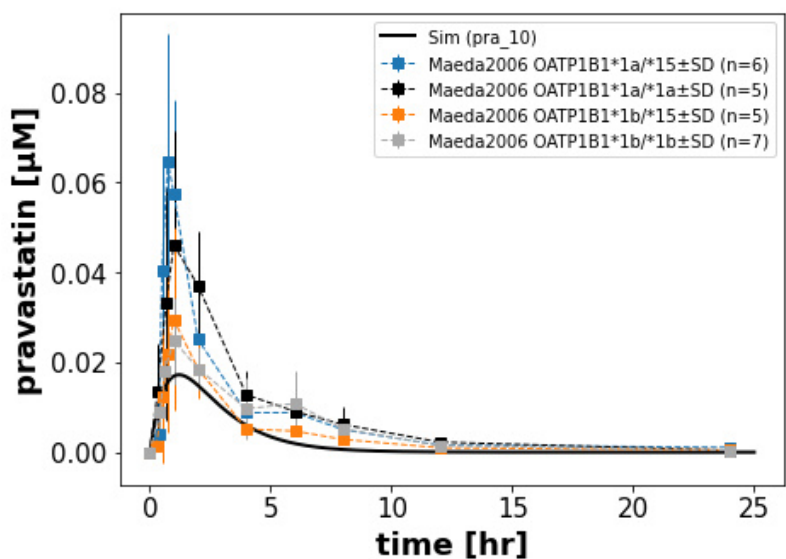


Figure 29: Simulation experiment Maeda2006 [42].

Mwinyi2004 Fig1

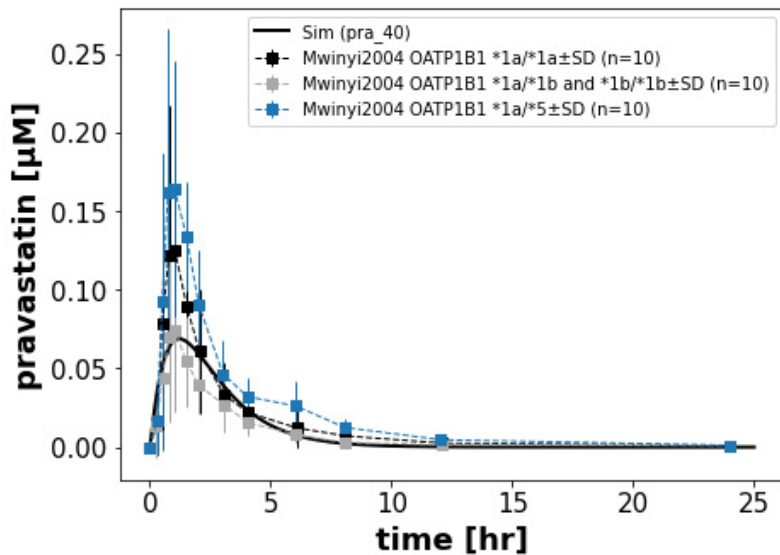


Figure 30: Simulation experiment Mwinyi2004 [45].

Neuvonen1998 Fig3

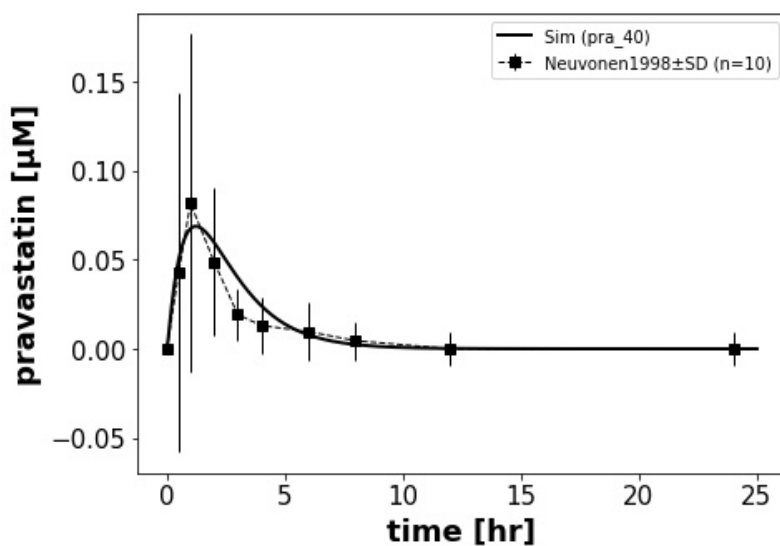


Figure 31: Simulation experiment Neuvonen1998 [47].

Niemi2006 Fig1

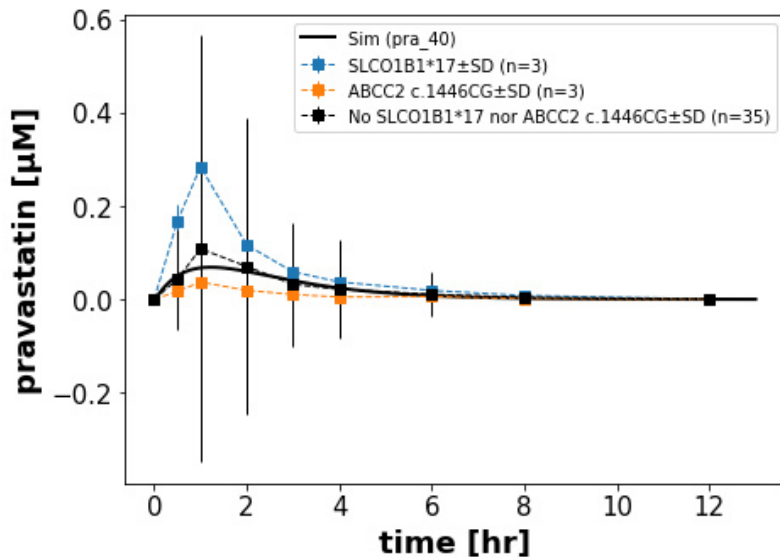


Figure 32: Simulation experiment Niemi2006 [49].

Niemi2004 Fig1

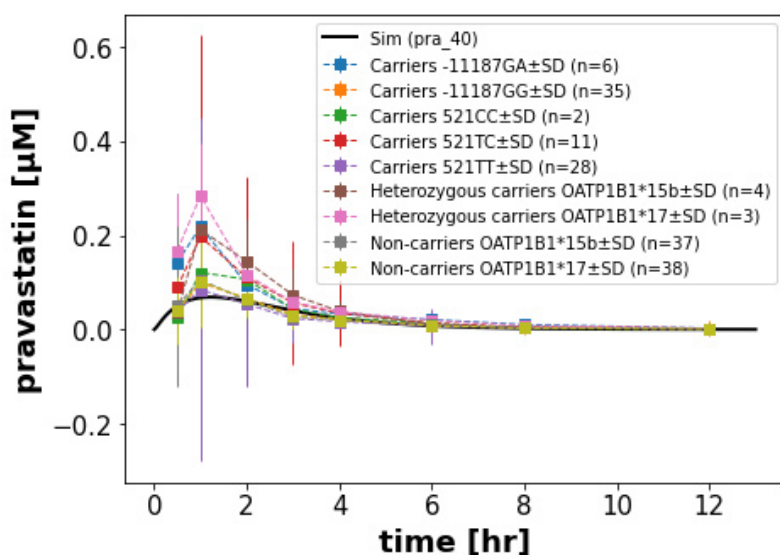


Figure 33: Simulation experiment Niemi2004 [51].

Nishizato2003 Fig1

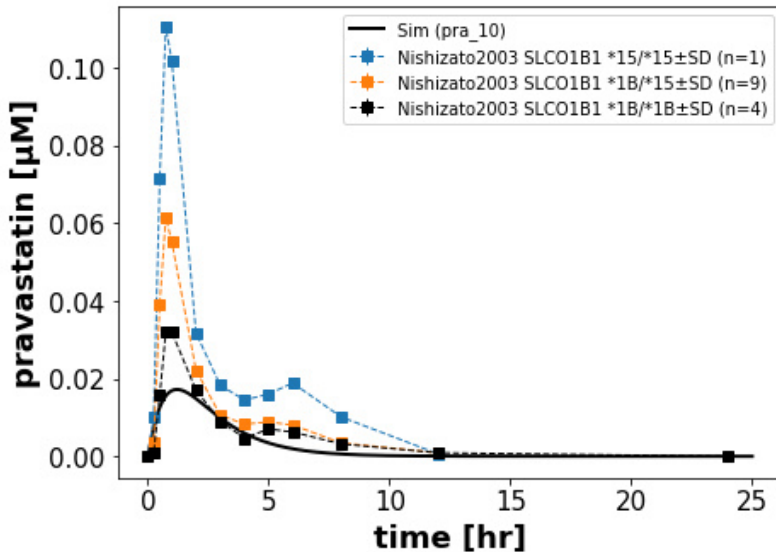


Figure 34: Simulation experiment Nishizato2003 [52].

Pan1993a Fig1

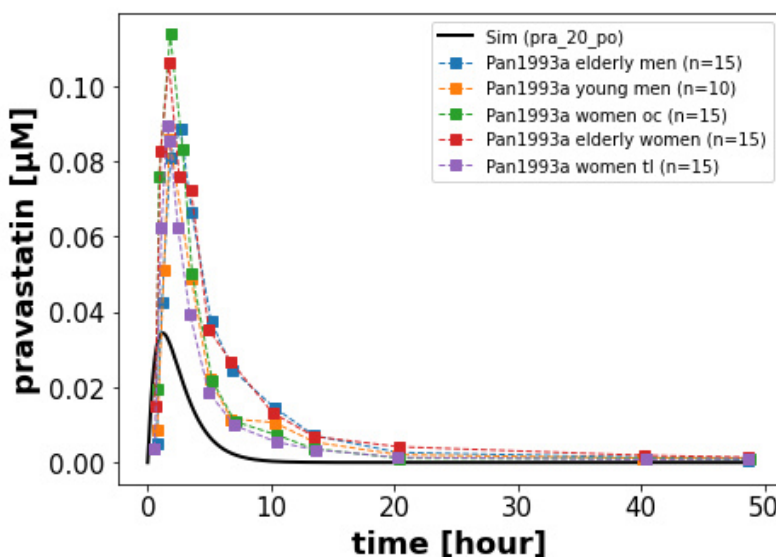


Figure 35: Simulation experiment Pan1993a [57].

Sigurbjoernsson1998 Fig3

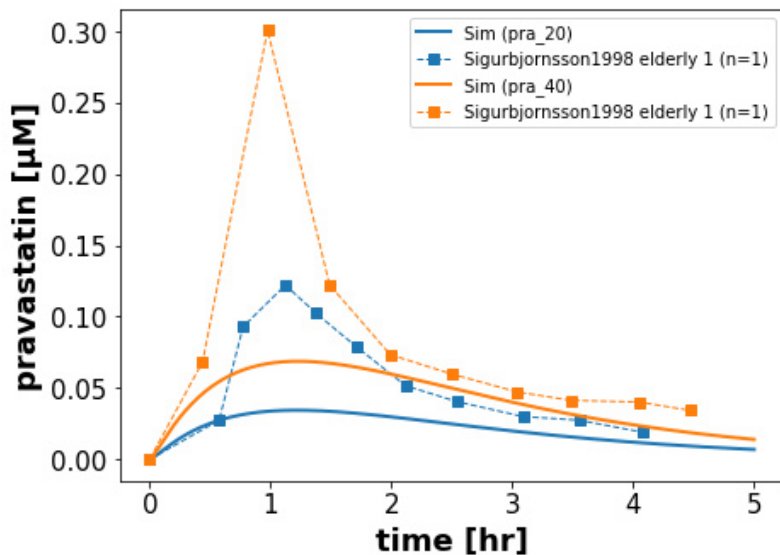


Figure 36: Simulation experiment Sigurbjoernsson1998, Figure 3 [66].

Sigurbjoernsson1998 Fig4

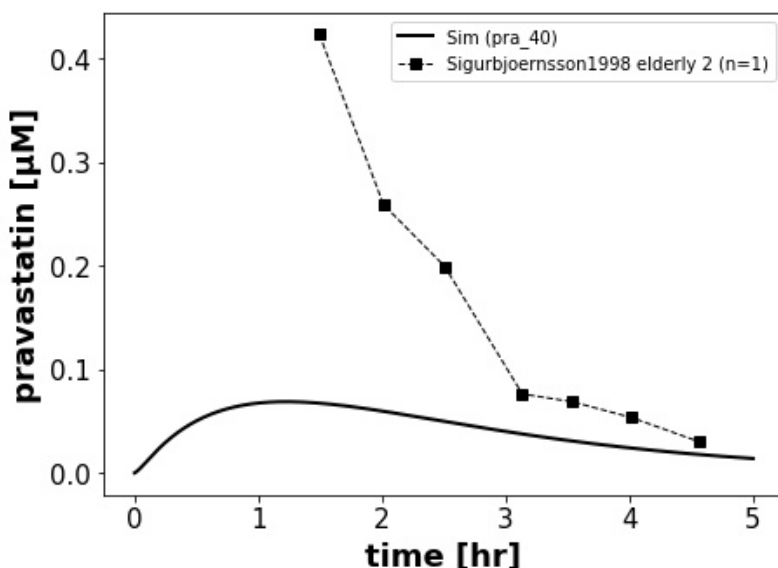


Figure 37: Simulation experiment Sigurbjoernsson1998, Figure 4 [66].

Sigurbjoernsson1998 Fig5

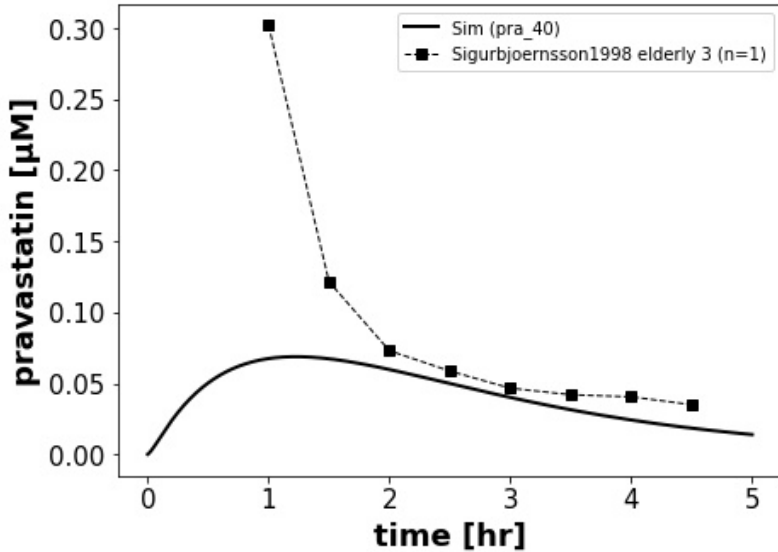


Figure 38: Simulation experiment Sigurbjoernsson1998, Figure 5 [66].

Sugimoto2001 Fig2

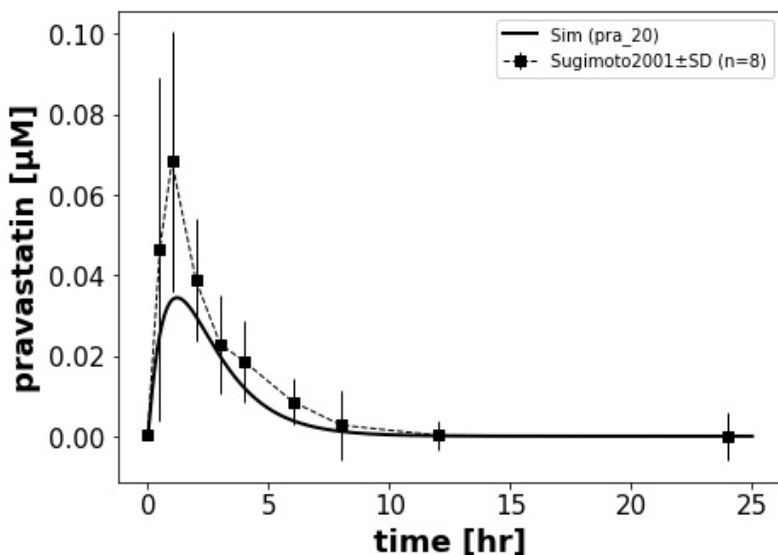


Figure 39: Simulation experiment Sugimoto2001, Figure 5 [70]

References

- [1] Lynne M Bang and Karen L Goa. "Pravastatin". In: *Drugs & aging* 20.14 (2003), pp. 1061–1082.
- [2] König Matthias Bartsch Florian Grzegorewski Janek. "Computational Modelling of Simvastatin - Effects on HMG-CoA Reductase Activity and Cholesterol". MA thesis. Humboldt-Universität zu Berlin, Nov. 2020.
- [3] Laurent Becquemont, Christian Funck-Brentano, and Patrice Jaillon. "Mibepradil, a potent CYP3A inhibitor, does not alter pravastatin pharmacokinetics". In: *Fundamental & clinical pharmacology* 13.2 (1999), pp. 232–236.
- [4] Leslie Z Benet and Parnian Zia-Amirhosseini. "Basic principles of pharmacokinetics". In: *Toxicologic pathology* 23.2 (1995), pp. 115–123.
- [5] JE Campbell and D Cohall. "Pharmacodynamics—A Pharmacognosy Perspective". In: *Pharmacognosy*. Elsevier, 2017, pp. 513–525.
- [6] Lucy CJ Ellis, Gabrielle M Hawksworth, and Richard J Weaver. "ATP-dependent transport of statins by human and rat MRP2/Mrp2". In: *Toxicology and applied pharmacology* 269.2 (2013), pp. 187–194.
- [7] DONALD W Everett, THEODORE J Chando, GERALD C Didonato, SAMPAT M Singhvi, HENRY Y Pan, and STEPHEN H Weinstein. "Biotransformation of pravastatin sodium in humans." In: *Drug metabolism and disposition* 19.4 (1991), pp. 740–748.
- [8] Food and Drug Administration, FDA. "Full Prescribing Information of Pravachol". In: (). URL: https://www.accessdata.fda.gov/drugsatfda_docs/label/2012/019898s062lbl.pdf. Reference ID: 3090896. Approved Mar. 1991. Last accessed 31.03.2022.
- [9] Jan Grzegorzewski, Janosch Brandhorst, Kathleen Green, Dimitra Eleftheriadou, Yannick Duport, Florian Barthorscht, Adrian Köller, Danny Yu Jia Ke, Sara De Angelis, and Matthias König. "PK-DB: pharmacokinetics database for individualized and stratified computational modeling". In: *Nucleic acids research* 49.D1 (2021), pp. D1358–D1364.
- [10] Charles E Halstenson, Joseph Triscari, Arthur DeVault, Bruce Shapiro, William Keane, and Henry Pan. "Single-dose pharmacokinetics of pravastatin and metabolites in patients with renal impairment". In: *The Journal of Clinical Pharmacology* 32.2 (1992), pp. 124–132.
- [11] Tomomi Hatanaka. "Clinical pharmacokinetics of pravastatin". In: *Clinical pharmacokinetics* 39.6 (2000), pp. 397–412.
- [12] Richard H Ho, Leena Choi, Wooin Lee, Gail Mayo, Ute I Schwarz, Rommel G Tirona, David G Bailey, C Michael Stein, and Richard B Kim. "Effect of drug transporter genotypes on pravastatin disposition in European-and African-American participants". In: *Pharmacogenetics and genomics* 17.8 (2007), p. 647.
- [13] Michael Hucka, Frank Bergmann, Stefan Hoops, Sarah Keating, Sven Sahle, and Darren Wilkinson. "The systems biology markup language (SBML): language specification for level 3 version 1 core (release 1 candidate)". In: *Nature Precedings* (2010), pp. 1–1.
- [14] Michael Hucka, Frank T Bergmann, Claudine Chaouiya, Andreas Dräger, Stefan Hoops, Sarah M Keating, Matthias König, Nicolas Le Novère, Chris J Myers, Brett G Olivier, et al. "The systems biology markup language (SBML): language specification for level 3 version 2 core release 2". In: *Journal of integrative bioinformatics* 16.2 (2019).
- [15] Donald B Hunninghake, Robert H Knopp, Gustav Schonfeld, Anne C Goldberg, W Virgil Brown, Ernst J Schaefer, Simeon Margolis, Adrian S Dobs, Margot J Mellies, William Insull Jr, et al. "Efficacy and safety of pravastatin in patients with primary hypercholesterolemia: I. A dose-response study". In: *Atherosclerosis* 85.1 (1990), pp. 81–89.
- [16] Takafumi Ide, Tomohiro Sasaki, Kazuya Maeda, Shun Higuchi, Yuichi Sugiyama, and Ichiro Ieiri. "Quantitative population pharmacokinetic analysis of pravastatin using an enterohepatic circulation model combined with pharmacogenomic Information on SLCO1B1 and ABCC2 polymorphisms". In: *The Journal of Clinical Pharmacology* 49.11 (2009), pp. 1309–1317.

- [17] Matthew K Ito. "Effects of extensive and poor gastrointestinal metabolism on the pharmacodynamics of pravastatin". In: *The Journal of Clinical Pharmacology* 38.4 (1998), pp. 331–336.
- [18] Jose Manuel Izquierdo-Palomares, Jesus Maria Fernandez-Tabera, Maria N Plana, Almudena Añino Alba, Pablo Gómez Álvarez, Inmaculada Fernandez-Esteban, Luis Carlos Saiz, Pilar Martin-Carrillo, and Óscar Pinar López. "Chronotherapy versus conventional statins therapy for the treatment of hyperlipidaemia". In: *Cochrane Database of Systematic Reviews* 11 (2016).
- [19] Wolfgang Jacobsen, Gabriele Kirchner, Katrin Hallensleben, Laviero Mancinelli, Michael Deters, Ingelore Hackbarth, Karen Baner, Leslie Z Benet, Karl-Friedrich Sewing, and Uwe Christians. "Small intestinal metabolism of the 3-hydroxy-3-methylglutaryl-coenzyme A reductase inhibitor lovastatin and comparison with pravastatin". In: *Journal of Pharmacology and Experimental Therapeutics* 291.1 (1999), pp. 131–139.
- [20] Terry A Jacobson. "Comparative pharmacokinetic interaction profiles of pravastatin, simvastatin, and atorvastatin when coadministered with cytochrome P450 inhibitors". In: *The American journal of cardiology* 94.9 (2004), pp. 1140–1146.
- [21] Gabriele Jedlitschky, Ulrich Hoffmann, and Heyo K Kroemer. "Structure and function of the MRP2 (ABCC2) protein and its role in drug disposition". In: *Expert opinion on drug metabolism & toxicology* 2.3 (2006), pp. 351–366.
- [22] HM Jones and Karen Rowland-Yeo. "Basic concepts in physiologically based pharmacokinetic modeling in drug discovery and development". In: *CPT: pharmacometrics & systems pharmacology* 2.8 (2013), pp. 1–12.
- [23] Annikka Kalliokoski and Mikko Niemi. "Impact of OATP transporters on pharmacokinetics". In: *British journal of pharmacology* 158.3 (2009), pp. 693–705.
- [24] Yoshio Kameyama, Keiko Yamashita, Kaoru Kobayashi, Masakiyo Hosokawa, and Kan Chiba. "Functional characterization of SLCO1B1 (OATP-C) variants, SLCO1B1* 5, SLCO1B1* 15 and SLCO1B1* 15+ C1007G, by using transient expression systems of HeLa and HEK293 cells". In: *Pharmacogenetics and genomics* 15.7 (2005), pp. 513–522.
- [25] Teemu Kantola, Janne T Backman, Mikko Niemi, Kari T Kivistö, and Pertti J Neuvonen. "Effect of fluconazole on plasma fluvastatin and pravastatin concentrations". In: *European journal of clinical pharmacology* 56.3 (2000), pp. 225–229.
- [26] Sarah M Keating, Dagmar Waltemath, Matthias König, Fengkai Zhang, Andreas Dräger, Claudine Chaouiya, Frank T Bergmann, Andrew Finney, Colin S Gillespie, Tomáš Helikar, et al. "SBML Level 3: an extensible format for the exchange and reuse of biological models". In: *Molecular systems biology* 16.8 (2020), e9110.
- [27] Jenni E Keskitalo, Marja K Pasanen, Pertti J Neuvonen, and Mikko Niemi. "Different effects of the ABCG2 c. 421C \rightarrow T SNP on the pharmacokinetics of fluvastatin, pravastatin and simvastatin". In: *Pharmacogenomics* 10.10 (2009), pp. 1617–1624.
- [28] Kari T Kivistö, Olaf Grisk, Ute Hofmann, Konrad Meissner, Klaus-Uwe Möritz, Christoph Ritter, Katja A Arnold, Dieter Lutjöhann, Klaus von Bergmann, Ingrid Klötting, et al. "Disposition of oral and intravenous pravastatin in MRP2-deficient TR-rats". In: *Drug Metabolism and Disposition* 33.11 (2005), pp. 1593–1596.
- [29] Kari T Kivistö and Mikko Niemi. "Influence of drug transporter polymorphisms on pravastatin pharmacokinetics in humans". In: *Pharmaceutical research* 24.2 (2007), pp. 239–247.
- [30] Daisuke Kobayashi, Takashi Nozawa, Kozue Imai, Jun-ichi Nezu, Akira Tsuji, and Ikumi Tamai. "Involvement of human organic anion transporting polypeptide OATP-B (SLC21A9) in pH-dependent transport across intestinal apical membrane". In: *Journal of pharmacology and experimental therapeutics* 306.2 (2003), pp. 703–708.
- [31] Adrian Köller, Jan Grzegorzewski, and Matthias König. "Physiologically based modeling of the effect of physiological and anthropometric variability on indocyanine green based liver function tests". In: *Frontiers in physiology* (2021), p. 2043.

- [32] Adrian Köller, Jan Grzegorzewski, Hans-Michael Tautenhahn, and Matthias König. “Prediction of survival after partial hepatectomy using a physiologically based pharmacokinetic model of indocyanine green liver function tests”. In: *Frontiers in physiology* (2021), p. 1975.
- [33] Matthias König. *sbmlsim: SBML simulation made easy*. Version 0.2.2. Sept. 2021. DOI: 10.5281/zenodo.5531088. URL: <https://doi.org/10.5281/zenodo.5531088>.
- [34] Matthias König. *sbmlutils: Python utilities for SBML*. Version 0.7.1. Feb. 2022. DOI: 10.5281/zenodo.5546603. URL: <https://doi.org/10.5281/zenodo.5546603>.
- [35] Matthias König, Andreas Dräger, and Hermann-Georg Holzhütter. “CySBML: a Cytoscape plugin for SBML”. In: *Bioinformatics* 28.18 (2012), pp. 2402–2403.
- [36] Matthias König and Helen Leal Pujol. *Pravastatin physiological based pharmacokinetics model (PBPK)*. Version 0.8.2. Apr. 2022. DOI: 10.5281/zenodo.6481380. URL: <https://doi.org/10.5281/zenodo.6481380>.
- [37] Matthias König and Nicolas Rodriguez. *matthiaskoenig/cy3sbml: cy3sbml-v0.3.0 - SBML for Cytoscape*. Version v0.3.0. Sept. 2019. DOI: 10.5281/zenodo.3451319. URL: <https://doi.org/10.5281/zenodo.3451319>.
- [38] Carl Kyrklund, Janne T Backman, Mikko Neuvonen, and Pertti J Neuvonen. “Effect of rifampicin on pravastatin pharmacokinetics in healthy subjects”. In: *British journal of clinical pharmacology* 57.2 (2004), pp. 181–187.
- [39] Carl Kyrklund, Janne T Backman, Mikko Neuvonen, and Pertti J Neuvonen. “Gemfibrozil increases plasma pravastatin concentrations and reduces pravastatin renal clearance”. In: *Clinical Pharmacology & Therapeutics* 73.6 (2003), pp. 538–544.
- [40] James H Lewis, Mary Ellen Mortensen, Steven Zweig, Mary Jean Fusco, Jeffrey R Medoff, Rene Belder, and Pravastatin in Chronic Liver Disease Study Investigators. “Efficacy and safety of high-dose pravastatin in hypercholesterolemic patients with well-compensated chronic liver disease: results of a prospective, randomized, double-blind, placebo-controlled, multicenter trial”. In: *Hepatology* 46.5 (2007), pp. 1453–1463.
- [41] Jari J Lilja, Kari T Kivistö, and Pertti J Neuvonen. “Grapefruit juice increases serum concentrations of atorvastatin and has no effect on pravastatin”. In: *Clinical Pharmacology & Therapeutics* 66.2 (1999), pp. 118–127.
- [42] Kazuya Maeda, Ichiro Ieiri, Kuninobu Yasuda, Akiharu Fujino, Hiroaki Fujiwara, Kenji Otsubo, Masaru Hirano, Takao Watanabe, Yoshiaki Kitamura, Hiroyuki Kusuhara, et al. “Effects of organic anion transporting polypeptide 1B1 haplotype on pharmacokinetics of pravastatin, valsartan, and temocapril”. In: *Clinical Pharmacology & Therapeutics* 79.5 (2006), pp. 427–439.
- [43] Asad Mansoor. “Volume of distribution”. In: *StatPearls*. (). U.S. National Library of Medicine. <https://www.ncbi.nlm.nih.gov/books/NBK545280/>. Jul 2021. Last accessed 16.01.2022.
- [44] Donna McTavish and Eugene M Sorkin. “Pravastatin”. In: *Drugs* 42.1 (1991), pp. 65–89.
- [45] Jessica Mwinyi, Andreas Johne, Steffen Bauer, Ivar Roots, and Thomas Gerloff. “Evidence for inverse effects of OATP-C (SLC21A6)* 5 and* 1b haplotypes on pravastatin kinetics”. In: *Clinical Pharmacology & Therapeutics* 75.5 (2004), pp. 415–421.
- [46] Noriaki Nakaya, Yasuhiko Homma, Hiromitsu Tamachi, Hiroshi Shigematsu, Yoshiya Hata, and Yuichiro Goto. “The effect of CS-514 on serum lipids and apolipoproteins in hypercholesterolemic subjects”. In: *Jama* 257.22 (1987), pp. 3088–3093.
- [47] Pertti J Neuvonen, Teemu Kantola, and Kari T Kivistö. “Simvastatin but not pravastatin is very susceptible to interaction with the CYP3A4 inhibitor itraconazole”. In: *Clinical pharmacology & therapeutics* 63.3 (1998), pp. 332–341.
- [48] Pertti J Neuvonen, Mikko Niemi, and Janne T Backman. “Drug interactions with lipid-lowering drugs: mechanisms and clinical relevance”. In: *Clinical Pharmacology & Therapeutics* 80.6 (2006), pp. 565–581.

- [49] Mikko Niemi, Katja A Arnold, Janne T Backman, Marja K Pasanen, Ute Gödtel-Armbrust, Leszek Wojnowski, Ulrich M Zanger, Pertti J Neuvonen, Michel Eichelbaum, Kari T Kivistö, et al. “Association of genetic polymorphism in ABCC2 with hepatic multidrug resistance-associated protein 2 expression and pravastatin pharmacokinetics”. In: *Pharmacogenetics and genomics* 16.11 (2006), pp. 801–808.
- [50] Mikko Niemi, Pertti J Neuvonen, Ute Hofmann, Janne T Backman, Matthias Schwab, Dieter Lütjohann, Klaus von Bergmann, Michel Eichelbaum, and Kari T Kivistö. “Acute effects of pravastatin on cholesterol synthesis are associated with SLCO1B1 (encoding OATP1B1) haplotype* 17”. In: *Pharmacogenetics and genomics* 15.5 (2005), pp. 303–309.
- [51] Mikko Niemi, Elke Schaeffeler, Thomas Lang, Martin F Fromm, Mikko Neuvonen, Carl Kyrlund, Janne T Backman, Reinhold Kerb, Matthias Schwab, Pertti J Neuvonen, et al. “High plasma pravastatin concentrations are associated with single nucleotide polymorphisms and haplotypes of organic anion transporting polypeptide-C (OATP-C, SLCO1B1)”. In: *Pharmacogenetics and Genomics* 14.7 (2004), pp. 429–440.
- [52] Yohei Nishizato, Ichiro Ieiri, Hiroshi Suzuki, Miyuki Kimura, Kiyoshi Kawabata, Takeshi Hirota, Hiroshi Takane, Shin Irie, Hiroyuki Kusuhara, Yoko Urasaki, et al. “Polymorphisms of OATP-C (SLC21A6) and OAT3 (SLC22A8) genes: consequences for pravastatin pharmacokinetics”. In: *Clinical Pharmacology & Therapeutics* 73.6 (2003), pp. 554–565.
- [53] Takashi Nozawa, Kozue Imai, Jun-Ichi Nezu, Akira Tsuji, and Ikumi Tamai. “Functional characterization of pH-sensitive organic anion transporting polypeptide OATP-B in human”. In: *Journal of Pharmacology and Experimental Therapeutics* 308.2 (2004), pp. 438–445.
- [54] Takashi Nozawa, Miki Nakajima, Ikumi Tamai, Kumiko Noda, Jun-ichi Nezu, Yoshimichi Sai, Akira Tsuji, and Tsuyoshi Yokoi. “Genetic polymorphisms of human organic anion transporters OATP-C (SLC21A6) and OATP-B (SLC21A9): allele frequencies in the Japanese population and functional analysis”. In: *Journal of Pharmacology and Experimental Therapeutics* 302.2 (2002), pp. 804–813.
- [55] Henry Y Pan, Arthur R DeVault, Barbara J Swites, Daisy Whigan, Eugene Ivashkiv, David A Willard, and Donald Brescia. “Pharmacokinetics and pharmacodynamics of pravastatin alone and with cholestyramine in hypercholesterolemia”. In: *Clinical Pharmacology & Therapeutics* 48.2 (1990), pp. 201–207.
- [56] Henry Y Pan, Arthur R DeVault, David Wang-Iverson, Eugene Ivashkiv, Brian N Swanson, and A Arthur Sugerman. “Comparative pharmacokinetics and pharmacodynamics of pravastatin and lovastatin”. In: *The Journal of Clinical Pharmacology* 30.12 (1990), pp. 1128–1135.
- [57] Henry Y Pan, Anthony P Waclawski, Phillip T Funke, and Daisy Whigan. *Pharmacokinetics of pravastatin in elderly versus young men and women*. 1993.
- [58] HY Pan. “Clinical pharmacology of pravastatin, a selective inhibitor of HMG-CoA reductase”. In: *European journal of clinical pharmacology* 40.1 (1991), S15–S18.
- [59] Ralph H Raasch. “Pravastatin sodium, a new HMG-CoA reductase inhibitor”. In: *Dicp* 25.4 (1991), pp. 388–394.
- [60] Laura B Ramsey, Samuel G Johnson, Kelly E Caudle, Cyrine E Haidar, Deepak Voora, Russell A Wilke, Whitney D Maxwell, Howard L McLeod, Ronald M Krauss, Dan M Roden, et al. “The clinical pharmacogenetics implementation consortium guideline for SLCO1B1 and simvastatin-induced myopathy: 2014 update”. In: *Clinical Pharmacology & Therapeutics* 96.4 (2014), pp. 423–428.
- [61] SPR Romaine, KM Bailey, AS Hall, and AJ Balmforth. “The influence of SLCO1B1 (OATP1B1) gene polymorphisms on response to statin therapy”. In: *The pharmacogenomics journal* 10.1 (2010), pp. 1–11.
- [62] Detlef Schuppan and Nezam H Afdhal. “Liver cirrhosis”. In: *The Lancet* 371.9615 (2008), pp. 838–851.

- [63] Annick Seithel, Hartmut Glaeser, Martin F Fromm, and Jörg König. “The functional consequences of genetic variations in transporter genes encoding human organic anion-transporting polypeptide family members”. In: *Expert opinion on drug metabolism & toxicology* 4.1 (2008), pp. 51–64.
- [64] Hassan Shahbaz. “Creatinine clearance”. In: *StatPearls*. (). U.S. National Library of Medicine. <https://www.ncbi.nlm.nih.gov/books/NBK544228/>. Jul 2021. Last accessed 29.12.2021.
- [65] Yoshiyuki Shirasaka, Takanori Mori, Yukiko Murata, Takeo Nakanishi, and Ikumi Tamai. “Substrate-and dose-dependent drug interactions with grapefruit juice caused by multiple binding sites on OATP2B1”. In: *Pharmaceutical research* 31.8 (2014), pp. 2035–2043.
- [66] S Sigurbjörnsson, T Kjartansdottir, M Johannsson, J Kristinsson, and G Sigurdsson. “A pharmacokinetic evaluation of pravastatin in middle-aged and elderly volunteers”. In: *European journal of drug metabolism and pharmacokinetics* 23.1 (1998), pp. 13–18.
- [67] SM Singhvi, HY Pan, RA Morrison, and DA Willard. “Disposition of pravastatin sodium, a tissue-selective HMG-CoA reductase inhibitor, in healthy subjects.” In: *British journal of clinical pharmacology* 29.2 (1990), pp. 239–243.
- [68] Lucian P Smith, Michael Hucka, Stefan Hoops, Andrew Finney, Martin Ginkel, Chris J Myers, Ion Moraru, and Wolfram Liebermeister. “SBML level 3 package: hierarchical model composition, version 1 release 3”. In: *Journal of integrative bioinformatics* 12.2 (2015), pp. 603–659.
- [69] Endre T Somogyi, Jean-Marie Bouteiller, James A Glazier, Matthias König, J Kyle Medley, Maciej H Swat, and Herbert M Sauro. “libRoadRunner: a high performance SBML simulation and analysis library”. In: *Bioinformatics* 31.20 (2015), pp. 3315–3321.
- [70] Koh-ichi Sugimoto, Masami Ohmori, Shuichi Tsuruoka, Kenta Nishiki, Atsuhiro Kawaguchi, Ken-ichi Harada, Masashi Arakawa, Koh-ichi Sakamoto, Mikio Masada, Isamu Miyamori, et al. “Different effects of St John’s wort on the pharmacokinetics of simvastatin and pravastatin”. In: *Clinical Pharmacology & Therapeutics* 70.6 (2001), pp. 518–524.
- [71] Ikumi Tamai, Jun-ichi Nezu, Hiroshi Uchino, Yoshimichi Sai, Asuka Oku, Miyuki Shimane, and Akira Tsuji. “Molecular identification and characterization of novel members of the human organic anion transporter (OATP) family”. In: *Biochemical and biophysical research communications* 273.1 (2000), pp. 251–260.
- [72] Ikumi Tamai, Hitomi Takanaga, Hiroshi Maeda, Takuo Ogihara, Masaru Yoneda, and Akira Tsuji. “Proton-cotransport of pravastatin across intestinal brush-border membrane”. In: *Pharmaceutical research* 12.11 (1995), pp. 1727–1732.
- [73] Rommel G Tirona, Brenda F Leake, Gracia Merino, and Richard B Kim. “Polymorphisms in OATP-C: identification of multiple allelic variants associated with altered transport activity among European-and African-Americans”. In: *Journal of Biological Chemistry* 276.38 (2001), pp. 35669–35675.
- [74] Marcello Tonelli, Chris Isles, Timothy Craven, Andrew Tonkin, Marc A Pfeffer, James Shepherd, Frank M Sacks, Curt Furberg, Stuart M Cobbe, John Simes, et al. “Effect of pravastatin on rate of kidney function loss in people with or at risk for coronary disease”. In: *Circulation* 112.2 (2005), pp. 171–178.
- [75] Andrea Tsoris. “Use of the child Pugh score in liver disease”. In: *StatPearls*. (). U.S. National Library of Medicine. <https://www.ncbi.nlm.nih.gov/books/NBK542308/>. Mar 2021. Last accessed 22.12.2021.
- [76] Masayuki Tsujimoto, Daisuke Hatozaki, Daisuke Shima, Hitoshi Yokota, Taku Furukubo, Satoshi Izumi, Tomoyuki Yamakawa, Tetsuya Minegaki, and Kohshi Nishiguchi. “Influence of serum in hemodialysis patients on the expression of intestinal and hepatic transporters for the excretion of pravastatin”. In: *Therapeutic Apheresis and Dialysis* 16.6 (2012), pp. 580–587.
- [77] Roger K Verbeeck. “Pharmacokinetics and dosage adjustment in patients with hepatic dysfunction”. In: *European journal of clinical pharmacology* 64.12 (2008), pp. 1147–1161.

- [78] Jonathan B Wagner, Melissa Ruggiero, J Steven Leeder, and Bruno Hagenbuch. “Functional consequences of pravastatin isomerization on OATP1B1-mediated transport”. In: *Drug Metabolism and Disposition* 48.11 (2020), pp. 1192–1198.
- [79] Andrew P Wright, Srinath Adusumalli, and Kathleen E Corey. “Statin therapy in patients with cirrhosis”. In: *Frontline gastroenterology* 6.4 (2015), pp. 255–261.

Eigenständigkeitserklärung

Hiermit erkläre ich, dass ich die vorliegende Arbeit selbstständig verfasst habe und sämtliche Quellen, einschließlich Internetquellen, die unverändert oder abgewandelt wiedergegeben werden, insbesondere Quellen für Texte, Grafiken, Tabellen und Bilder, als solche kenntlich gemacht habe. Ich versichere, dass ich die vorliegende Abschlussarbeit noch nicht für andere Prüfungen eingereicht habe. Mir ist bekannt, dass bei Verstößen gegen diese Grundsätze ein Verfahren wegen Täuschungsversuchs bzw. Täuschung gemäß der fachspezifischen Prüfungsordnung und/oder der Fächerübergreifenden Satzung zur Regelung von Zulassung, Studium und Prüfung der Humboldt-Universität zu Berlin (ZSP-HU) eingeleitet wird.



Berlin, den 03. Mai 2022, Helena Leal Pujol